Targets for personalized treatment of conjunctival melanoma

Cao, J.

Targets for Personalized Treatment of Conjunctival Melanoma

Jinfeng Cao

曹金峰

ISBN/EAN: 978-94-6299-799-8

Printed by: Ridderprint BV

Cover designed by Jinfeng Cao

Thesis layout by Jinfeng Cao

The research described in this thesis was financially supported by the Chinese Scholarship Council (CSC) with “Chinese government graduate student overseas study program” as a PhD scholarship (File no. 201206170141), the Nelly Reef Fund, the Bontius Uveal Melanoma Fund, Ms. I. Brouwer, and LOOF.

Targets for Personalized Treatment of Conjunctival Melanoma

Proefschrift

Ter verkrijging van

De graad van Doctor aan de Universiteit Leiden,

Op gezag van Rector Magnificus prof.mr. C.J.J.M. Stolker,

Volgens het besluit van het college voor promoties

Te verdedigen op donderdag 07 december 2017

Klokke 13:45 uur

door

Jinfeng Cao

曹金峰

Geboren te Changchun, Jilin Province, P. R. China

In 1982

Promotor

Prof. Dr. M. J. Jager

Co-promotores

Dr. R. M. Verdijk (Erasmus University Medical Center, The Netherlands)

Dr. A. G. Jochemsen

Promotiecommissie

Prof. Dr. L. Heindl (University of Cologne, Germany)

Prof. Dr. G.P.M. Luyten

Dr. M. Wang

Dr. R. Jia (Shanghai Jiao Tong University, China)

Dr. T. van Hall

“Cheerfulness and content are great beautifiers,
and are famous preservers of youthful looks.”

Charles Dickens
Barnaby Rudge, 1841

Table of contents

Chapter 1

Introduction and aims of the thesis

Melanoma is a type of cancer that originates from melanin-producing cells that are derived from the neural crest cells [1]. Melanoma frequently occurs in the skin, but the eye, and the mucosa of head and neck may also be involved. Ocular melanoma, the second most common type of melanoma, consists of two types: 1. those that develop in the conjunctiva, the tissue that covers the eye, and 2. those that grow intraocularly in the uvea (iris, ciliary body and choroid). This thesis focuses on the first type, the conjunctival melanoma (CM), which arises from the melanocytes within the basal layer of the conjunctival epithelium, and accounts for 5-6% of all ocular melanoma [2,3]. CM occurs mainly in the non-Hispanic white population, and is rare in young people [4]. The annual incidence is increasing and is now up to 0.8/million in Caucasians [5]. Between 1973 and 1999, the incidence in the United States increased by 295% in white males [6]. The risk factors of CM are not well understood. However, the population-based studies in Northern Europe suggest that, like cutaneous melanoma, the increasing incidence of CM is possibly associated with increased exposure to ultraviolet light radiation [5,7].

Malignant CM originates in primary acquired melanosis (PAM) (74%), de novo (19%), or in a pre-existing nevus (7%) [8]. CM may occur in any area of the conjunctiva, such as the bulbar, palpebral, caruncular, limbal and forniceal conjunctiva, and the cornea (Figure 1). CM frequently (up to 60%) recurs locally after primary treatment [9], and can be lethal because of metastasis. Intraocular extension may occur after primary surgical removal [10]. The first site of metastatic CM is often in the preauricular, submandibular or cervical lymph nodes after diagnosis of an invasive melanoma lesion, suggesting lymphatic vessels may be the main route of regional dissemination of CM [11]. However, distant metastasis may develop without first having a regional metastasis [9]. The lung, brain, liver, skin, bone, and gastrointestinal tract may be sites of distant metastases. The incidence rate

of metastatic CM varies from 12% to 25%, and the melanoma-related mortality at 10 years varies from 13% to 32% [5,9,12-14].

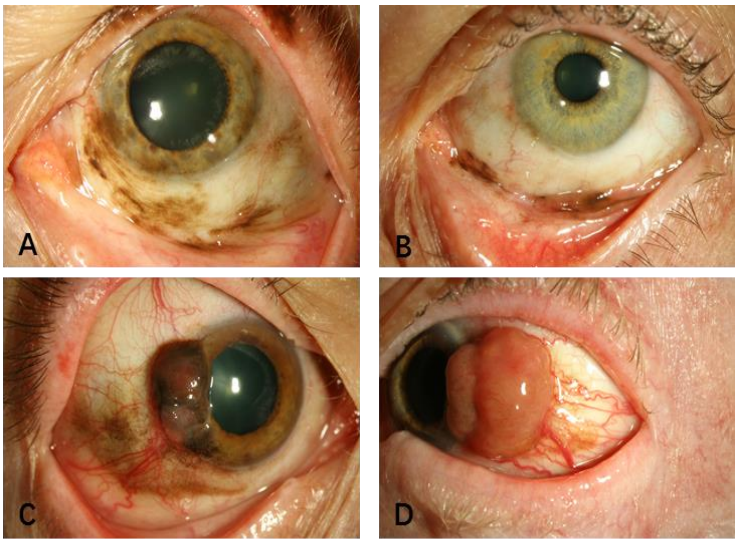

Figure. 1: **Conjunctival lesions**. **A**. Extensive primary acquired melanosis involving half the ocular surface and the corneal limbus. **B**. Pigmented CM in the fornix. Large pigmented (**C**) and non-pigmented (**D**) CM overlaying the corneal limbus.

Predisposing factors for malignancy

Conjunctival nevi, both pigmented and non-pigmented, are often found in childhood; they may be quite bulky. Although this type of lesion frequently carries a *BRAF* V600E mutation [15], it rarely progresses into melanoma [12]. On the other hand, the flat pigmented lesion known as PAM, usually detected in adults, indicates an increased risk of progression to malignant melanoma. A greater extent of PAM and/or PAM with severe atypia may potentially increase the chances of malignant transformation [16,17].

Prognostic factors

Many attempts have been made to elucidate the risk factors that predict the prognosis of CM. Firstly, the origin of melanoma may be an indicator of metastasis and death: Shields et al. reported that de novo melanoma have a higher risk of metastasis and mortality than tumors derived from PAM and nevi [8]. The presence of PAM with atypia also correlates with the development of local recurrences after biopsy or cryotherapy treatment [18]. Secondly, tumors located in the non-bulbar regions, i.e. the fornix, caruncle, or palpebra, and those with positive pathological margins are associated with local recurrence and metastasis after primary surgical treatment [8], and with a poor survival [5,9,19,20]. Thirdly, tumor thickness has prognostic value: an increased risk of local recurrence is observed in melanoma with a thickness over 0.5 mm [21], and more metastases and melanoma-related deaths are seen in thicker tumors [12,22,23]. Correspondingly, tumors thinner than 1 mm carry a low risk of mortality [9]. Lastly, other features, such as excision without adjuvant therapies, a large basal diameter, eyelid involvement and tumor lymphangiogenesis have been associated with worse clinical outcomes [5,9,11,24].

Treatment of conjunctival melanoma

Treating conjunctival lesions may start at the level of PAM, because, as we mentioned above, PAM is associated with an abnormal vascularity and melanoma transformation; Gloor and Alexandrakis therefore recommended surgical removal of widespread and thickened PAM [25]. However, the use of topical chemotherapies using mitomycin C or interferon alfa-2b without surgical excision have in recent years shown their effectiveness in decreasing the pigmentation and presence of PAM [26-28]. Regarding primary CM, extensive surgical excision used to be the conventional treatment. Whereas, growing evidence has shown a high local recurrence rate after surgery only [29,30]. Consequently, the current trend is towards surgical excision combined with adjuvant therapies.

Adjuvant therapies for CM are comprised of cryotherapy, topical chemotherapy and radiotherapy. Historically, cryotherapy was applied on the surgical margins after excision. However, Damato and Coupland found a significant higher recurrence rate and many complications after cryotherapy [31]. Therefore, cryotherapy has almost completely been replaced by topical chemotherapy as an adjuvant approach [32]. The most favorable topical drug for intraepithelial and superficial CM is mitomycin C, which has been investigated in several series [26,33,34]. Another topical drug is interferon α-2b with a treatment benefit shown in a few studies, in rather small cohorts [27,28,34]. The ideal dosage of mitomycin C and interferon α-2b are dependent on the clinical experience of doctors since there is no golden standard yet. Despite this adjuvant treatment, high recurrence rates, ranging from 33%-50%, are still being recorded after topical mitomycin C application [34-36].

Unlike topical chemotherapy, adjuvant radiotherapy may be applied for deeper malignant conjunctival lesions. Plaque brachytherapy significantly decreases the recurrence rates [30]. Similarly, proton beam radiotherapy has been applied to patients with non-bulbar primary CM. However, Wuestemeyer and colleagues demonstrated a 30% recurrence rate and 30% metastasis rate of CM upon proton beam radiotherapy [37].

Preventing patients from developing metastasis is a dilemma for treating CM. The traditional chemotherapies have limited effects, and because of the rarity, patients with advanced CM are often not included in clinical trials evaluating the effectiveness of novel therapies.

Animal models

The rarity of CM significantly limits the possibility of recruiting enough patients for randomized clinical trials to test new therapies. Therefore, it is urgent to develop animal models which can properly mimic the original disorder. However, unlike uveal melanoma, only a few models have been introduced to study CM. Successful models for CM are restricted to mice, while a model of PAM has been established

in rabbits [39]. De Waard and colleagues [38] recently developed a murine CM metastasis model, using nonobese diabetic (NOD)/severe combined immunodeficiency (SCID) IL-2 $r\gamma^{null}$ mice in which three human primary CM cell lines were subconjunctivally injected. Although tumor growth was observed in all cases after this approach, no metastasis occurred. Subsequently, cells obtained from the subconjunctival xenografts were inoculated into the subconjunctival space of a second group of these immunodeficient mice, and this *in vivo* passaging method led to frequent lung metastases. Schlereth et al. [12] implanted two murine melanoma cell lines subconjunctivally into C57BL/6N immuno-competent mice, and observed successful primary tumor growth as well as metastases in the lymph node, lung and spleen. In the future, more attention should be paid and more effort should be taken to establish ideal models for CM.

Genetics of conjunctival melanoma

Cancer is a human genetic disorder. Investigations have shown that CM, distinct from intraocular uveal melanoma, shares many molecular similarities with cutaneous melanoma; *BRAF* and *NRAS* are both known oncogenes that contribute to the formation of cutaneous melanoma. Activating mutations in *BRAF* or *NRAS* (mutually exclusive) are frequently detected in CM as well, and have been identified in up to 47% of all CMs [40-42]. Similar to cutaneous melanoma, more than 90% of mutations in the *BRAF* gene in CM occur at the V600E position.

BRAF is a crucial component in the mitogen-activated protein kinase (MAPK) pathway, while NRAS may participate in activities of the MAPK and PI3K/AKT pathways. Tumor-driven mutations in *BRAF* and *NRAS* genes activate MAPK and PI3K/AKT pathways, thereby promoting intracellular signaling, cell proliferation and cell cycle dysregulation (Figure 2).

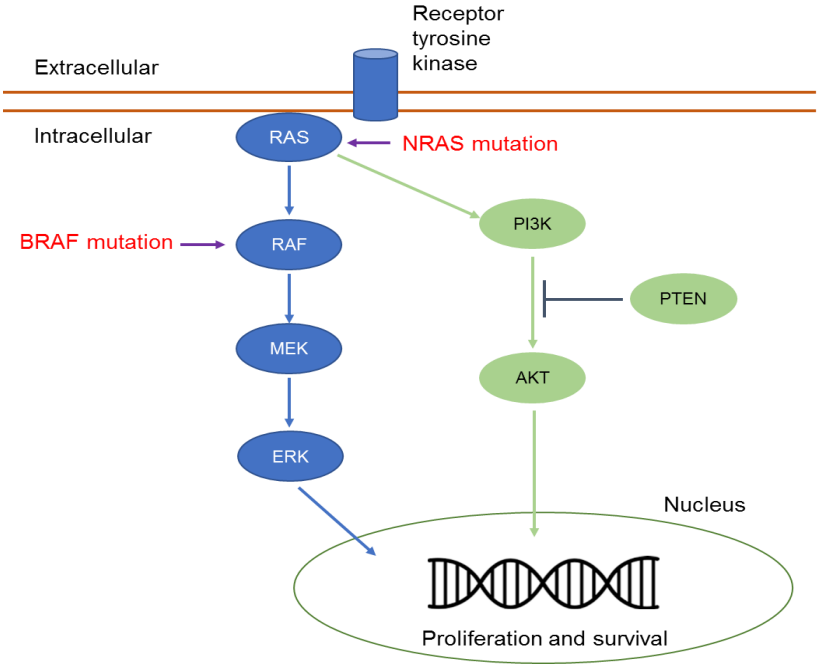

Figure 2. MAPK and PI3K/AKT signaling pathways. Oncogenic BRAF and NRAS mutations lead to phosphorylation of ERK and AKT, thereby activating the MAPK and PI3K/AKT pathways and stimulating cells to grow into a malignancy and survive.

Mutations in *GNAQ* or *GNA11*, which are oncogenes in uveal melanoma, however, are not found in CM, indicating different oncogenic triggers in these two types of ocular melanoma. Interestingly, in a large series, the *BRAF* V600E mutation was detected in conjunctival nevi and melanoma, but not in PAM with or without atypia [16]. One may speculate about the role of the *BRAF* V600E mutation in melanoma transformation, because in contrast to PAM with atypia, conjunctival nevi rarely develop into melanoma. We believe that additional mutations or oncogenic factors promote this tumor formation. Activating mutations of another hotspot oncogene of cutaneous melanoma and mucosal melanoma, KIT, are seldom identified in CM [43]. In contrast to activating mutations, abnormalities of tumor-suppressor genes like *p53*, *p16* and *PTEN* have not been well characterized in CM.

One study using a monoclonal antibody and immunohistochemistry has demonstrated a significantly lower protein expression of p16 in CM, compared to nevi and PAM with or without atypia [44], and suggested p16 expression could be used as a diagnostic marker to distinguish nevi and PAM from CM.

Many chromosomal aberrations have been discovered in CM, such as gain of 1q, 3p, 6p, 7, 17q and loss of 9p, 10q, 11, and 12q, 16q [45-47]. These biologic data are of great importance to further understand the basis of this malignancy, and to promote the development of new therapies.

Targeted therapy

The need for developing new treatments for advanced CM is urgent since the current approaches to treat metastases have limited effects. The new era of cancer personalized treatment involves comprehensive genomic or immunohistochemical analysis, thus unlike conventional chemotherapy, the new types of targeted therapies can attack tumor cells precisely with little damage to normal cells. The goal of personalized medicine is to tailor suitable therapies with the right medical decisions and medicines, at the right dose and at the right time in the right patient [48]. In cancer, personalized medicine will create more specific approaches to the individuals and their genomes. Early diagnoses and better drug development are believed to be achievable by personalized medicine. As we described above, the mutant genes in the MAPK pathway lead to abnormal activation of cell growth and survival. Therefore, personalized treatment with therapeutic agents aimed at these specific oncogenes is being applied in several types of cancer and has shown promising clinical outcomes [49]. However, only a few studies have evaluated the potential benefit of targeted therapies in CM. Pahlitzsch and Maleka et al. showed induction of good clinical responses in primary and metastatic CM patients upon Vemurafenib treatment [50,51], whereas Weber et al. reported a failed case using Vemurafenib for a metastatic CM patient with a *BRAF* V600E mutation [52]. We encourage clinical trials to recruit more CM patients using targeted compounds.

Other therapeutic approaches involve epigenetic changes: the term “epigenetics” refers to heritable changes which are not caused by alterations in the DNA sequence [53]. Aberrant patterns of epigenetics are considered a hallmark of cancer. Not only mutations and chromosomal translocations, but also aberrant chromatin-related proteins may lead to alterations in gene expression and signaling pathways, and thus result in cancer formation. The dynamic feature of epigenetic enzymes offers the opportunity to develop new drugs for cancer therapeutics. Enhancer of zeste homolog 2 (EZH2) is a core subunit of the polycomb repressive complex 2 (PRC2) family, and is of importance in regulating cellular processes. EZH2 catalyzes trimethylation of lysine 27 in histone H3 (H3K27me3) and results in the transcriptional repression of target genes [54,55]. Heterozygous somatic mutations of EZH2 are often observed in diffuse large B cell lymphomas and follicular lymphomas [56], but is not frequently found in solid tumors [57]. However, overexpression of EZH2 has been detected in many cancers, including cutaneous melanoma [58]. Targeting EZH2 with specific small molecule inhibitors has shown a high *in vitro* and *in vivo* potency against EZH2-mutant or EZH2-wildtype cancers [59]. CM may be a good target for blocking EZH2 with genetic or pharmacological approaches to inhibit cell growth *in vitro* and in *vivo*. We believe more potential molecular targets will be discovered with the evolvement of cancer research.

Immunotherapy

Immunotherapy boosts the activity of a person’s immune cells to fight against malignancies. It can be done by either stimulating the immune system or giving humanized antibodies. In the last few decades, immunotherapy has gained a revolutionary success in treating some types of cancer, especially advanced cutaneous melanoma.

Cytokine immunotherapy (with interferon and interleukin-2) has been applied for cutaneous melanoma patients, providing some good responses. However, many

complications have been noticed with this approach, making this method less favorable compared to other options [60].

The discovery of immune checkpoints is a milestone of immunological research. Immune checkpoints switch signals on or off, and cancer usually protects itself from T cell attack by blocking T cell signals. For example, when the T cell surface receptor known as programmed cell death 1 (PD-1) binds to programmed death ligand 1 (PD-L1) on the surface of a cancer cell, this will suppress the T-cell's function, impair cytokine production, and induce T cell apoptosis. To reverse this immunologically-non-responder state, antibodies against the inhibitory checkpoints have been developed, which target PD-1 and cytotoxic T-lymphocyte-associated protein 4 (CTL-A4), with promising results [61,62]. Very recently, Nivolumab (PD-1 inhibitor) showed a successful clinical response in a CM patient with breast metastasis [63]. However, very few clinical trials have recruited CM patients. It is therefore essential to study the expression of these ligands in CM.

The human leukocyte antigen (HLA) complex plays a pivotal role in immunology: cytotoxic T cells (CTL) function when HLA class I molecules are present. Cancer cells attempt to escape immune surveillance in many ways, one of which is downregulating HLA class I expression, which helps to avoid an attack from CTL. Downregulation of HLA class I expression usually is a predictive biomarker of poor prognosis in many cancer types, although opposite outcomes have been reported in colorectal cancer and uveal melanoma [64-66]. T cell receptor (TCR)-based immunotherapies have been extensively studied in the past years, especially in cutaneous melanoma. In this context, HLA class I is required to present tumor antigens to $CD8^+$ cells, letting cytotoxic $CD8^+$ cells kill tumor cells. Therefore, it is worthwhile to examine the HLA class I status in CM to help determine the therapeutic options. However, not all melanoma may express the same target antigens. A special interest focuses on the identification of T cell clones that recognize tumor-specific antigens. One study showed that a new cancer-testis antigen PRAME (Melanoma antigen preferentially expressed in tumors), is highly expressed in CM [67]. As the LUMC has extensive experience with this antigen, we

decided to test the newly designed PRAME-specific HLA-A2 restricted T cell clones on CM cell lines, and found that the HLA-A*02:01 transduced melanoma cells could be recognized by those PRAME-specific T cell clones, indicating a potential approach for treating CM (Figure 3). However, T cells only respond when the appropriate HLA antigen is expressed on the target, and we therefore studied expression of HLA class I antigens on a series of CM.

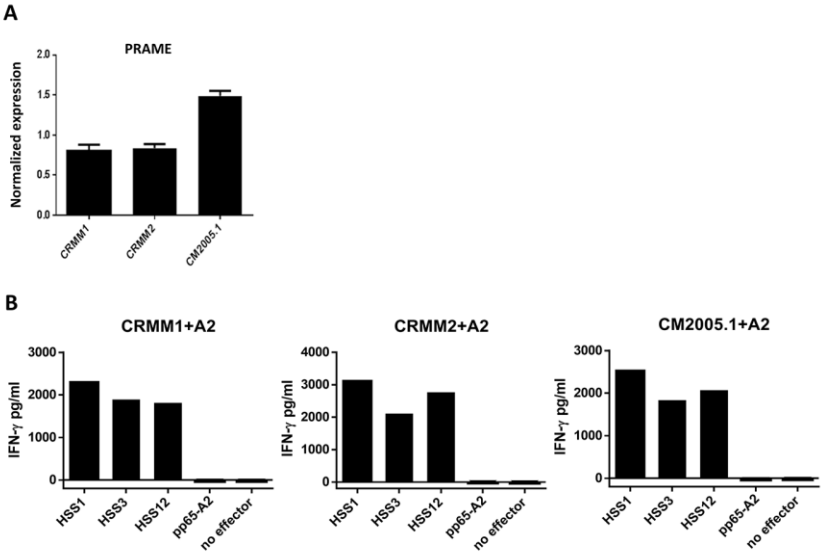

Figure 3. Three PRAME-positive CM cell lines are efficiently recognized by PRAME-specific T-cells. (**A**) The mRNA expression of PRAME in three CM cell lines (CRMM1, CRMM2 and CM2005.1) was determined using quantitative real-time polymerase chain reaction (qPCR). (**B**) The PRAME-specific T-cell clones HSS1 and HSS3 identified all CM cell lines. CM cell lines had been retrovirally transduced with HLA-A*02:01 (+ A2). USP11 (housekeeping gene)-specific T-cell clone HSS12 was used to verify that HLA-A2 was positive in CM cells. Clone pp65-A2, reacting with a peptide of pp65 in the context of HLA-A2, served as the negative control. Data are provided by DM van der Steen and MHM Heemskerk, Department of Hematology, LUMC.

There are several new directions in the immune-oncology field. For instance, dendritic cell (DC) vaccines can enhance $CD8^+$ T cell response to neoantigens (encoded by tumor-specific mutated genes) in cutaneous melanoma [68], and combining DC vaccines with immune checkpoint blocking therapy may be a future regimen [69]. Another promise lies in the combination of epigenetic therapy and

immunotherapy to enhance the immune system and thereby improve the outcome [70]. In addition, chimeric antigen receptor T-cell (CAR-T) therapy is a global focus for cancer treatment. T cells extracted from the tumor-bearing patient are genetically reengineered to express CAR that recognize a specific tumor antigen, and are subsequently reinfused into the patient. CAR-T therapy was initially designed for hematopoietic malignancies, but currently, a great effort targeting solid tumors is ongoing, although many obstacles still need to be overcome.

Aims of this thesis

Two different yet related topics are described in this thesis. The first part of the thesis identifies specific targets, illustrates the role of these targets, and explores personalized therapeutic possibilities to inhibit tumor growth by using new treatment strategies. The second part starts with the description of a new animal model for CM. A proper model can mimic the human disorder and provide opportunities for studying tumor biology, and for seeking novel effective therapies to inhibit the dissemination of malignant cells. Subsequently, the potential role of immune checkpoint molecules and the presence of HLA class I antigens are studied.

New animal models and therapeutic targets will broaden our understanding of CM, and help us to develop better treatments for primary and metastatic CM, thus prolonging patients' survival.

Scope and outline

Given the challenges described above, this thesis aims to discover targets of personalized treatment for CM. Figure 4 illustrates the different aspects of this thesis. *i*) targeting oncogenes and epigenetics, *ii*) establishment of a murine metastatic CM model and *iii*) studying the immunology and potential of using immunotherapy for CM.

In **Chapter 2**, we examine the presence of *BRAF* V600E mutation, and the

expression of phosphorylated-ERK and phosphorylated-AKT on sections of human conjunctival lesions by immunohistochemistry. We show that *BRAF* V600E mutations occur frequently in conjunctival nevi and melanoma, and ERK and AKT are expressed in these lesions as well as in PAM. Furthermore, we treated human CM cell lines with BRAF, MEK and AKT inhibitors, and reveal that although a single drug can inhibit cell growth, it is not always cytotoxic. We demonstrate that *in vitro* BRAF inhibitors (Vemurafenib and Dabrafenib) are effective on *BRAF* V600E-mutated CM cell lines, while the MEK inhibitor MEK162 and AKT inhibitor MK2206 work on all cell lines, regardless of mutation status. The combination of MEK and AKT inhibitors results in more cell cycle arrest and cell death.

Another area of targeted therapy lies in epigenetic regulators. The dynamic and versatile character of epigenetics makes seeking epigenetic targets attractive. In **Chapter 3**, we focus on the crucial epigenetic gene EZH2, and observe frequent overexpression of EZH2 in primary CM. Inhibiting EZH2 with genetic knockdown or small molecule EZH2 inhibitors impairs CM cell growth and EZH2-mediated protein expression and induces cell cycle arrest *in vitro*. Additionally, one EZH2 inhibitor reduces cell proliferation in a zebrafish model. These findings suggest that targeting EZH2 may provide an alternative treatment for CM.

To facilitate the understanding of the tumor behavior and testing potential therapeutic compounds, we created a mouse metastatic CM model (**Chapter 4**). Our model mimics the way of metastatic spread of human CM, thereby especially providing opportunities for novel treatments to prevent metastatic dissemination.

As resistance to targeted therapies may develop, it is worthwhile to look for alternative therapeutic targets. Therefore, to determine whether blocking the PD-1/PD-L1 axis can be a potential treatment, we examine the expression of PD-1, PD-L1 and tumor-infiltrating lymphocytes (TILs) of primary CM using immunofluorescence staining in **Chapter 5**. The results show that PD-L1 is expressed in some CM, and this expression is correlated with distant metastases and a worse melanoma-related survival. Large tumors contain a lower density of TILs

than small tumors. Our explorative study indicates that immunotherapy targeting the PD-1/PD-L1 axis should be considered for patients with CM.

In **Chapter 6**, we reveal that downregulation of HLA class I expression occurs frequently in CM, and thick tumors show a low HLA class I expression. Moreover, HLA class I expression is not correlated with PD-L1/PD-1 status, but respectively associates and tends to associate with macrophages and $CD8^+$ T cells, which produce interferon gamma, an essential cytokine for HLA class I regulation. Therefore, to mimic the tumor environment, CM cell lines were incubated with interferon gamma, which indeed led to elevation of mRNA and protein expression of HLA class I. Thick tumors that lack HLA class I may be inappropriate targets for T cell mediated therapies, unless cytokines are added that will upregulate their expression.

Finally, in **Chapter 7** we summarize and discuss the conclusions according to the studies presented in the thesis.

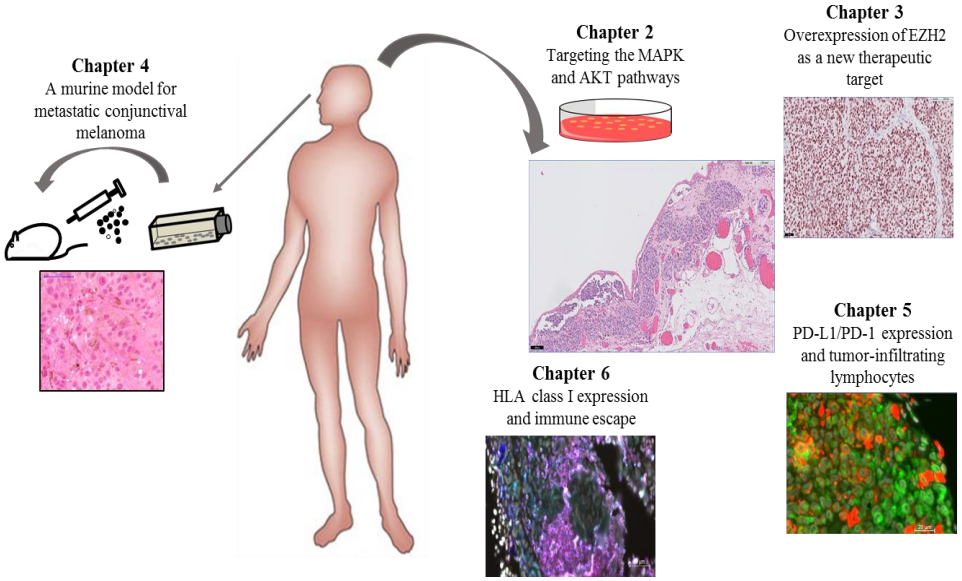

Figure 4. Overview of different chapters.

References

[1] Cramer, SF. The origin of epidermal melanocytes. Implications for the histogenesis of nevi and melanomas. Arch Pathol Lab Med. 1991;115:115-119.

[2] McLaughlin CC, Wu XC, Jemal A, Martin HJ, Roche LM, Chen VW. Incidence of noncutaneous melanomas in the U. S. Cancer. 2005;103:1000–1007.

[3] Isager P, Engholm G, Overgaard J, Storm H. Uveal and conjunctival malignant melanoma in denmark 1943-97: observed and relative survival of patients followed through 2002. Ophthalmic Epidemiol. 2006;13:85–96.

[4] Taban M, Traboulsi EI. Malignant melanoma of the conjunctiva in children: a review of the international literature 1965-2006. J Pediatr Ophthalmol Strabismus. 2007;44:277-82; quiz 298-9.

[5] Tuomaala S, Eskelin S, Tarkkanen A, Kivelä T. Populationbased assessment of clinical characteristics predicting outcome of conjunctival melanoma in whites. Invest Ophthalmol Vis Sci. 2002;43:3399-3408.

[6] Yu GP, Hu DN, McCormick S, Finger PT. Conjunctival melanoma: is it increasing in the United States? Am J Ophthalmol. 2003; 135:800-806.

[7] Triay E, Bergman L, Nilsson B, All-Ericsson C, Seregard S. Time trends in the incidence of conjunctival melanoma in Sweden. Br J Ophthalmol. 2009; 93:1524–1528.

[8] Shields CL, Markowitz JS, Belinsky I, Schwartzstein H, George NS, Lally SE, Mashayekhi A, Shields JA. Conjunctival melanoma: outcomes based on tumor origin in 382 consecutive cases. Ophthalmology. 2011;118:389-395.e1-2.

[9] Missotten GS, Keijser S, De Keizer RJ, De Wolff-Rouendaal D. Conjunctival melanoma in the Netherlands: a nationwide study. Invest Ophthalmol Vis Sci. 2005; 46:75-82.

[10] Wenkel H, Rummelt V, Naumann GO. Malignant melanoma of the conjunctiva with intraocular extension. Arch Ophthalmol. 2000;118:557-560.

[11] Schlereth SL, Iden S, Mescher M, Ksander BR, Bosch JJ, Cursiefen C, Heindl LM. A novel model of metastatic conjunctival melanoma in immune-competent mice. Invest Ophthalmol Vis Sci. 2015;56:5965-5973.

[12] Shields CL, Shields JA, Gunduz K, Cater J, Mercado GV, Gross N, et al. Conjunctival melanoma: risk factors for recurrence, exenteration, metastasis, and death in 150 consecutive patients. Archives of ophthalmology. 2000;118:1497-507.

[13] Kujala E, Tuomaala S, Eskelin S, Kivelä T. Mortality after uveal and conjunctival melanoma: which tumour is more deadly? Acta Ophthalmol. 2009;87(2):149-53.

[14] Shildkrot Y, Wilson MW. Conjunctival melanoma: pitfalls and dilemmas in management. Curr Opin Ophthalmol. 2010;21:380–386.

[15] Cao J, Heijkants RC, Jochemsen AG, Dogrusöz M, de Lange MJ, van der Velden PA, van der Burg SH, Jager MJ, Verdijk RM. Targeting of the MAPK and AKT pathways in conjunctival melanoma shows potential synergy. Oncotarget. 2016. doi: 10.18632/oncotarget.10770.

[16] Jakobiec FA, Folberg R, Iwamoto T. Clinicopathologic characteristics of premalignant and malignant melanocytic lesions of the conjunctiva. Ophthalmology. 1989;96:147-166.

[17] Shields JA, Shields CL, Mashayekhi A, Marr BP, Benavides R, Thangappan A, Phan L, Eagle RC Jr. Primary acquired melanosis of the conjunctiva. Risks for progression to melanoma in

311 eyes. The 2006 Lorenz E. Zimmerman Lecture. Ophthalmology. 2008;115:511-519.

[18] Shields JA, Shields CL, Mashayekhi A, Marr BP, Benavides R, Thangappan A, Phan L, Eagle RC Jr. Primary acquired melanosis of the conjunctiva: experience with 311 eyes. Trans Am Ophthalmol Soc 2007;105:61-71.

[19] Paridaens AD, Minassian DC, McCartney AC, Hungerford JL. Prognostic factors in primary malignant melanoma of the conjunctiva: a clinicopathological study of 256 cases. Br J Ophthalmol 1994;78:252–259.

[20] Werschnik C, Lommatzsch PK. Long-term follow-up of patients with conjunctival melanoma. Am J Clin Oncol 2002;25:248–255.

[21] Yousef YA, Finger PT. Predictive Value of the Seventh Edition American Joint Committee on Cancer Staging System for Conjunctival Melanoma AJCC Staging for Conjunctival Melanoma. Arch Ophthalmol 2012;130:599-606.

[22] Tuomaala S, Kivela T. Metastatic pattern and survival in disseminated conjunctival melanoma: implications for sentinel lymph node biopsy. Ophthalmology 2004;111:816–821.

[23] Savar A, Ross MI, Prieto VG, Ivan D, Kim S, Esmaeli B. Sentinel lymph node biopsy for ocular adnexal melanoma: experience in 30 patients. Ophthalmology 2009;116:2217-2223.

[24] Heindl LM, Hofmann-Rummelt C, Adler W, Bosch JJ, Holbach LM, Naumann GO, Kruse FE, Cursiefen C. Prognostic significance of tumor-associated lymphangiogenesis in malignant melanomas of the conjunctiva. Ophthalmology 2011;118:2351-2360.

[25] Gloor P, Alexandrakis G. Clinical characterization of primary acquired melanosis. Invest Ophthalmol Vis Sci. 1995;36:1721-1729.

[26] Pe'er J, Frucht-Pery J. The treatment of primary acquired melanosis (PAM) with atypia by topical Mitomycin C. Am J Ophthalmol 2005;139:229–234.

[27] Finger PT, Sedeek RW, Chin KJ. Topical interferon alfa in the treatment of conjunctival melanoma and primary acquired melanosis complex. Am J Ophthalmol 2008;145:124–129.

[28] Herold TR, Hintschich C. Interferon alpha for the treatment of melanocytic conjunctival lesions. Graefes Arch Clin Exp Ophthalmol. 2010;248:111-115.

[29] Lim LA, Madigan MC, Conway RM. Conjunctival melanoma: a review of conceptual and treatment advances. Clin Ophthalmol. 2013;6:521-531.

[30] Damato B, Coupland SE. An audit of conjunctival melanoma treatment in Liverpool. Eye (Lond). 2009;23:801-809.

[31] Damato B, Coupland SE. Management of conjunctival melanoma. Expert Rev Anticancer Ther. 2009;9:1227-1239.

[32] Kao A, Afshar A, Bloomer M, Damato B. Management of primary acquired melanosis, nevus, and conjunctival melanoma. Cancer Control. 2016;23:117-125.

[33] Finger PT, Czechonska G, Liarikos S. Topical mitomycin C chemotherapy for conjunctival melanoma and PAM with atypia. Br J Ophthalmol. 1998;82:476-479.

[34] Ditta LC, Shildkrot Y, Wilson MW. Outcomes in 15 patients with conjunctival melanoma treated with adjuvant topical mitomycin C: complications and recurrences. Ophthalmology. 2011;118:1754-1759.

[35] Demirci H, McCormick SA, Finger PT. Topical mitomycin chemotherapy for conjunctival malignant melanoma and primary acquired melanosis with atypia: clinical experience with histopathologic observations. Arch Ophthalmol. 2000;118:885-891.

[36] Kurli M, Finger PT. Topical mitomycin chemotherapy for conjunctival malignant melanoma and primary acquired melanosis with atypia: 12 years' experience. Graefes Arch Clin Exp Ophthalmol. 2005;243:1108-1114.

[37] Wuestemeyer H, Sauerwein W, Meller D, Chauvel P, Schueler A, Steuhl KP, Bornfeld N, Anastassiou G. Proton radiotherapy as an alternative to exenteration in the management of extended conjunctival melanoma. Graefes Arch Clin Exp Ophthalmol. 2006;244:438-446.

[38] de Waard NE, Cao J, McGuire SP, Kolovou PE, Jordanova ES, Ksander BR, Jager MJ. A murine model for metastatic conjunctival melanoma. Invest Ophthalmol Vis Sci. 2015;56:2325-2333.

[39] Folberg R, Baron J, Reeves RD, Stevens RH, Bogh LD. Animal model of conjunctival primary acquired melanosis. Ophthalmology. 1989;96:1006-1013.

[40] Griewank KG, Westekemper H, Murali R, et al. Conjunctival melanomas harbor BRAF and NRAS mutations and copy number changes similar to cutaneous and mucosal melanomas. Clin Cancer Res. 2013;19:3143-3152.

[41] Gear H, Williams H, Kemp EG, Roberts F. BRAF mutations in conjunctival melanoma. Invest Ophthalmol Vis Sci. 2004; 45:2484-2488.

[42] Spendlove HE, Damato BE, Humphreys J, Barker KT, Hiscott PS, Houlston RS. BRAF mutations are detectable in conjunctival but not uveal melanomas. Melanoma Res. 2004; 14:449-452.

[43] Alessandrini L, Parrozzani R, Bertorelle R, Valentini E, Candiotto C, Giacomelli L, Midena E, Blandamura S. C-Kit SCF receptor (CD117) expression and KIT gene mutation in conjunctival pigmented lesions. Acta Ophthalmol. 2013;91:e641-e645.

[44] Zoroquiain P, Fernandes BF, Gonzalez S, Novais GN, Schalper KA, Burnier MN Jr. p16ink4a expression in benign and malignant melanocytic conjunctival lesions. Int J Surg Pathol. 2012;20:240-245.

[45] Vajdic CM, Hutchins AM, Kricker A, Aitken JF, Armstrong BK, Hayward NK, Armes JE. Chromosomal gains and losses in ocular melanoma detected by comparative genomic hybridization in an Australian population-based study. Cancer Genet Cytogenet. 2003;144:12-17.

[46] Lake SL, Jmor F, Dopierala J, Taktak AF, Coupland SE, Damato BE. Multiplex ligation-dependent probe amplification of conjunctival melanoma reveals common BRAF V600E gene mutation and gene copy number changes. Invest Ophthalmol Vis Sci. 2011;52:5598-5604.

[47] Busam KJ, Fang Y, Jhanwar SC, Pulitzer MP, Marr B, Abramson DH. Distinction of conjunctival melanocytic nevi from melanomas by fluorescence in situ hybridization. J Cutan Pathol. 2010;37:196-203.

[48] Lazarou J, Pomeranz BH, Corey PN. Incidence of adverse drug reactions in hospitalized patients. JAMA. 1998; 279:1200-1205.

[49] Cheng Y, Zhang G, Li G. Targeting MAPK pathway in melanoma therapy. Cancer Metastasis Rev. 2013;32:567-584.

[50] Pahlitzsch M, Mai C. Conjunctival melanoma and BRAF inhibitor therapy. J Clin Exp Ophthalmol. 2014;5:322.

[51] A. Maleka, G. Åström, P. Byström, G. J. Ullenhag. A case report of a patient with metastatic ocular melanoma who experienced a response to treatment with the BRAF inhibitor vemurafenib. BMC Cancer. 2016;16:634.

[52] Weber JL, Smalley KS, Sondak VK, Gibney GT. Conjunctival melanomas harbor BRAF and NRAS mutations--Letter. Clin Cancer Res. 2013;19:6329-6330.

[53] Handy DE, Castro R, Loscalzo J. Epigenetic modifications: basic mechanisms and role in cardiovascular disease. Circulation. 2011;123:2145-2156.

[54] Ciferri C, Lander GC, Maiolica A, Herzog F, Aebersold R, Nogales E. Molecular architecture of human polycomb repressive compex 2. eLife. 2012;1:e00005. doi: 10.7554/eLife.00005.

[55] Riquelme E, Behrens C, Lin HY, Simon G, Papadimitrakopoulou V, Izzo J, Moran C, Kalhor N, Lee JJ, Minna JD, Wistuba II. Modulation of EZH2 expression by MEK-ERK or PI3K-AKT signaling in lung cancer is dictated by different KRAS oncogene mutations. Cancer Res. 2016;76:675-685.

[56] Morin RD, Johnson NA, Severson TM, et al. Somatic mutations altering EZH2 (Tyr641) in follicular and diffuse large B-cell lymphomas of germinal-center origin. Nat Genet. 2010; 42:181–185.

[57] Tiffen J, Gallagher SJ, Hersey P. EZH2: an emerging role in melanoma biology and strategies for targeted therapy. Pigment Cell Melanoma Res. 2015;28:21-30.

[58] Bachmann IM, Halvorsen OJ, Collett K, Stefansson IM, Straume O, Haukaas SA, Salvesen HB, Otte AP, Akslen LA. EZH2 expression is associated with high proliferation rate and aggressive tumor subgroups in cutaneous melanoma and cancers of the endometrium, prostate, and breast. J Clin Oncol. 2006;24:268-273.

[59] Kim KH, Roberts CW. Targeting EZH2 in cancer. Nat Med. 2016;22:128-134.

[60] Becker JC, Terheyden P, Kämpgen E, Wagner S, Neumann C, Schadendorf D, Steinmann A, Wittenberg G, Lieb W, Bröcker EB. Treatment of disseminated ocular melanoma with sequential fotemustine, interferon alpha, and interleukin 2. Br J Cancer. 2002;87:840-845.

[61] Weber JS, D'Angelo SP, Minor D, et al. Nivolumab versus chemotherapy in patients with advanced melanoma who progressed after anti-CTLA-4 treatment (CheckMate 037): a randomised, controlled, open-label, phase 3 trial. Lancet Oncol. 2015;16:375-384.

[62] Mahoney KM, Freeman GJ, McDermott DF. The next immune checkpoint inhibitors: PD-1/PD-L1 blockade in melanoma. Clinical Ther. 2015;37:765-782.

[63] Ford J, Thuro BA, Thakar S, Hwu WJ, Richani K, Esmaeli B. Immune checkpoint inhibitors for treatment of metastatic melanoma of the orbit and ocular adnexa. Ophthal Plast Reconstr Surg. 2016. doi: 10.1097/IOP.0000000000000790.

[64] Speetjens FM, de Bruin EC, Morreau H, Zeestraten EC, Putter H, van Krieken JH, van Buren MM, van Velzen M, Dekker-Ensink NG, van de Velde CJ, Kuppen PJ. Clinical impact of HLA class I expression in rectal cancer. Cancer Immunol Immunother. 2008;57:601-609.

[65] Ericsson C, Seregard S, Bartolazzi A, Levitskaya E, Ferrone S, Kiessling R, Larsson O. Association of HLA class I and class II antigen expression and mortality in uveal melanoma. Invest Ophthalmol Vis Sci. 2001;42:2153-2156.

[66] Jager MJ, Hurks HM, Levitskaya J, Kiessling R. HLA expression in uveal melanoma: there is no rule without some exception. Hum Immunol. 2002;63:444-451.

[67] Westekemper H, Karimi S, Süsskind D, Anastassiou G, Freistühler M, Meller D, Zeschnigk M, Steuhl KP, Bornfeld N, Schmid KW, Grabellus F. Expression of MCSP and PRAME in conjunctival melanoma. Br J Ophthalmol. 2010;94:1322-1327.

[68] Carreno BM, Magrini V, Becker-Hapak M, Kaabinejadian S, Hundal J, Petti AA, Ly A, Lie WR, Hildebrand WH, Mardis ER, Linette GP. Cancer immunotherapy. A dendritic cell

vaccine increases the breadth and diversity of melanoma neoantigen-specific T cells. Science. 2015;348:803-808.

[69] Garg AD, Coulie PG, Van den Eynde BJ, Agostinis P. Integrating next-generation dendritic cell vaccines into the current cancer immunotherapy landscape. Trends Immunol. 2017. doi: 10.1016/j.it.2017.05.006.

[70] Dunn J, Rao S. Epigenetics and immunotherapy: The current state of play. Mol Immunol. 2017;87:227-239.

Chapter 2

Targeting of the MAPK and AKT pathways in conjunctival melanoma shows potential synergy

Jinfeng Cao, Renier C. Heijkants, Aart G. Jochemsen, Mehmet Dogrusöz, Mark J. de Lange, Pieter A. van der Velden, Sjoerd H. van der Burg, Martine J. Jager, Robert M. Verdijk

Published: Oncotarget. 2016; 8: 58021-58036.

DOI: 10.18632/oncotarget.10770.

Abstract

Purpose. Conjunctival melanoma (CM) is a rare but lethal form of cancer. Similar to cutaneous melanoma, CM frequently carries activating mutations in *BRAF* and *NRAS*. We studied whether CM as well as conjunctival benign and premalignant melanocytic lesions express targets in the mitogen-activated protein kinase (MAPK) and AKT pathways, and whether specific inhibitors can suppress CM growth *in vitro*.

Methods. 131 conjunctival lesions obtained from 129 patients were collected. The presence of *BRAF* V600E mutation and expression of phosphorylated (p)-ERK and p-AKT were assessed by immunohistochemistry. We studied cell proliferation, phosphorylation, cell cycling and apoptosis in three CM cell lines using two BRAF inhibitors (Vemurafenib and Dabrafenib), a MEK inhibitor (MEK162) and an AKT inhibitor (MK2206).

Results. The *BRAF* V600E mutation was present in 19% of nevi and 26% of melanomas, but not in primary acquired melanosis (PAM). Nuclear and cytoplasmic p-ERK and p-AKT were expressed in all conjunctival lesions. Both BRAF inhibitors suppressed growth of both *BRAF* mutant CM cell lines, but only one induced cell death. MEK162 and MK2206 inhibited proliferation of CM cells in a dose-dependent manner, and the combination of these two drugs led to synergistic growth inhibition and cell death in all CM cell lines.

Conclusions. ERK and AKT are constitutively activated in conjunctival nevi, PAM and melanoma. While BRAF inhibitors prohibited cell growth, they were not always cytotoxic. Combining MEK and AKT inhibitors led to more growth inhibition and cell death in CM cells. The combination may benefit patients suffering from metastatic conjunctival melanoma.

Key words: conjunctival melanoma, MAPK, AKT, nevus, kinase inhibitor.

Introduction

Conjunctival melanoma (CM) is a rare malignant ocular surface tumor, arising from melanocytes in the conjunctiva. Although CM accounts for 5% of all ocular melanoma, over the past decades, an increase in occurrence has been reported from Finland [1], Sweden [2] and the United States [3]. CM has a high local recurrence rate after treatment [4, 5]. Surgical excision combined with adjuvant cryotherapy, brachytherapy, and/or topical chemotherapy helps to prevent local recurrences of primary CM [5, 6]. A melanoma-related death rate of up to 29% at 10 years has been reported [5, 7]. However, the current therapeutic strategies are limited with regard to metastases.

Most CM originate in primary acquired melanosis (PAM) with atypia, while a small proportion arises from a preexisting nevus or de novo [8, 9]. The term "PAM", created by Zimmerman [10], is used to describe the appearance of conjunctival pigmentation at some time after birth. PAM occurs with or without atypia: PAM without atypia consists of an increased amount of melanin pigment in the basal layer of the epithelium and/or melanocytic hyperplasia [11], and generally does not develop into melanoma. In contrast, PAM with atypia contains atypical melanocytic hyperplasia that can extend into the more superficial non-basal portion of the epithelium and/or contains epithelioid melanocytes [12]. Up to 71% of CM has been reported to arise from PAM with atypia, while only up to 17% of CM is associated with conjunctival nevi [5, 13].

CM shares more similarities with cutaneous melanoma than with intraocular uveal melanoma. Like cutaneous melanoma, CM frequently harbors a *BRAF* mutation [14-16], as opposed to *GNAQ/GNA11* mutations which are found in most cases of uveal melanoma. In a recent study, a *BRAF* V600E mutation was found in 29% of CM, and an *NRAS* mutation in 18% [17]. C-*KIT* mutations are seldom found in CM [18-20]. Mutant *BRAF* and *NRAS* are both known to activate the downstream kinases MEK1/2 and ERK1/2, thereby promoting tumor proliferation [21]. BRAF inhibitors (BRAFi), including Vemurafenib and Dabrafenib, can prolong survival of

metastatic cutaneous melanoma patients [22, 23]. In CM, Vemurafenib has been used to target metastases and a primary melanoma with opposite outcomes: the metastatic tumor progressed after 2 months of treatment while the primary tumor was controlled for 16 months [24, 25]. MEK inhibitor (MEKi) treatment is being tested in phase II and III clinical trials of metastatic cutaneous melanoma. Recently, it was found that the PI3K/AKT signaling pathway plays a major role in the initiation, progression, invasion, and drug resistance of cutaneous melanoma [26, 27]. Overactivity of PI3K/AKT pathway can be induced by loss of activity of PTEN or by activating mutations in oncogene *NRAS*. A number of clinical trials using PI3K or AKT inhibitors (AKTi) are ongoing in patients with BRAF wild type (WT), BRAFi-resistant and NRAS-mutant cutaneous melanoma, colon cancer and ovarian carcinoma [28].

To determine whether the above-mentioned inhibitors are of use in CM, we tested the effect of several potentially useful drugs on three CM cell lines, each of which has either a *BRAF* or *NRAS* mutation. We furthermore evaluated the phosphorylation of ERK and AKT in a substantial series of conjunctival nevi, PAM without atypia, PAM with atypia and primary CM tissues.

Results

Phosphorylation of ERK and AKT in conjunctival melanoma

We determined the presence of *BRAF* V600E mutation in 131 pigmented conjunctival lesions from 129 patients and analyzed the expression of phosphorylated (p)-ERK and p-AKT by immunohistochemistry (Table 1). We observed *BRAF* V600E mutation in 19% of nevi (n=51) and 26% of melanoma (n=42) (Figure 1G). No *BRAF* V600E mutation was seen in any case of PAM without atypia (n=20) or PAM with atypia (n=18). One of the *BRAF* mutated melanomas evolved from a background of PAM.

The presence of p-ERK and p-AKT was studied by immunohistochemistry. AKT activation is associated with phosphorylation of two residues: serine 473

Table 1. Frequency of positively-staining cells in an immunohistological analysis of BRAF V600E mutation, p-ERK and p-AKT, in conjunctival lesions.

	Nevi	**PAM without atypia**	**PAM with atypia**	**CM**	***P* value [c] (Nevi vs. CM)**
	***n*=51 (%)**	***n*=20 (%)**	***n*=18 (%)**	***n*=42 (%)**	
BRAF V600E mutation [a]					
Negative	30 (81)	17 (100)	13 (100)	29 (74)	0.48
Positive	7 (19)	0 (0)	0 (0)	10 (26)	
expression [b]					
Absent	27 (75)	12 (75)	8 (44)	26 (72)	0.79
Present	9 (25)	4 (25)	10 (56)	10 (28)	
P-ERK nuclear expression [b]					
Absent	29 (83)	13 (81)	8 (44)	28 (78)	0.59
Present	6 (17)	3 (19)	10 (56)	8 (22)	
P-AKT Ser473 cytoplasmic expression [b]					
Absent	31 (82)	10 (83)	7 (78)	29 (74)	0.41
Present	7 (18)	2 (17)	2 (22)	10 (26)	
P-AKT Ser473 nuclear expression [b]					
Absent	9 (24)	2 (17)	3 (33)	5 (13)	0.24
Present	29 (76)	10 (83)	6 (67)	33 (87)	
P-AKT Thr308 cytoplasmic expression [b]					
Absent	12 (33)	10 (91)	8 (80)	14 (37)	0.75
Present	24 (67)	1 (9)	2 (20)	24 (63)	
P-AKT Thr308 nuclear expression [b]					
Absent	22 (61)	5 (45)	7 (70)	26 (68)	0.51
Present	14 (39)	6 (55)	3 (30)	12 (32)	

[a] *BRAF* V600E mutation was scored as positive or negative.
[b] The phosphorylated protein expression was evaluated according to IRS scoring system, 0-1 was regarded as absent, and 2-12 was regarded as present.
[c] Pearson chi-square test was applied to compare nevi group versus CM group for indicated protein expression. All tests were two-sided, and *P* values of ≤0.05 were considered significant.

(Ser473) and threonine 308 (Thr308) [29]. Using the antibody p-AKT Ser473, most p-AKT staining was observed in nuclei (Figure 1n), while the p-AKT Thr308 antibody gave both nuclear and cytoplasmic staining (Figure 1m). In all 4 groups (nevi, PAM with and without atypia, and melanoma), expression of nuclear and cytoplasmic p-ERK and p-AKT was observed. P-ERK cytoplasmic staining was seen more frequently in PAM with atypia than in nevi ($P = 0.027$) or CM ($P = 0.046$). Similarly, p-ERK nuclear expression was seen more often in PAM with atypia than in nevi ($P = 0.004$), PAM without atypia ($P = 0.028$) or CM ($P = 0.014$). In groups of nevi and CM, neither cytoplasmic nor nuclear expression was associated with the presence of a *BRAF* mutation.

Molecular effects of Vemurafenib, Dabrafenib, MEK162 and MK2206

Western blot analysis was performed to determine the baseline protein levels of BRAF, p-ERK, ERK, p-AKT and AKT in two *BRAF*-mutant CM cell lines CRMM1 and CM2005.1 and the *NRAS*-mutant cell line CRMM2 (Figure 2A). BRAF is expressed in all three cell lines, with the highest level observed in CRMM1.

To determine whether the responses to drugs are pathway specific, we treated different cell lines with BRAFi (Vemurafenib, Dabrafenib), MEKi (MEK162) or AKTi (MK2206) for 24 hours and analyzed the effects on p-ERK and p-AKT levels by western blotting (Table 2). In CRMM1 (Figure 2B), the lowest dose of Vemurafenib (0.4 μM) and Dabrafenib (0.005 μM) already inhibited p-ERK. In contrast, in CM2005.1 (Figure 2D), increasing dosages of Vemurafenib and Dabrafenib decreased p-ERK gradually, while total ERK levels were not suppressed. However, p-ERK expression was increased after BRAFi treatment of the *BRAF* WT CRMM2 cells (Figure 2C). This phenomenon is similar to what has been observed in *BRAF* WT cutaneous melanoma cell lines [30]. The effects on p-ERK levels, combined with cell viability data, indicate that the MAPK pathway plays an important role in growth of CM cell lines. In CRMM1 and CM2005.1, p-AKT was slightly attenuated after BRAFi and MEKi treatment without influencing total AKT, which might be an indirect effect due to the growth inhibition caused by these drugs.

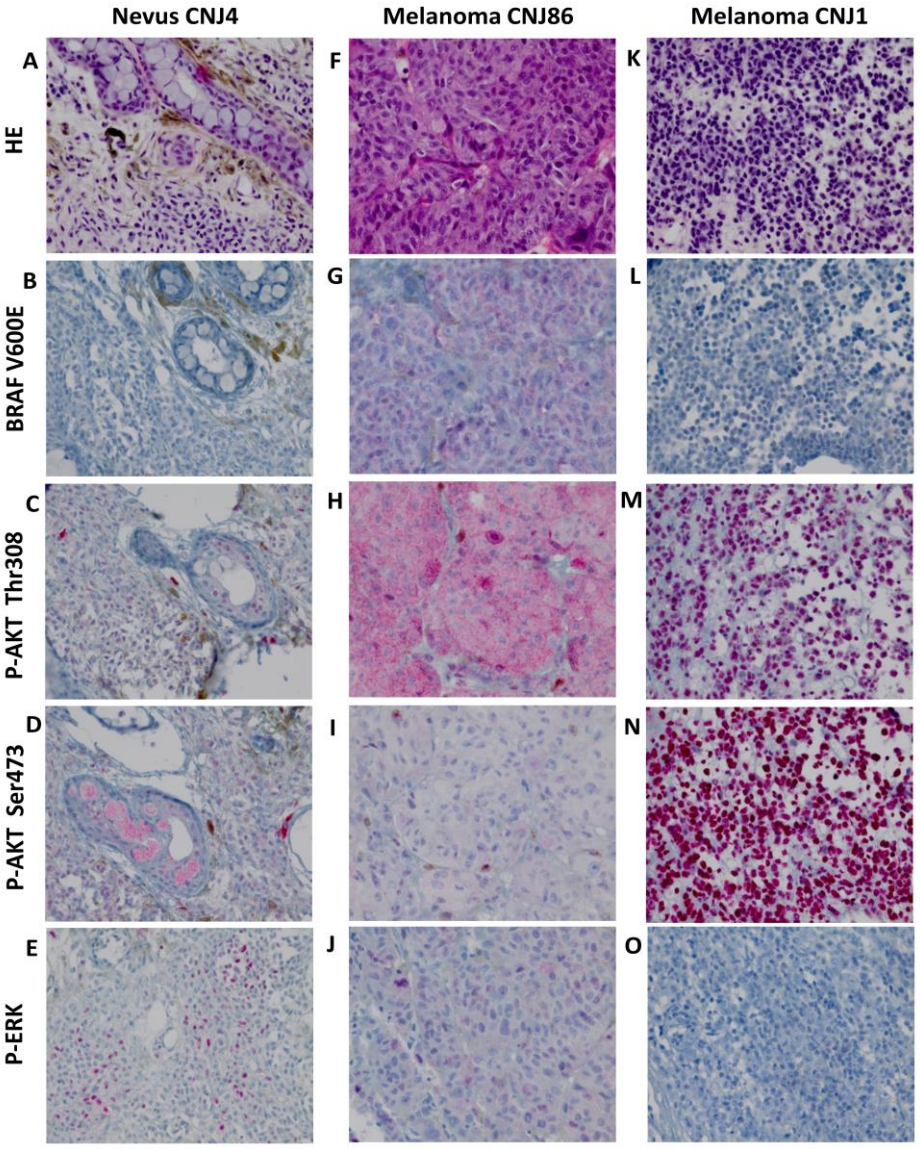

Figure 1. HE staining, BRAF V600E expression and phosphorylation of ERK and AKT in CM. A-E. nevus, **F-J.** BRAF V600E mutated melanoma, **K-O**. BRAF V600E negative melanoma. HE staining (A, F, K). Positive staining for p-AKT Thr308, p-AKT Ser473 and p-ERK occurred in a cytoplasmic (H, I) and nuclear (C, M, N) fashion and in combination (D, E, J). Negative staining (B, L, O). Staining patterns for these proteins did not correlate with malignant progression. All images were taken at the magnification of ×400.

In CRMM2, p-AKT was upregulated by BRAFi, but downregulated by MEKi. Low concentrations of MK2206 (CRMM1 0.5 μM, CRMM2 2μM and CM2005.1 4μM) reduced the level of p-AKT, but higher concentrations were needed to suppress cell growth (Figure 3). To investigate whether the AKT pathway was effectively inhibited by MK2206, we determined the p-PRAS40 level, since PRAS40 is a direct downstream target molecule of AKT. As shown in Figure 3E, levels of p-PRAS40 were strongly reduced in all three cell lines upon MK2206 treatment at relative low concentrations, indicating that AKT activity was decreased by MK2206; however, this inhibition was not sufficient to decrease the cell growth of CRMM2 and CM2005.1.

Table 2. Summary of drugs effects on cell proliferation and protein expression in vitro.

	CRMM1	**CRMM2**	**CM2005.1**
Mutations [a]			
BRAF V600E	+	-	+
NRAS Q61L	-	+	-
Inhibitiont of cell proliferation [b]			
BRAFi			
Vemurafenib	+	-	+
Dabrafenib	+	-	+
MEKi			
MEK162	+	+	+
AKTi			
MK2206	+	+	+
Drug effect on phosphorylated protein expression [c]			
Vemurafenib	p-ERK↓	p-ERK↑	p-ERK↓
Dabrafenib	p-ERK↓	p-ERK↑	p-ERK↓
MEK162	p-ERK↓	p-ERK↓	p-ERK↓
MK2206	p-AKT↓	p-AKT↓	p-AKT↓

[a] "+" means mutant, and "-" indicates wild type.

[b] "+" shows cell proliferation was inhibited, while "-" demonstrates cell viability was not influenced.

[c] "↑" represents phosphorylation of proteins was increased, while "↓" implies phosphorylation of proteins was decreased.

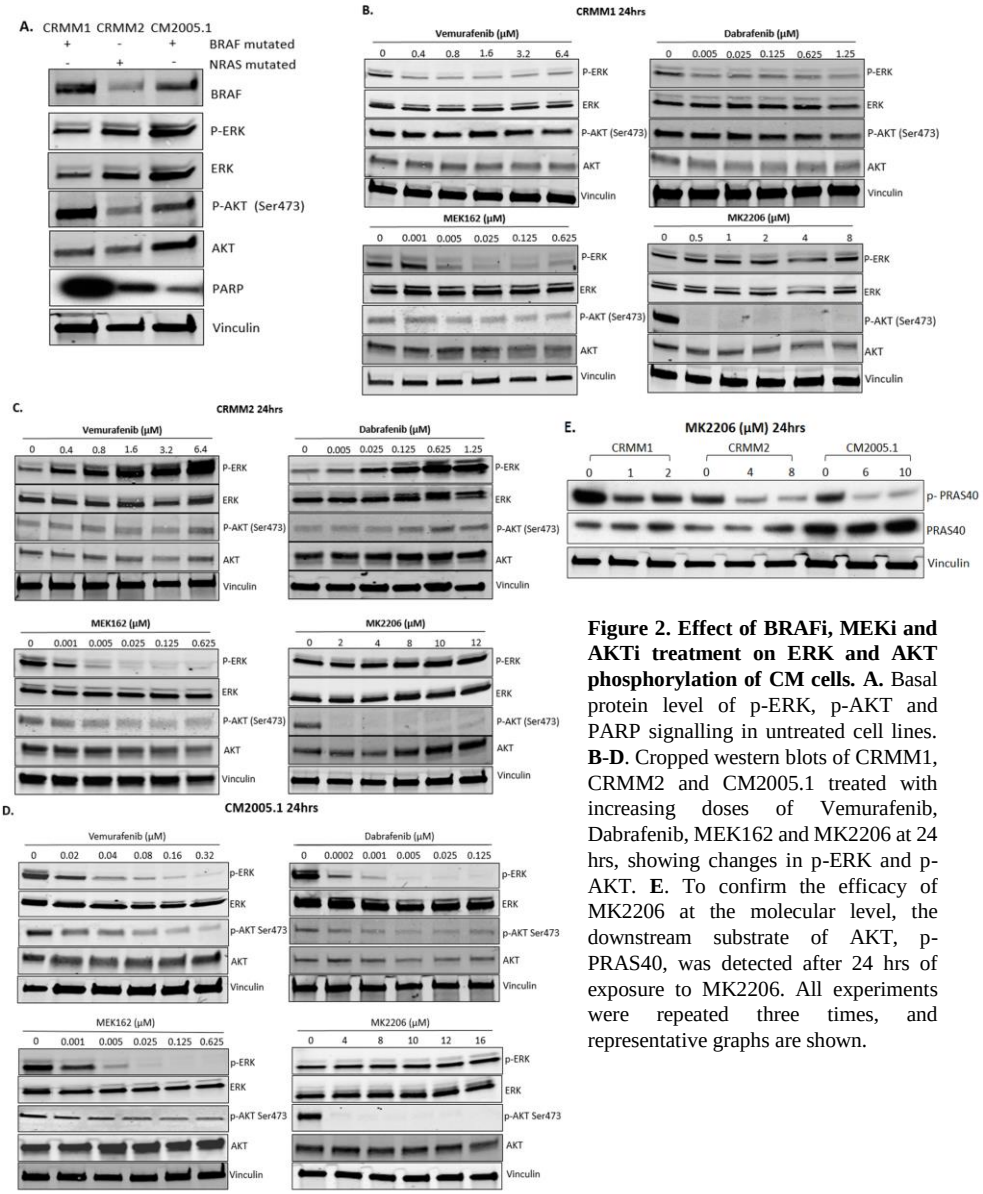

Figure 2. Effect of BRAFi, MEKi and AKTi treatment on ERK and AKT phosphorylation of CM cells. A. Basal protein level of p-ERK, p-AKT and PARP signalling in untreated cell lines. **B-D**. Cropped western blots of CRMM1, CRMM2 and CM2005.1 treated with increasing doses of Vemurafenib, Dabrafenib, MEK162 and MK2206 at 24 hrs, showing changes in p-ERK and p-AKT. **E**. To confirm the efficacy of MK2206 at the molecular level, the downstream substrate of AKT, p-PRAS40, was detected after 24 hrs of exposure to MK2206. All experiments were repeated three times, and representative graphs are shown.

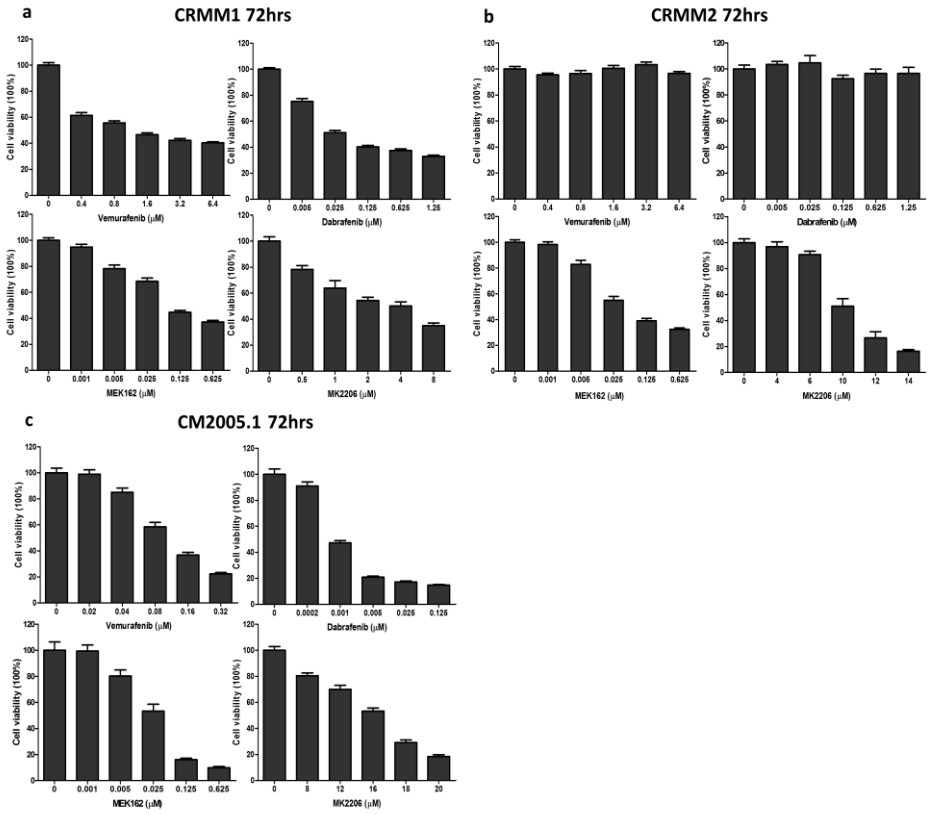

Figure 3. Cell viability assessed by In-cell western assay. a-c. CRMM1, CRMM2 and CM2005.1 were counted and seeded, and drugs were added one day later at indicated concentrations. Cell viability was measured after 72hrs. All experiments were repeated three times, and the representative data were expressed as mean ± standard error of the mean (SEM).

In vitro activity of BRAF, MEK and AKT inhibitors in CM cell lines

Cells were treated with each drug at 5 different concentrations and survival was determined 72 hours later (Figure 3). As shown in Figure 3, Vemurafenib and Dabrafenib inhibited the growth of the *BRAF*-mutant cell lines CRMM1 and CM2005.1, but not of the *NRAS*-mutant cell line CRMM2. MEK162 and MK2206 inhibited growth of all CM cell lines in a dose-dependent manner, although only high concentrations of MK2206 were able to suppress the proliferation of CRMM2

and CM2005.1. Table 3 summarizes the IC_{50} values of each agent for the three CM cell lines. Although CRMM1 and CM2005.1 both harbor the *BRAF* V600E mutation, their sensitivity to BRAFi differed very much. No indications for *PTEN* loss of function were found in the *BRAF* V600E mutated cell lines that could explain this difference. However, we did find a deletion in exon 2 of *PTEN* in the *NRAS* mutant cell line CRMM2.

Table 3. The sensitivity of conjunctival melanoma cell lines to Vemurafenib, Dabrafenib, MEK162 and MK2206.

Cell line	Mutation	Vemurafenib (μM)	Dabrafenib (μM)	MEK162 (μM)	MK2206 (μM)
CRMM1	*BRAF* V600E	0.99±0.07	0.10±0.01	0.09±0.02	4.90±1.25
CRMM2	*NRAS* Q61L	>6.4	>1.25	0.05±0.01	9.67±0.91
CM2005.1	*BRAF* V600E	0.10±0.01	0.003±0.001	0.03±0.01	16.4±1.61

Cells were exposed to the single agent for 72 hrs to assess the cell viability. And the dose-response IC_{50} values were calculated using Compusyn software. Data were presented as the mean ± SD from at least 3 independent experiments.

G1 arrest and apoptosis after exposure to single drug treatment

To obtain more insight into the effects of kinase inhibitors on cell growth and survival, we investigated their impact on cell cycle profiles using flow cytometry (Figure 4 A-C). Treatment with 4 different kinase inhibitors of cell line CRMM1 resulted in strong G1 arrest. MEK162 and MK2206 increased the sub-G1 fraction, indicating that these two drugs were able to induce cell death. As expected, BRAFi did not induce any cell cycle change in CRMM2. Both MEK162 and MK2206 treatment led to G1 arrest, a modest increase in the sub-G1 fraction and a reduced number of S-phase cells (Supplementary Figure 2), although the effect of MK2206 was not very strong. In CM2005.1, G1 arrest and depletion of S-phase cells were found after all drug treatments, although MK2206 treatment did not result in a reduced G2/M phase. Some increase in sub-G1 cells was detected upon all treatments, although it was very modest after MK2206 treatment.

Poly (ADP-ribose) polymerase (PARP) cleavage is often associated with apoptotic cell death and has served as a marker for apoptosis and caspase activity [31]. CRMM1 showed high baseline level of PARP (Figure 2A), while CRMM2 and CM2005.1 showed modest and low PARP expression, respectively. Figure 4D shows that at the indicated concentrations, Vemurafenib and Dabrafenib promoted PARP cleavage in CM2005.1, but not in CRMM1 and CRMM2. MEK162 induced some cleaved PARP in cell line CM2005.1, while PARP cleavage was weak in CRMM1 and CRMM2. MK2206 treatment led to low PARP cleavage in all cell lines.

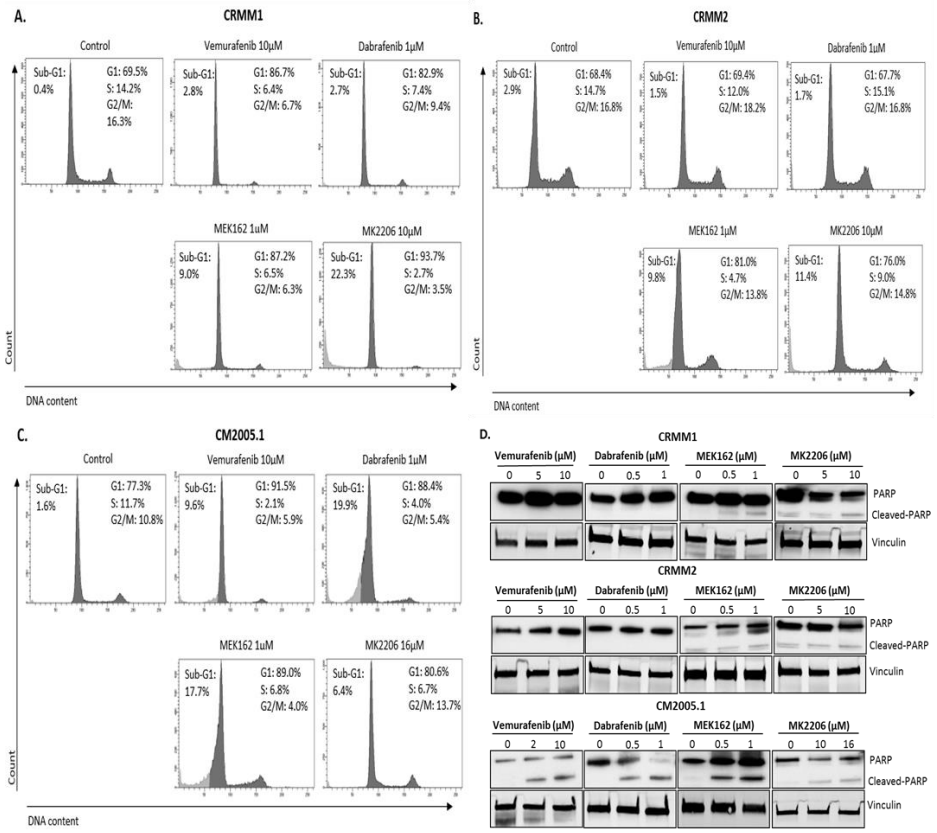

Figure 4. BRAFi, MEKi and AKTi induce cell cycle alteration and apoptosis. A-C. Representative flow cytometry analysis 72hrs post treatment as indicated. **D**. Cropped western blots of PARP cleavage in cell lines treated with inhibitors at 72hrs.

Synergistic growth inhibition and cell cycle arrest by combining MEK162 with MK2206

Treatment of MEKi combined with AKTi has been used to treat *BRAF*-mutant, *BRAF*-WT and *NRAS*-mutant cutaneous melanoma patients [28] . We tested whether combining a MEK and AKT inhibitor would be effective in CM cell lines. We treated CRMM1, CRMM2 and CM2005.1 with varied concentrations of MEK162, MK2206 or the combination of MEK162 and MK2206 for 72 hours, and evaluated cell growth. Synergy studies were performed using the method of Chou [32]. Figure 5 shows that MEK162 and MK2206 were synergistic in all cell lines, with synergy confirmed by CI values. These results suggest that at low concentrations, the two drugs may be used clinically to inhibit cell growth effectively.

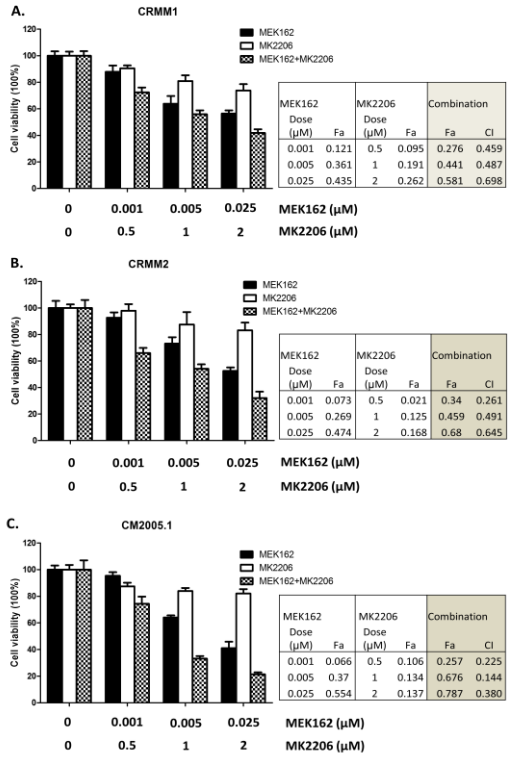

MEK162 Dose (μM)	MEK162 Fa	MK2206 Dose (μM)	MK2206 Fa	Combination Fa	Combination CI
0.001	0.121	0.5	0.095	0.276	0.459
0.005	0.361	1	0.191	0.441	0.487
0.025	0.435	2	0.262	0.581	0.698

MEK162 Dose (μM)	MEK162 Fa	MK2206 Dose (μM)	MK2206 Fa	Combination Fa	Combination CI
0.001	0.073	0.5	0.021	0.34	0.261
0.005	0.269	1	0.125	0.459	0.491
0.025	0.474	2	0.168	0.68	0.645

MEK162 Dose (μM)	MEK162 Fa	MK2206 Dose (μM)	MK2206 Fa	Combination Fa	Combination CI
0.001	0.066	0.5	0.106	0.257	0.225
0.005	0.37	1	0.134	0.676	0.144
0.025	0.554	2	0.137	0.787	0.380

Figure 5. Synergistic growth inhibition using the combination of MEK162 and MK2206. Mono or combination treatments were performed on CRMM1 **A**., CRMM2 **A**. and CM2005.1 **C**. using MEK162 and MK2206 with indicated concentrations. Cell proliferation was measured after 72hrs treatment, and the effects of drug as fraction of untreated control cells were calculated. The combination index (CI), reflecting the extent of synergy or antagonism for two drugs, was obtained for each drug combination. CI<0.9, synergy; 0.9<CI<1.1, additive effect; CI>1.1, antagonism. The experiments were performed three times and representative data were expressed as mean ± SEM.

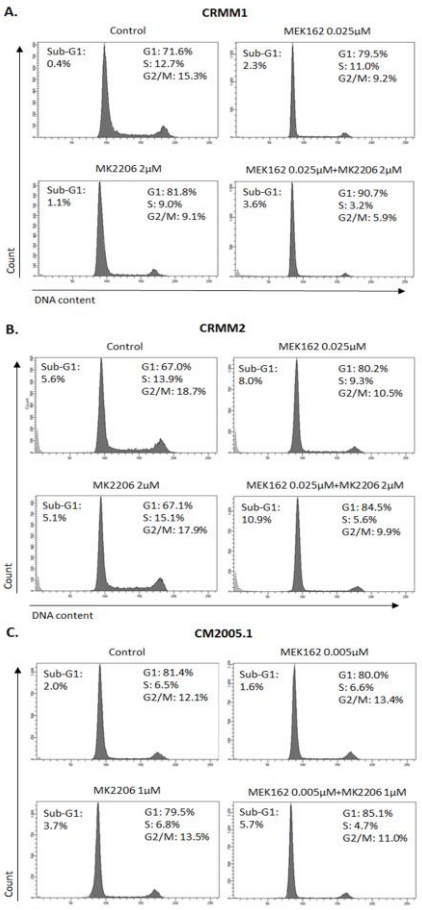

Figure 6. Enhanced G1 arrest induced by MEK162 combined with MK2206 at low concentrations. Single or combination treatments were performed in CRMM1 **A**. and CRMM2 **B**. using 0.025µM MEK162 and 2µM MK2206 and in CM2005.1 **C**. using 0.005µM MEK162 and 1µM MK2206. Flow cytometry was analyzed after 72hrs of treatment.

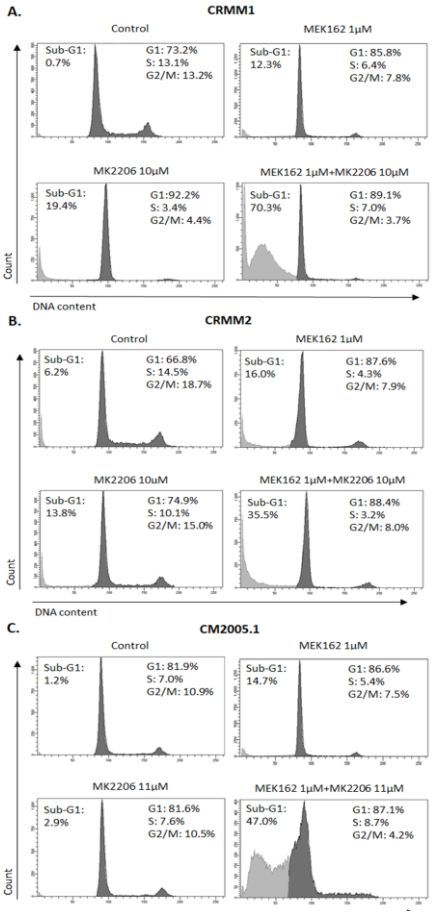

Figure 7. Increased sub-G1 fractions induced by MEK162 combined with MK2206 at high concentrations. Mono or combination treatments were performed in CRMM1 **A**. and CRMM2 **B**. using 1µM MEK162 and 10µM MK2206 and in CM2005.1 **C**. using 11µM MEK162 and 1µM MK2206. Flow cytometry was studied after 72hrs of treatment.

To investigate whether combination treatments would inhibit cell cycle progression and induce more cell death than single treatments, we performed flow cytometry. In all cell lines, the combination of MEK162 and MK2206 at low concentrations caused slightly stronger G1 arrest and depletion of S-phase compared

to single treatments (Figure 6). The combination of high concentrations induced stronger sub-G1 fractions than single agents (Figure 7).

Discussion

Uveal melanomas, in contrast to conjunctival melanomas, lack *BRAF* or *NRAS* mutations but frequently have mutations in *GNAQ*, *GNA11*, *BAP1*, *SF3B1* or *EIF1AX* [33]. To date, the reports describing the impact of kinase pathways in conjunctival melanoma are limited. Our results show that MAPK and AKT-signaling pathways are activated in both benign, premalignant and malignant conjunctival melanocytic lesions. In our series, *BRAF* V600E mutations occur in 19% of nevi and 26% of CM, but not in PAM, which confirms previous results [16]. Likewise, *BRAF* V600E mutations have been described to be less frequent in lentigo maligna lesions of the skin which show a comparable lentiginous histopathology as PAM [34]. Furthermore, similar to the findings in melanocytic nevi and cutaneous melanoma [35, 36], we report that *BRAF* mutations do not determine the tumor's ERK phosphorylation status. It is unlikely that technical problems such as tissue fixation and the high temperature used for antigen retrieval impaired the staining of p-ERK, because positive p-ERK cells were abundant in positive control tissues (data not shown). Recently, loss of function mutations in NF1 have been described in a high percentage of cutaneous melanoma. NF1 suppression can lead to increased RAS activation in melanoma, which may explain the lack of correlation between ERK phosphorylation and BRAF mutational status [37, 38].

Although p-ERK and p-AKT are regarded as being predominantly situated in the cytoplasm, the phosphorylation of ERK and AKT in the nucleus is essential for nuclear translocation and activation of transcription factors [39, 40]; we therefore scored the staining in nuclei as well as in the cytoplasm. Our data show that, in general, p-ERK and p-AKT are indeed expressed in both nuclei and cytoplasm among all diagnostic groups of conjunctival melanocytic lesions, although with

variable percentages. These results indicate that MAPK and PI3K/AKT pathways are both potential targets for pharmacologic therapies in CM.

To investigate the effect of different drugs on cell proliferation and cell death, we tested BRAF, MEK and AKT inhibitors on three CM cell lines. Vemurafenib and Dabrafenib are selective BRAF inhibitors, and have been approved by the FDA as single agents for treatment of metastatic cutaneous melanoma. MEK162 and MK2206 target MEK and AKT respectively. Although CRMM1 and CM2005.1 both harbor a *BRAF* V600E mutation, their sensitivity to BRAFi differed greatly: CRMM1 required a much higher dose of Dabrafenib to inhibit cell growth compared to CM2005.1. This could not be explained by loss of function in *PTEN*. Additionally, we demonstrate that BRAFi induced apoptosis of CM2005.1 cells. The cell cycle analysis indicates that BRAFi inhibited cell growth of CRMM1 by inducing a G1 arrest. In contrast, Vemurafenib and Dabrafenib did not inhibit cell proliferation of CRMM2, and they led to an increased p-ERK expression. This finding is in agreement with other preclinical studies in other malignancies, in which selective BRAFi stimulated cell growth and ERK phosphorylation in *BRAF* WT and *NRAS* mutant cutaneous melanoma cell lines [41-43]. The mechanism of the detrimental effects is through paradoxical-activation of RAS and receptor tyrosine kinases, which subsequently cause MAPK pathway hyperactivation through CRAF [44].

MEK162 inhibits the downstream RAS/RAF pathway target MEK, thereby decreasing p-ERK levels and suppressing cell growth. We did not find other studies that have treated CM cells with this novel drug. Proliferation of all three cell lines was inhibited through downregulation of p-ERK upon MEK162 treatment. Furthermore, the data of cell cycle profiles and PARP cleavage show that in addition to cytostatic effects, MEK162 alone can prompt apoptosis, regardless of *BRAF* or *NRAS* mutations. Importantly, IC_{50} values for cell cultures are much lower than known plasma levels of MEK162 in patients (0.6-1μM). However, similar to BRAFi, the disadvantage is that constitutive activation of the MAPK pathway can frequently lead to cross-talk with other signal transduction pathways, enabling melanoma cells

to escape from MEK inhibition [45]. Current MEKi have more clinical side effects than Vemurafenib and Dabrafenib.

The PI3K/AKT signal transduction pathway is considered a potential co-target for *BRAF* and *NRAS* mutant cutaneous melanoma [22]. To the best of our knowledge, we are the first to attempt AKT inhibition in CM *in vitro*. Our results show that MK2206 inhibited proliferation in all CM cell lines, but at variable doses, and independent of their effect on p-AKT and p-PRAS40, indicating that the growth inhibitory effect induced by MK2206 is not specific or at least partly caused by off-target effects.

With the clinical availability of PI3K, AKT and mTOR inhibitors, a number of trials are now ongoing in cutaneous melanoma. Our studies show that combining MEK162 with MK2206 has a synergistic inhibitory effect on proliferation of three CM cell lines, regardless of their sensitivity to the individual agents. Mutations in the G-α-proteins *GNAQ* and *GNA11* that occur in 91% of uveal melanoma also activate MAPK and PI3K/AKT pathways, which implies that the combination of MEK and AKT inhibitors may also be profitable for this patient group. Future studies on cutaneous and uveal melanoma cell lines are therefore warranted to evaluate the efficacy of combination treatment of MEK and AKT inhibitors. In clinical treatment, one may argue that multi-signal pathway blockades generate more side effects than individual kinase inhibitor. On the other hand, we have shown that combined treatment could be effective at considerably lower drug dosages and potentially ameliorate detrimental side effects.

In summary, our data suggest that the ERK and AKT are constitutively activated in all conjunctival melanocytic lesions. Our *in vitro* study shows some growth inhibition and cytotoxic effect of kinase inhibitors and provides a rationale for the clinical application of these compounds in CM. Our results indicate that co-inhibition of the MAPK and AKT pathways may improve their efficacy. Clinical studies are now indicated to test the efficacy of MAPK and AKT inhibitors in metastatic CM.

Materials and Methods

Patients and samples

Paraffin-embedded tissue specimens were retrieved from the archive of the Department of Pathology of the Erasmus University Medical Center from patients with a conjunctival melanocytic lesion diagnosed between 1987 and 2013. The Institutional Review Board of the Erasmus University Medical Center waived the need for approval because of the retrospective and non-interventional character of the study. The study adhered to the tenets of the Declaration of Helsinki. Two hundred and seventy-eight samples obtained from 131 conjunctival lesions of 129 patients contained enough material for the study. In our patient cohort, CM were derived from PAM (59.5%, *n*=25), de novo (28.6%, *n*=12) and nevi (11.9%, *n*=5). All melanomas described were invasive. The metastatic rate was 21.4% (*n*=9). Out of 18 PAM with atypia, 8 had severe atypia and 10 moderate atypia. No cases with minor atypia were included. The diagnosis was reviewed and the original slides were assessed according to the AJCC criteria. Because of the high recurrence rate, some patients underwent multiple surgeries.

Construction of Tissue Microarray (TMA) Samples

Carefully selected cores of 1 mm in diameter were taken from paraffin-embedded conjunctival tumor samples and assembled in a grid pattern into seven tissue microarrays. Positive control samples consisted of brain, liver, tonsil, heart, lung, gut and skin. The 4-μm sections were cut from TMA and were stained with hematoxylin and eosin (HE), and anti-Melan A to confirm the presence of the expected tissue histology within each tissue core. Additional sections were cut for further immunohistochemical analysis.

Immunohistochemistry (IHC)

We assessed the expression of p-ERK, p-AKT Ser473, p-AKT Thr 308 and BRAF V600E. Immunohistochemistry was performed with an automated staining system (Ventana BenchMark ULTRA, Ventana Medical Systems Inc., Tucson, AZ, USA)

using the alkaline-phosphatase method for all antibodies and a red chromogen. Briefly, following deparaffinization and heat-induced antigen retrieval for 60 minutes, the tissue sections were incubated with primary antibody anti-MAP kinase diphosphorylated ERK 1/2 (1:1000; M8159, Sigma-Aldrich, St. Louis, MO, USA), p-AKT Ser473 (sc-135651; 1:25, Santa Cruz Biotechnology; Dallas, TX, USA), p-AKT Thr 308 (sc-135650, 1:50, Santa Cruz Biotechnology), BRAF-V600E (26039,1:50, NewEast Biosciences, Malvern, PA, USA) or Melan A (clone A103, Ventana) for 1 hour at 36°C. A subsequent amplification step was followed by incubation with hematoxylin II counter stain for 8 minutes and then bluing reagent for 8 minutes according to the manufacturer's instructions (Ventana). The immunostained TMAs were analyzed with light microscopy (Leica DM 300, Leica, Eindhoven, the Netherlands) by two different observers at different time points. The samples were scored using the immunoreactive scoring (IRS) method, described by Remmele and Stegner [46]. The IRS evaluates the staining intensity and the proportion of positive cells, which results in two scores: an intensity score (IS) and a proportion score (PS). The value of the IS varies from 0 to 3 points and the value of the PS varies from 0 to 4 points. Multiplying these scores yields the IRS (0 - 12 points). The representative pictures of staining were taken with an Olympus DP25 camera, and acquired by Olympus CellSens Entry 1.9 software.

The immunohistochemical markers stained the cytoplasm of the melanocytes. Some markers also stained the nucleus. For these markers, the staining of the cytoplasm and nucleus were analyzed and scored separately.

Reagents

Vemurafenib (PLX4032, S1267), Dabrafenib (GSK2118436, S2807), MEK162 (ARRY-162, S7007) and MK2206 (S1078) were purchased from Selleck Chemicals (Huissen, The Netherlands). All drugs were dissolved in dimethyl sulfoxide (DMSO) to reach a stock concentration of 10 mM. For *in vitro* tests, the stock solution was diluted in the indicated fresh medium.

Cell lines and cell culture

CM cell lines CRMM1 and CRMM2 were established by G. Nareyeck, Essen, Germany [47], and kindly provided by M. Madigan, Sydney, Australia. The cells were cultured in F-12K nutrient mixture, Kaighn's modification (Gibco, Life Technologies, The Netherlands), with added heat-inactivated 10% fetal bovine serum (FBS, Greiner Bio-one, The Netherlands) and 1% Penicillin/Streptomycin (Gibco). CM2005.1 was created by S. Keijser, LUMC, Leiden, The Netherlands [48]. These cells were grown in RPMI 1640 Dutch modified media (Gibco) supplemented with 10% FBS (Greiner Bio-one), 1% GlutaMAX and 1% Penicillin/Streptomycin (Gibco). Our previous studies [49, 50] have shown that CRMM1 and CM2005.1 harbor a *BRAF* V600E mutation, and CRMM2 contains an *NRAS* Q61L mutation. These mutations were confirmed at Erasmus University Medical Center, Rotterdam in May 2016 by next generation sequencing (NGS). Inactivating molecular changes in *PTEN* were tested by NGS as described before [51].

Cell line authentication

Short tandem repeat analysis was performed using the AmpFLSTR® Identifiler™ PCR Amplification Kit (Life Technologies, UK) based on the procedure recommended by *The International Cell Line Authentication Committee* (ICLAC) in Baseclear (Baseclear, Leiden, The Netherlands) in April, 2014, setting the standard for these three cell lines [50]. They were confirmed at Erasmus University Medical Center, Rotterdam in October 2014.

Immunoblotting

Cells were lysed in M-PER Mammalian Protein Extraction Reagent (78501, Thermo Scientific, OH, USA), supplemented with protease and phosphatase inhibitors (78415 and 78420, Thermo Scientific). Proteins (15-25 µg total protein lysates) were separated on Mini-PROTEAN TGX Precast Gels (4-15%, Bio-Rad) using the Mini-PROTEAN Tetra system (Bio-Rad, Hercules, CA). Proteins were blotted onto polyvinylidene difluoride (PVDF) membranes (Immobilon-P, Millipore, Billerica,

MA, USA) using the Trans-Blot Turbo System (Bio-Rad). Subsequently, the membranes were incubated with the appropriate primary antibodies and IRdye-680 or IRdye-800 dyes (LI-COR), and analyzed with the Odyssey Infrared Imaging System (LI-COR). Signal intensity was analyzed with Odyssey 3.0 software. Alternatively, membranes were incubated with HRP-conjugated secondary antibodies, and the bands were visualized by chemoluminescence (West Dura, Pierce Biotechnology, Rockford, IL, USA) and exposed to X-ray films (Fuji Super RX, Japan). Antibodies are listed below: BRAF (1:1000; ab33899, Abcam, Cambridge, UK); anti-MAP kinase diphosphorylated ERK 1/2 (1:1000; M8159, Sigma-Aldrich); p44/42 MAPK (ERK1/2) (1:1000; 4695, Cell Signaling Technology (CST) , Leiden, The Netherlands); p-AKT (Ser473) (1:1000; 4060, CST); AKT (pan) (1:2000; 2920, CST); PARP (1:1000; 9542, CST); p-PRAS40 (Thr246) (1:1000; 2640, CST) , PRAS40 (1:1000; 2610, CST) and Vinculin (1:1000; V9131, Sigma-Aldrich).

Cell proliferation assay

Cells were seeded in triplicate in 96-well plates at a density of 2500 (CRMM1 and CRMM2) or 5000 (CM2005.1) cells per well, in a total volume of 100 µl medium. The next day, the media were refreshed and cells were treated with drugs at various concentrations. Cell survival was determined 72 hours later by an In-cell western assay (Supplementary Figure 1): after removing the medium, the cells were fixed in 4% formaldehyde and incubated with DRAQ5, a far-red fluorescent DNA dye (1:8000, DR50050, Biostatus Ltd.,UK) for 1 hour. After washing with 0.1% Tween-PBS (phosphate-biffered saline) buffer, the plates were scanned with an Odyssey Infrared Imaging System (LI-COR, Leusden, The Netherlands). Odyssey 3.0 software was used to quantify the signal intensity. IC_{50} values were calculated on the basis of the growth inhibition curves and determined with CompuSyn software [32]. For synergy studies, drug effects were evaluated as “affected fraction” of treated versus untreated cells [52]. Dose-effect analyzes and Combination Index (CI) were calculated using CompuSyn. CI reflects the extent of synergy or antagonism for two drugs: $CI<0.9$, synergy; $0.9<CI<1.1$, additive effect; $CI>1.1$, antagonism.

Flow cytometry

Cells were harvested, washed in PBS and fixed in ice-cold 70% ethanol and stored at -20°C. Subsequently, cells were washed with 2%FBS/PBS and suspended in 2%FBS/PBS containing 50 μg/ml propidium iodide (PI) and 50 μg/ml RNase. Flow cytometry was performed in the BD LSR II system (BD Biosciences, Sparks, MD, USA) and the data were analyzed with FACSDiva software (BD).

Statistical analysis

Statistical analyses were performed with SPSS version 22.0 software (SPSS, Inc., Chicago, IL, USA). The Pearson chi-square test was used to compare the protein expression *in vivo*. Two-tailed *P* values equal to or below 0.05 were considered to be statistically significant. The plots of cell proliferation and cell cycle profiles were drawn with GraphPad Prism 5 software (La Jolla, CA, USA).

Acknowledgements

We thank Kiran Baran, MSc. for technical assistance. We thank the Rotterdam Ocular Melanoma Study group for sharing the patient tissue specimens for the immunohistochemical study.

Conflict of interests

The authors declare no conflict of interest.

Grant support

This work was supported partly by grants from the China Scholarship Council, the Dutch Cancer Society (UL 2013-5757) and the Stichting Nederlands Oogheelkundig Onderzoek (SNOO2012-13).

References

[1] Tuomaala S, Eskelin S, Tarkkanen A,Kivela T. Population-based assessment of clinical characteristics predicting outcome of conjunctival melanoma in whites. Invest Ophthalmol Vis Sci. 2002; 43:3399-3408.

[2] Triay E, Bergman L, Nilsson B, All-Ericsson C, Seregard S. Time trends in the incidence of conjunctival melanoma in Sweden. Br J Ophthalmol. 2009; 93:1524-1528.

[3] Yu GP, Hu DN, McCormick S, Finger PT. Conjunctival melanoma: is it increasing in the United States? Am J Ophthalmol. 2003; 135:800-806.

[4] Shields CL, Shields JA, Gunduz K, Cater J, Mercado GV, Gross N, Lally B. Conjunctival melanoma: risk factors for recurrence, exenteration, metastasis, and death in 150 consecutive patients. Arch Ophthalmol. 2000; 118:1497-1507.

[5] Missotten GS, Keijser S, De Keizer RJ, De Wolff-Rouendaal D. Conjunctival melanoma in the Netherlands: a nationwide study. Invest Ophthalmol Vis Sci. 2005; 46:75-82.

[6] Larsen AC, Dahmcke CM, Dahl C, Siersma VD, Toft PB, Coupland SE, Prause JU, Guldberg P, Heegaard S. A Retrospective Review of Conjunctival Melanoma Presentation, Treatment, and Outcome and an Investigation of Features Associated With BRAF Mutations. JAMA Ophthalmol. 2015; 133:1295-303.

[7] Werschnik C, Lommatzsch PK. Long-term follow-up of patients with conjunctival melanoma. Am J Clin Oncol. 2002; 25:248-255.

[8] Folberg R, McLean IW, Zimmerman LE. Conjunctival melanosis and melanoma. Ophthalmology. 1984; 91:673-678.

[9] Paridaens AD, Minassian DC, McCartney AC, Hungerford JL. Prognostic factors in primary malignant melanoma of the conjunctiva: a clinicopathological study of 256 cases. Br J Ophthalmol. 1994; 78:252-259.

[10] Zimmerman LE. Criteria for management of melanosis [letter]. Arch Ophthalmol. 1966; 76:307-308.

[11] Harooni H, Schoenfield LR, Singh AD. Current appraisal of conjunctival melanocytic tumors: classification and treatment. Future Oncol. 2011; 7:435-446.

[12] Shields JA, Shields CL, Mashayekhi A, Marr BP, Benavides R, Thangappan A, Phan L, Eagle RC Jr. Primary acquired melanosis of the conjunctiva: experience with 311 eyes. Trans Am Ophthalmol Soc. 2007; 105:61-71.

[13] Seregard S, Kock E. Conjunctival malignant melanoma in Sweden 1969-91. Acta Ophthalmol. 1992; 70:289-296.

[14] Gear H, Williams H, Kemp EG, Roberts F. BRAF mutations in conjunctival melanoma. Invest Ophthalmol Vis Sci. 2004; 45:2484-2488.

[15] Spendlove HE, Damato BE, Humphreys J, Barker KT, Hiscott PS, Houlston RS. BRAF mutations are detectable in conjunctival but not uveal melanomas. Melanoma Res. 2004; 14:449-452.

[16] Goldenberg-Cohen N, Cohen Y, Rosenbaum E, Herscovici Z, Chowers I, Weinberger D, Pe'er J, Sidransky D. T1799A BRAF mutations in conjunctival melanocytic lesions. Invest Ophthalmol Vis Sci. 2005; 46:3027-3030.

[17] Griewank KG, Westekemper H, Murali R, Mach M, Schilling B, Wiesner T, Schimming T,

Livingstone E, Sucker A, Grabellus F, Metz C, Susskind D, Hillen U, et al. Conjunctival melanomas harbor BRAF and NRAS mutations and copy number changes similar to cutaneous and mucosal melanomas. Clin Cancer Res. 2013; 19:3143-3152.

[18] Beadling C, Jacobson-Dunlop E, Hodi FS, Le C, Warrick A, Patterson J, Town A, Harlow A, Cruz F, Azar S, Rubin BP, Muller S, West R, et al. KIT Gene Mutations and Copy Number in Melanoma Subtypes. Clin Cancer Res. 2008; 14:6821-6828.

[19] Alessandrini L, Parrozzani R, Bertorelle R, Valentini E, Candiotto C, Giacomelli L, Midena E, Blandamura S. C-Kit SCF receptor (CD117) expression and KIT gene mutation in conjunctival pigmented lesions. Acta Ophthalmol. 2013; 91:e641-e645.

[20] Wallander ML, Layfield LJ, Emerson LL, Mamalis N, Davis D, Tripp SR, Holden JA. KIT mutations in ocular melanoma: frequency and anatomic distribution. Mod Pathol. 2011; 24:1031-1035.

[21] Banerji U, Affolter A, Judson I, Marais R and Workman P. BRAF and NRAS mutations in melanoma: potential relationships to clinical response to HSP90 inhibitors. Mol Cancer Ther. 2008; 7:737-739.

[22] Flaherty KT, Puzanov I, Kim KB, Ribas A, McArthur GA, Sosman JA, O'Dwyer PJ, Lee RJ, Grippo JF, Nolop K and Chapman PB. Inhibition of mutated, activated BRAF in metastatic melanoma. N Engl J Med. 2010; 363:809-819.

[23] Hauschild A, Grob JJ, Demidov LV, Jouary T, Gutzmer R, Millward M, Rutkowski P, Blank CU, Miller WH Jr., Kaempgen E, Martin-Algarra S, Karaszewska B, Mauch C, et al. Dabrafenib in BRAF-mutated metastatic melanoma: a multicentre, open-label, phase 3 randomised controlled trial. Lancet. 2012; 380:358-365.

[24] Weber JL, Smalley KS, Sondak VK, Gibney GT. Conjunctival melanomas harbor BRAF and NRAS mutations--Letter. Clin Cancer Res. 2013; 19:6329-6330.

[25] Pahlitzsch M BE, Mai C. Conjunctival melanoma and BRAF inhibitor therapy. J Clin Exp Ophthalmol. 2014; 5:322.

[26] Carnero A. The PKB/AKT pathway in cancer. Curr Pharm Des. 2010; 16:34-44.

[27] Lazo JS, Wipf P. Phosphatases as targets for cancer treatment. Curr Opin Investig Drugs. 2009; 10:1297-1304.

[28] Fedorenko IV, Gibney GT, Sondak VK, Smalley KS. Beyond BRAF: where next for melanoma therapy? Br J Cancer. 2015; 112:217-226.

[29] Vincent EE, Elder DJ, Thomas EC, Phillips L, Morgan C, Pawade J, Sohail M, May MT, Hetzel MR, Tavare JM. Akt phosphorylation on Thr308 but not on Ser473 correlates with Akt protein kinase activity in human non-small cell lung cancer. Br J Cancer. 2011; 104:1755-1761.

[30] Hatzivassiliou G, Song K, Yen I, Brandhuber BJ, Anderson DJ, Alvarado R, Ludlam MJ, Stokoe D, Gloor SL, Vigers G, Morales T, Aliagas I, Liu B, et al. RAF inhibitors prime wild-type RAF to activate the MAPK pathway and enhance growth. Nature. 2010; 464:431-435.

[31] Yang Y, Zhao S, Song J. Caspase-dependent apoptosis and -independent poly(ADP-ribose) polymerase cleavage induced by transforming growth factor beta1. Int J Biochem Cell Biol. 2004; 36:223-234.

[32] Chou TC and Martine N. CompuSyn Software for Drug Combinations and for General Dose-Effect Analysis, and User's Guide 9-2-2007. ComboSyn, Inc. 2007:Paramus, NJ.

[33] Decatur CL, Ong E, Garg N, Anbunathan H, Bowcock AM, Field MG, Harbour JW. Driver

mutations in uveal melanoma: associations with gene expression profile and patient outcomes. JAMA Ophthalmol. 2016. doi:10.1001/jamaophthalmol.2016.0903. Epub ahead of print.

[34] Stadelmeyer E, Heitzer E, Resel M, Cerroni L, Wolf P, Dandachi N. The BRAF V600K mutation is more frequent than the BRAF V600E mutation in melanoma in situ of lentigo maligna type. J Invest Dermatol. 2014; 134:548-550.

[35] Houben R, Vetter-Kauczok CS, Ortmann S, Rapp UR, Broecker EB, Becker JC. Phospho-ERK staining is a poor indicator of the mutational status of BRAF and NRAS in human melanoma. J Invest Dermatol. 2008; 128:2003-2012.

[36] Uribe P, Andrade L, Gonzalez S. Lack of association between BRAF mutation and MAPK ERK activation in melanocytic nevi. J Invest Dermatol. 2006; 126:161-166.

[37] Xia J, Jia P, Hutchinson KE, Dahlman KB, Johnson D, Sosman J, Pao W and Zhao Z. A meta-analysis of somatic mutations from next generation sequencing of 241 melanomas: a road map for the study of genes with potential clinical relevance. Mol Cancer Ther. 2014; 13:1918-1928.

[38] Cancer Genome Atlas N. Genomic Classification of Cutaneous Melanoma. Cell. 2015; 161:1681-1696.

[39] Aplin AE, Hogan BP, Tomeu J, Juliano RL. Cell adhesion differentially regulates the nucleocytoplasmic distribution of active MAP kinases. J Cell Sci. 2002; 115:2781-2790.

[40] Martelli AM, Tabellini G, Bressanin D, Ognibene A, Goto K, Cocco L, Evangelisti C. The emerging multiple roles of nuclear Akt. Biochim Biophys Acta. 2012; 1823:2168-2178.

[41] Halaban R, Zhang W, Bacchiocchi A, Cheng E, Parisi F, Ariyan S, Krauthammer M, McCusker JP, Kluger Y, Sznol M. PLX4032, a selective BRAF(V600E) kinase inhibitor, activates the ERK pathway and enhances cell migration and proliferation of BRAF melanoma cells. Pigment Cell Melanoma Res. 2010; 23:190-200.

[42] Kaplan FM, Shao Y, Mayberry MM, Aplin AE. Hyperactivation of MEK-ERK1/2 signaling and resistance to apoptosis induced by the oncogenic B-RAF inhibitor, PLX4720, in mutant N-RAS melanoma cells. Oncogene. 2011; 30:366-371.

[43] Poulikakos PI, Zhang C, Bollag G, Shokat KM, Rosen N. RAF inhibitors transactivate RAF dimers and ERK signalling in cells with wild-type BRAF. Nature. 2010; 464:427-430.

[44] Su F, Viros A, Milagre C, Trunzer K, Bollag G, Spleiss O, Reis-Filho JS, Kong X, Koya RC, Flaherty KT, Chapman PB, Kim MJ, Hayward R, et al. RAS mutations in cutaneous squamous-cell carcinomas in patients treated with BRAF inhibitors. N Engl J Med. 2012; 366:207-215.

[45] Wang D, Boerner SA, Winkler JD, LoRusso PM. Clinical experience of MEK inhibitors in cancer therapy. Biochim Biophys Acta. 2007; 1773:1248-1255.

[46] Remmele W, Stegner HE. Recommendation for uniform definition of an immunoreactive score (IRS) for immunohistochemical estrogen receptor detection (ER-ICA) in breast cancer tissue. Pathologe. 1987; 8:138-140.

[47] Nareyeck G, Wuestemeyer H, von der Haar D, Anastassiou G. Establishment of two cell lines derived from conjunctival melanomas. Exp Eye Res. 2005; 81:361-362.

[48] Keijser S, Maat W, Missotten GS, de Keizer RJ. A new cell line from a recurrent conjunctival melanoma. Br J Ophthalmol. 2007; 91:1566-1567.

[49] de Waard NE, Cao J, McGuire SP, Kolovou PE, Jordanova ES, Ksander BR, Jager MJ. A Murine Model for Metastatic Conjunctival Melanoma. Invest Ophthalmol Vis Sci. 2015; 56:2325-2333.

[50] de Waard NE, Kolovou PE, McGuire SP, Cao J, Frank NY, Frank MH, Jager MJ, Ksander BR. Expression of Multidrug Resistance Transporter ABCB5 in a Murine Model of Human Conjunctival Melanoma. Ocul Oncol Patho. 2015; 1:182-189.

[51] Dubbink HJ, Atmodimedjo PN, Kros JM, French PJ, Sanson M, Idbaih A, Wesseling P, Enting R, Spliet W, Tijssen C, Dinjens WN, Gorlia T, van den Bent MJ. Molecular classification of anaplastic oligodendroglioma using next-generation sequencing: a report of the prospective randomized EORTC Brain Tumor Group 26951 phase III trial. Neuro Oncol. 2016; 18: 388-400.

[52] de Lange J, Ly LV, Lodder K, Verlaan-de Vries M, Teunisse AF, Jager MJ, Jochemsen AG. Synergistic growth inhibition based on small-molecule p53 activation as treatment for intraocular melanoma. Oncogene. 2012; 31:1105-1116.

Supplementary files

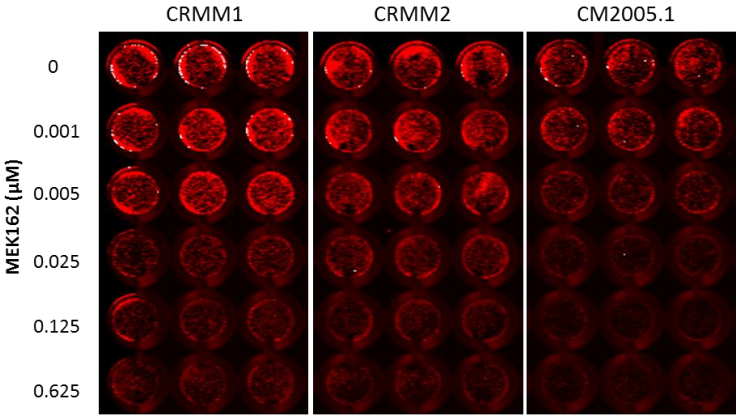

Supplementary Figure 1. In-cell western assay for CM cell lines treated with MEK162 for 72 hrs. MEK162 inhibited cell growth of CRMM1, CRMM2 and CM2005.1. Cells were seeded in triplicate in a 96-well plate for 24 h, and then MEK162 (0.001-0.625μM) was added from top line to bottom. In-cell western assay with DRAQ5 stained the DNA content (red) in each well, and the intensity was measured to interpret the cell growth.

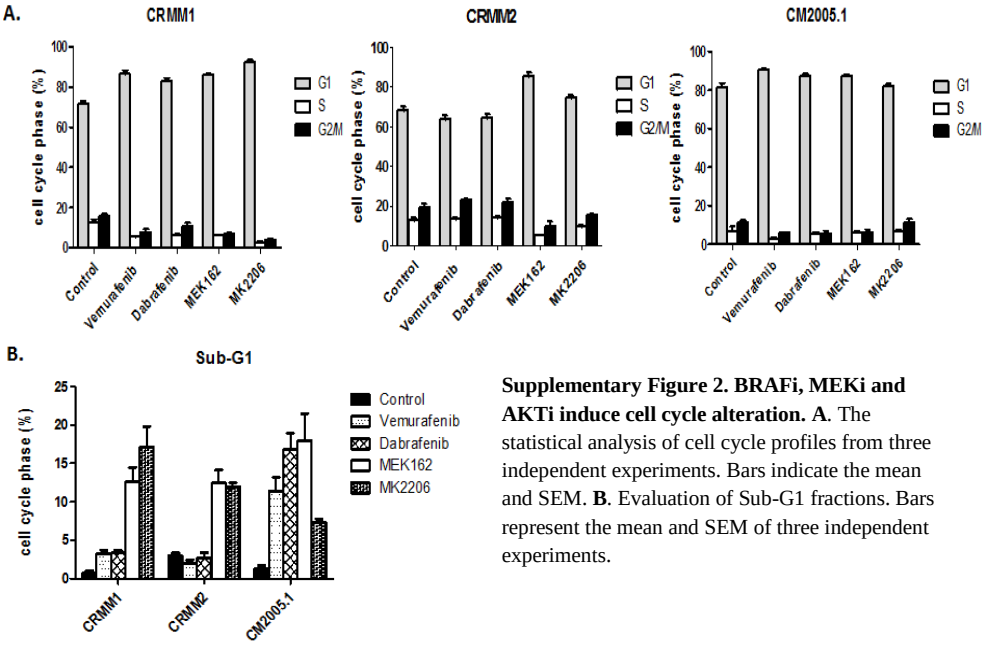

Supplementary Figure 2. BRAFi, MEKi and AKTi induce cell cycle alteration. A. The statistical analysis of cell cycle profiles from three independent experiments. Bars indicate the mean and SEM. **B**. Evaluation of Sub-G1 fractions. Bars represent the mean and SEM of three independent experiments.

Chapter 3

Overexpression of EZH2 in conjunctival melanoma offers a new therapeutic target

Jinfeng Cao, Kelly C. S. Pontes, Renier C. Heijkants, Niels J. Brouwer, Arwin Groenewoud, Ekaterina Jordanova, Marina Marinkovic, Sjoerd. van Duinen, Amina F. A. S. Teunisse, Robert M. Verdijk, Ewa Snaar-Jagalska, Aart G. Jochemsen, Martine J. Jager

Submitted for publication

Abstract

Malignant melanoma of the conjunctiva (CM) is an uncommon but potentially deadly disorder. Many malignancies show an increased activity of the epigenetic modifier Enhancer of zeste homolog 2 (EZH2). We studied whether EZH2 is expressed in CM, and whether it may be a target for therapy in this malignancy. Immunohistochemical analysis showed that EZH2 protein expression was absent in normal conjunctival melanocytes and primary acquired melanosis, while EZH2 was highly expressed in 13 (50%) of 26 primary CM and seven (88%) of eight lymph node metastases. An increased expression was positively associated with tumor thickness (p=0.03). Next, we targeted EZH2 with specific inhibitors (GSK503 and UNC1999) or depleted *EZH2* by stable shRNA knockdown in three primary CM cell lines. Both pharmacological as well as genetic inactivation of EZH2 inhibited cell growth and colony formation, and influenced EZH2-mediated protein expression and cell cycle profile *in vitro*. The tumor suppressor gene *p21* was especially upregulated in CM cells after *EZH2* knockdown CM cells. Additionally, the potency of GSK503 against CM cells was monitored in zebrafish xenografts. GSK503 profoundly attenuated tumor growth in CM xenografts using a well-tolerated concentration. Our results indicate that elevated levels of EZH2 are relevant to CM tumorigenesis and progression, and that EZH2 may become a potential therapeutic target for patients with CM.

Key words: conjunctival melanoma, EZH2, histone methylation, cell death, zebrafish.

Introduction

Conjunctival melanoma (CM) is a rare malignancy on the ocular surface, showing an increasing incidence in Europe and the United States [1-3]. CM recur frequently after surgical removal and can lead to death due to metastases [4,5]. The melanoma-related death rate can reach 29% at 10 years [5,6]. Once distant metastases occur, there are few therapeutic options.

CM share many characteristics with cutaneous melanoma, such as the presence of *BRAF* or *NRAS* mutations, which respectively occur in 29% and 18% of CM, and lead to activation of the MAPK pathway [7]. We recently showed that BRAF inhibitors are effective on *BRAF*-mutated CM cell lines [8] and at least two patients have been treated with these drugs [9,10]. As resistance to these drugs may develop, there is a need for alternative targets. One option is to investigate drugs that affect proteins involved in epigenetic regulation. Many epigenetic processes are regulated through the polycomb repressive complex 2 (PRC2), and overexpression of one of its catalytic subunits, Enhancer of zeste homolog 2 (EZH2), has been observed in a broad spectrum of cancer types including cutaneous melanoma, breast cancer, and endometrial carcinoma [11,12]. EZH2 is a histone methyltransferase which catalyzes trimethylation of lysine 27 in histone H3 (H3K27me3); this leads to transcriptional silencing of many genes, including tumor suppressor genes, rendering *EZH2* a potential oncogene [13,14]. EZH2 is not expressed in the normal tissues of adults, except in actively dividing cells, such as stem cells [15]. Somatic mutations including gain-of-function alterations of *EZH2* have primarily been discovered in hematopoietic malignancies, but sporadic activating mutations have also been identified in 3% of cutaneous melanoma [16]. While EZH2 expression is not detectable in benign nevi, it is expressed in cutaneous melanoma cells, suggesting a role for EZH2 in melanoma progression [17]. Indeed, EZH2 depletion or inhibition has been shown to repress melanoma growth and metastasis in a murine model of cutaneous melanoma [17].

Drugs that target EZH2 have shown promising preclinical results, and some phase 1/2 clinical trials using small molecule inhibitors have been initiated for lymphoma [18]. These inhibitors also show strong growth inhibitory effects on *EZH2* wild-type lymphoma cells *in vitro* [19,20]. We propose that EZH2 may also be overexpressed in CM, as in many ways CM resembles cutaneous melanoma, and blocking EZH2 may therefore inhibit the growth of CM cells.

We show that EZH2 expression is absent in normal conjunctival melanocytes and primary acquired melanosis (PAM), but is elevated in primary tumors and metastases of CM patients. In addition, we reveal that pharmacological inhibition of EZH2 activity or genetic depletion of *EZH2* leads to robust anticancer effects *in vitro* and *in vivo*. These results indicate that targeting EZH2 may provide a novel therapeutic strategy against CM.

Materials and Methods

Study population

Paraffin-embedded tissue specimens of nine PAM, 26 primary CM and one lymph node metastasis were collected through archive of the Department of Pathology, Leiden University Medical Center, Leiden, from patients who had been diagnosed with conjunctival melanocytic lesion between 1990 and 2014. Paraffin-embedded material of seven lymph node metastases of CM were retrieved from the Department of Pathology of the Erasmus University Medical Center. All the specimens contained enough material for the study. Five normal conjunctival samples were obtained from uveal melanoma-containing enucleated eyes. The use of human materials was approved by the Ethical Committee Board of Leiden University Medical Center and waived by Erasmus University Medical Center because it was a retrospective and non-interventional study. The diagnosis was reviewed and the original slides were assessed according to the 7th edition of the AJCC TNM cancer staging [21].

Immunohistochemistry (IHC) staining and evaluation

Immunohistochemistry (IHC) was carried out as previously described [22]. In short, after 10m (minute) of hot (100°C) antigen retrieval in a microwave and 1h (hour) cool down at room temperature (RT), sections were blocked with normal goat serum (1:10, X0907; DAKO, Glostrup, Denmark) for 1h at RT, after which the slides were incubated with anti-EZH2 monoclonal antibody (1:100, 612667; BD Biosciences, The Netherlands) overnight at 4°C. Thereafter, the slides were incubated with a goat-anti-mouse secondary antibody (K4000; EnVision+ System- HRP, Labelled Polymer, Dako) at RT for 1h. The staining was visualized with NovaRED substrate kit (SK-4800; VECTOR Laboratories, USA) for 15m at RT. Slides were then counterstained with hematoxylin and mounted with Kaiser's glycerin. Human placental tissue served as the positive control. The isotype control was obtained by replacing the primary antibody with the mouse IgG1 reagent (X9031, DAKO). Evaluation was done by two independent observers (JC and EJ) in a blinded manner. In case of divergent scores, a consensus was reached by simultaneous evaluation. Images were taken using Philips Image Management System 2.2. A staining index (SI) system, evaluating both intensity (0 = no staining, 1 = weak, 2 = moderate, and 3 = strong) and percentage of cells with nuclear EZH2 staining (1 ≤10%, 2 = 11%–50%, and 3 ≥50%) was used [12,23]. Multiplying intensity and percentage produced total scores (0-9). After considering the distribution plots and number of cases, the median (SI=3) was set as the cut-off value between low expression and high expression, as previously described [12,23].

Cell lines, lentiviral transduction and chemical reagents

Human CM cell lines CRMM1 and CRMM2 were established by G. Nareyeck, Essen, Germany [24], and kindly provided by M. Madigan, Sydney, Australia. CM2005.1 was established by S. Keijser, LUMC, Leiden, The Netherlands [25]. Human cutaneous melanoma cell lines A375 and MEL93.05 were kindly provided by E. M. E. Verdegaal, LUMC, Leiden, The Netherlands. The media and methods of cell culture have been described before [8]. Two validated MISSION®shRNA constructs (TRCN0000040-075 and TRCN0000040-077, Sigma Aldrich, USA)

were used to silence EZH2. Control shRNA vectors from the same library target green fluorescent protein (GFP) (shc005) or luciferase (shc007). HEK293T were transfected with the shRNA constructs together with helper plasmids encoding HIV-1 gag-pol, HIV-1 rev, and the VSV-G envelope as described previously [26]. To determine virus titers, p24 antigen levels were determined using a HIV-1 p24 antigen enzyme-linked immunosorbent assay (ELISA) kit (ZeptoMetrix Corp., USA). The CM cell lines were transduced with a MOI (multiplicity of infection) of 2.0 for 16h in medium containing 8.0 μg/mL polybrene. Virus-containing medium was replaced with fresh medium containing puromycin (1 μg/mL) for 72h to select transduced cells. GSK503 (S7804) and UNC1999 (S7165) were purchased from Selleck Chemicals (Huissen, The Netherlands). All drugs were dissolved in dimethyl sulfoxide (DMSO) to obtain a stock solution of 20 mM.

Immunoblotting

Protein lysates were extracted using 1.5× SDS sample buffer (75mM Tris HCl pH 6.8, 3% SDS, 15% glycerol). SDS-PAGE was carried out by loading 15-20 μg of total protein lysate on Mini-PROTEAN TGX Precast Gels (4-15%, Bio-Rad). Proteins were blotted onto Polyvinylidene difluoride (PVDF) membranes (Immobilon-P, Millipore, USA). Next, the membranes were incubated overnight with primary antibodies diluted with Odyssey blocking buffer (927-5000; LI-COR, The Netherlands) at 4°C, and visualized using IRdye-680 or IRdye-800 secondary antibodies (LI-COR). Blots were scanned and analyzed with the Odyssey Infrared Imaging System (LI-COR). Alternatively, membranes were incubated with horseradish peroxidase (HRP)-conjugated secondary antibodies and bands visualized by autoradiography. Primary antibodies are listed in Supplementary Table 1.

Cell proliferation and colony assay

The In-cell western assay was used to determine the growth rate, as previously described [8]. In brief, cells were seeded in triplicate in 96-well plates. EZH2 inhibitors at different concentrations were added 1 day later. After 5-day treatment

(pharmacological EZH2 inhibition), or treatment at day 1, day 4 and day 7 (*EZH2* knockdown), the cells were fixed in 4% formaldehyde and stained with DRAQ5 (1:7000, DR50050, Biostatus Ltd.). For a colony assay, cells were seeded in triplicate in 6-well or 12-well plates. Drugs at different concentrations were added 24h later. Medium was replaced with or without drugs every 4 days. After a 2-week incubation, cells were fixed in 4% formaldehyde and stained with 0.05% crystal violet. The plates were scanned with the Odyssey Infrared Imaging System.

Flow cytometry

Harvested cells were washed in cold PBS, fixed in 70% ethanol and stored at -20°C. Afterwards, cells were washed in PBS and resuspended in 2% fetal bovine serum/PBS with 50 μg/ml propidium iodide and 50 μg/ml RNase. Cell cycle analysis was carried out using BD LSR II system (BD Biosciences) and FACSDiva software (BD Biosciences).

RNA isolation, cDNA synthesis and real-time quantitative PCR (qRT-PCR)

RNA was isolated using the SV total RNA isolation kit (Promega, USA), after which cDNA was synthesized using the reverse transcriptase reaction mixture as indicated by Promega. qRT-PCR was performed using SYBR green mix (Roche Diagnostics, USA) in a C1000 touch Thermal Cycler (Bio-Rad laboratories, USA). Levels of *p14ARF*, *p21/CDKN1A*, *p16INK4a* and *p27KIP1* mRNAs were determined, corrected for housekeeping genes CAPNS1 and SRPR. The primer sequences are shown in Supplementary Table 2.

Fluorescent cell labeling and zebrafish model

To generate CM cells with red fluorescence, cells were stably transduced with lentivirus expressing both tdTomato and Blasticidin-S, as previously described [27]. Virus-containing medium was replaced with fresh medium containing Blasticidin-S (2 μg/mL) to select transduced cells. Transduction of the cells with the tdTomato-expressing virus did not alter the growth pattern of parental cells.

The (fli: GFP) Casper zebrafish embryos were maintained according to standard protocols (http://ZFIN.org, in the public domain) [28,29], in compliance with the Dutch animal welfare regulations. The research followed the statement on the use of animals in research as published by the Association for Research in Vision and Ophthalmology and was described previously [30]. To test drug toxicity, non-injected 3dpf (fli: GFP) Casper zebrafish embryos were put in a 24-well plate; each well contained 1ml of egg water, and different concentrations of GSK503. Six embryos were put into each well, maintained at 34°C, and monitored daily until 8dpf. The test was performed in triplicate and the media were refreshed every second day. When the survival was equal or higher than 80%, the concentration was considered nontoxic to the embryos.

After choosing the appropriate concentration, the same experimental conditions were applied for the treatment of tumor-cell injected embryos. Thus, at 2dpf, 350 to 450 cells of CRMM1, CRMM2, or CM2005.1 cells were injected inside the duct of Cuvier of (fli: GFP) Casper zebrafish embryos. At 1dpi, drug treatment was started and continued until 6dpi, completing a 5-day treatment. At 1dpi and 6dpi, injected embryos were anaesthetized with 0.160mg/ml tricaine (Sigma-Aldrich) to facilitate imaging under a stereo fluorescence microscope (Leica M205FA, Leica Microsystems, Inc.). The red pixels representing the number of cells inside the embryo were counted using Image J software (Schneider *et al*, 2012).

Statistical analysis

Statistical analyses were performed with either SPSS version 23.0 software (SPSS, Inc., USA) or R version 2.15.1 [31]. Pearson's chi-square, Fisher's exact and Mann-Whitney U tests were used for comparing categorical or numerical data of clinico-pathological characteristics. Two-tailed p values ≤ 0.05 were considered statistically significant. The plots of cell proliferation and cell cycle profiles were made with GraphPad Prism 6 software (La Jolla, USA). IC_{50} of drugs was calculated with CompuSyn software, according to relative 5-day growth inhibition [32]. The effect of GSK503 *in vivo* was analyzed using a generalized linear model after square-root transformation of the data.

Results

EZH2 is overexpressed in CM

We determined EZH2 expression in CM with IHC staining, analyzing the intensity and percentage of positive cells. Representative samples of different EZH2 expression patterns in CM are shown in Figure 1 (clinicopathological characteristics in Table 1, and clinical information in Supplementary Table 3). In normal conjunctiva, we observed some nuclear staining of keratinocytes, but not of melanocytes. EZH2 was also negatively expressed in PAM tissues (Supplementary Table 4). In contrast, EZH2 was highly expressed in 13 (50%) of the CM specimens, and was absent or marginally expressed in the other 13 (50%) primary CMs. In addition, seven (88%) out of eight lymph node metastases of CM showed strong EZH2 expression (Supplementary Table 5). In primary tumors, EZH2 expression positively correlated with tumor thickness (p=0.03). A high EZH2 expression was correlated with worse overall-survival and tended to associate with worse melanoma-related survival (Supplementary Figure 1). However, EZH2 expression was not correlated with tumor location, tumor stage, local recurrence, or distant metastasis (Table 1).

Pharmacological inhibition of EZH2 in CM cells

We determined EZH2 protein expression in three CM cell lines, a cutaneous melanocyte cell culture (07-11), and two cutaneous melanoma cell lines, one of which (A375) has previously been used extensively in determining the function of EZH2 [33]. Compared to the normal cutaneous melanocytes, all melanoma cell lines overexpressed EZH2 (Figure 2A). To investigate a putative growth stimulatory function of EZH2 in CM we treated the cells with small molecule EZH2 inhibitors GSK503 and UNC1999, since these had been shown to successfully inhibit the function of EZH2 in lymphoma and cutaneous melanoma *in vitro* and *in vivo* [17,34].

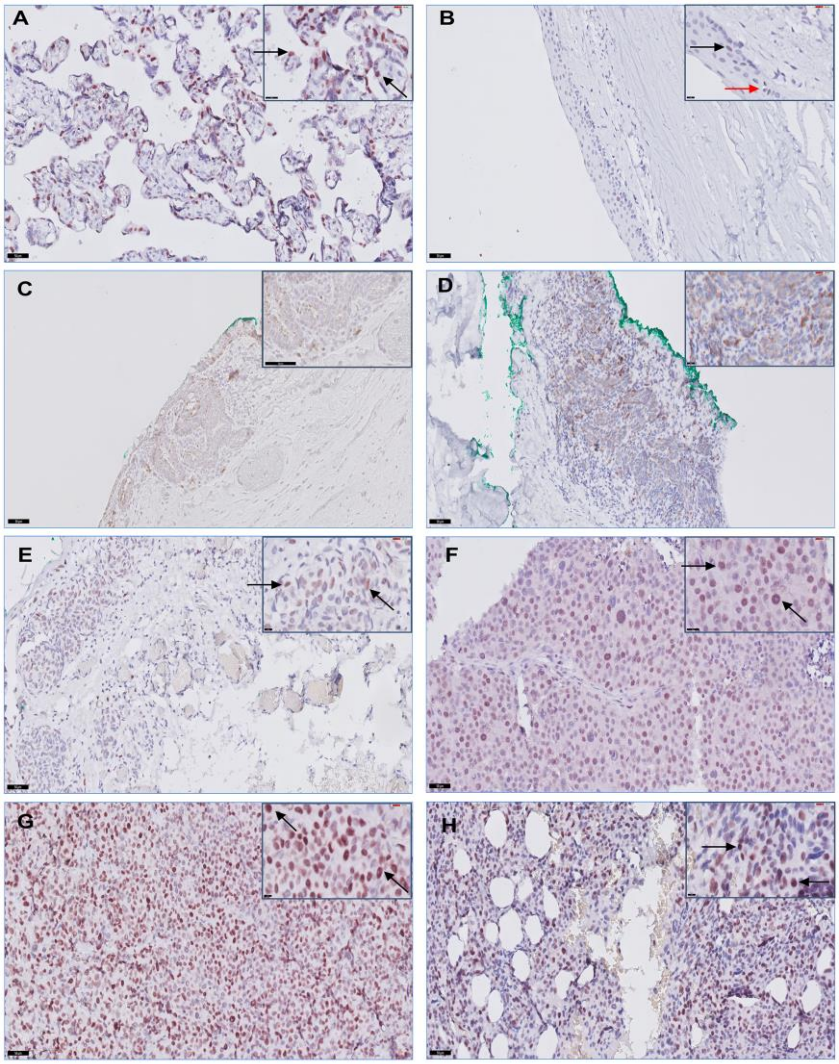

Figure 1. **Representative images of EZH2 IHC staining in CM**. (**A**) Positive control staining of placental tissue. (**B**) EZH2-positive keratinocytes (black arrow), and EZH2-negative melanocytes in the normal conjunctiva (red arrow). (**C**) EZH2 is absent in primary acquired melanosis. (**D**) CM with negative nuclear staining in all tumor cells. (**E**) CM with weak, (**F**) moderate, or (**G**) strong nuclear staining in >50% of tumor cells. (**H**) Strong nuclear staining in tumor cells in a lymph node metastasis. D and E were considered EZH2 low expression (scored ≤3); F, G and H were scored >3 and considered EZH2 high expression. Scale bar is 50μM in the original images. Black arrows indicate EZH2 positive cells.

Table 1. Clinicopathological characteristics according to low and high EZH2 expression.

	All cases	**EZH2 low**	**EZH2 high**	**Significance**
Characteristic	*Cases (%)*	*Cases (%)*	*Cases (%)*	*p value*
Overall	**26 (100)**	**13 (50)**	**13 (50)**	
Sex				
Male	11 (42)	8 (62)	3 (23)	*0.05**
Female	15 (58)	5 (38)	10 (77)	
Age at diagnosis				
Median [range], years	60.3 [21.2-86.3]	56.5 [21.2-73.0]	67.1 [48.7-86.3]	*0.03***
Tumor size, thickness	***N=23***	***N=11***	***N=12***	
Median [range], mm	1.0 [0.1-16.0]	0.6 [0.2-2.5]	3.3 [0.1-16.0]	*0.03***
Tumor size, LBD	***N=23***	***N=13***	***N=10***	
Median [range], mm	10.0 [2.0-30.0]	9.0 [2.0-30.0]	11.0 [5.0-20.0]	0.45**
Location				
Epibulbar	19 (73)	11 (85)	8 (62)	0.38&
Non-epibulbar	7 (27)	2 (15)	5 (38)	
cTNM				
T1	19 (73)	11 (85)	8 (62)	0.38&
T2	7 (27)	2 (15)	5 (38)	
Local recurrence				
No	16 (62)	7 (54)	9 (69)	0.42*
Yes	10 (38)	6 (46)	4 (31)	
Distant metastasis				
No	23 (88)	12 (92)	11 (85)	1.00&
Yes	3 (12)	1 (8)	2 (15)	

Abbreviation: LBD = largest basal diameter, cTNM = clinical TNM stage, based on the first occurring conjunctival melanoma. P value calculation: * = Pearson's chi-square; ** = Mann-Whitney U test; & = Fisher's exact test. Italic p values ≤ 0.05. Scoring method for EZH2 is described in the material and methods.

Figure 2B and 2F show that the level of H3K27me3 in CM cells decreased following increasing concentrations of GSK503 and UNC1999. EZH2 expression in CRMM2 and CM2005.1 was slightly decreased by GSK503, and UNC1999 clearly reduced EZH2 expression in CRMM2 at a high dose (6μM). IC_{50} values are shown in Table 2.

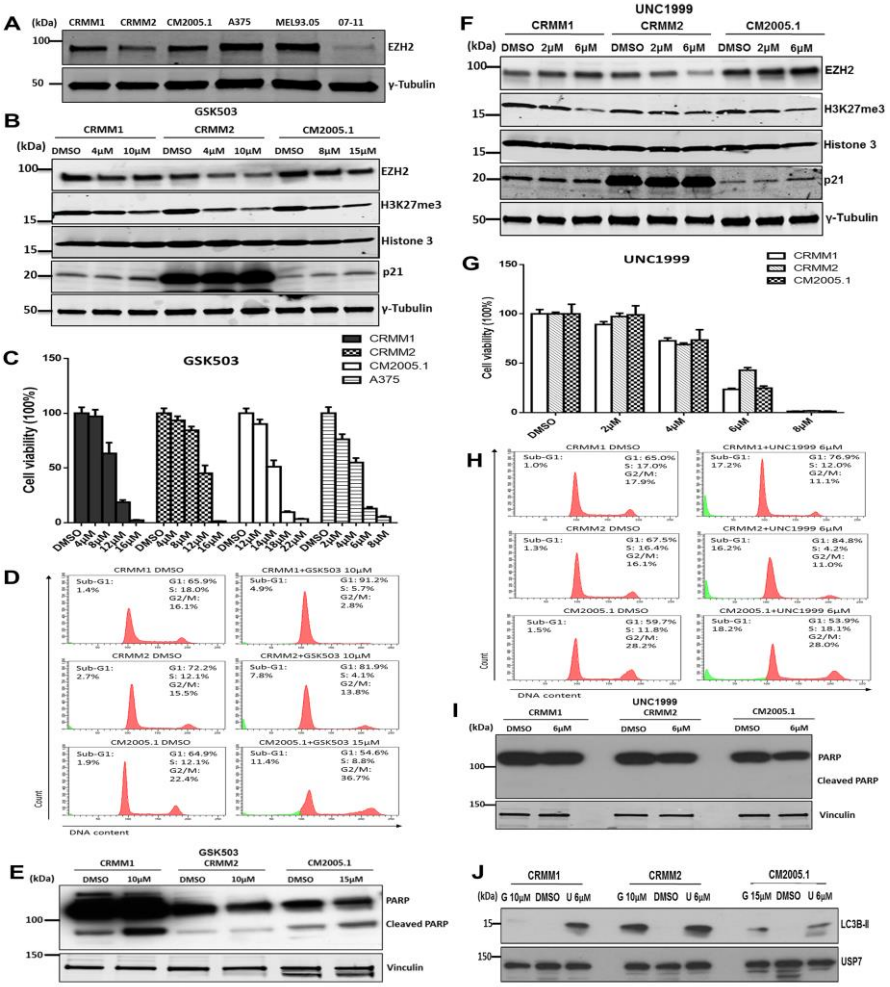

Figure 2. Effect of the EZH2 inhibitors GSK503 and UNC1999 on CM cell lines. (**A**) Western blot analysis of EZH2 protein in a panel of cell lines: CRMM1, CRMM2 and CM2005.1 are CM cell lines, A375 and MEL93.05 are cutaneous melanoma cell lines; 07-11 is a human melanocyte culture. Western blot analysis of CM cells upon 120h GSK503 (**B**) or UNC1999 (**F**) treatment. Representative bar graphs show the proliferation of melanoma cell lines exposed for 120h to GSK503 (**C**) or UNC1999 (**G**), respectively. The intensity (Y axis) was normalized to DMSO-treated control cells. Data were presented as means ± SEM (standard error of the mean), from one representative experiment. Histograms representing DNA content (**D, H**) and western blot analysis of (cleaved) PARP (**E, J**) following 120h incubation of GSK503 or UNC1999, respectively. (**J)** LC3B-II levels are increased following 120h incubation of GSK503 (G) or UNC1999 (U).

It has been reported that *EZH2* depletion increases p21 expression in cancer cell lines, and thereby induces cellular senescence [35,36]. Therefore, we examined p21 expression after drug treatment. However, we found that the p21 protein levels were only marginally elevated in CRMM1 and CM2005.1 cell lines exposed to either drug. Basal levels of p21 are very high in CRMM2 and the increase is hard to evaluate. Treatment for 5 days with GSK503 reduced the relative survival of CM cells, although the inhibitory effects on CM2005.1 cells required higher concentrations than the other cell lines (Figure 2C). Similarly, the proliferation of all CM cell lines was suppressed following UNC1999 treatment (Figure 2G). The colony formation assay confirmed the findings of the cell growth assay (Supplementary Figure 2).

Genes like *p14ARF*, *p16INK4a*, *p21/CDKN1A* and *p27KIP1* have been described as targets of EZH2 inhibition in several cancer types [35,37]. We therefore investigated whether GSK503 or UNC1999 affected the transcription of these genes in CM cells. However, mRNA expression of *p14ARF*, *p16INK4a*, *p21/CDKN1A* or *p27KIP1* was not significantly affected by these drugs (Supplementary Figure 3). However, results show that CM2005.1 does not express *p14ARF* nor *p16INK4a*, while CRMM2 lacks *p16INK4a* expression.

To determine the effects of EZH2 inhibition on cell cycle and apoptosis, we performed flow cytometry analysis after propidium Iodide staining (Figure 2D, 2H) and western blot analysis to investigate PARP cleavage (Figure 2E, 2I). Flow cytometry analysis of GSK503-treated CRMM1 and CRMM2 cells demonstrated a G1 arrest concomitant with S phase-depletion and slightly increased numbers of sub-G1 cells. In CM2005.1, on the other hand, we noticed an increase in the proportion of cells in G2/M phase (Figure 2D), also with an increase in the sub-G1 fraction. Some cleaved PARP could be detected in lysates from treated CRMM1 and CM2005.1 cells (Figure 2E). Following UNC1999 treatment, CRMM1 and CRMM2 cells showed an S-phase reduction concomitant with an increase of G1-phase cells. Furthermore, more sub-G1 cells were observed, indicating cell death (Figure 2H). In CM2005.1 cells, UNC1999 exposure did not have a strong effect on the cell cycle profile, but possibly the cells progress more slowly through S-phase since that

fraction is somewhat increased. A clearly increased sub-G1 fraction was identified, again indicating cell death. After UNC1999 treatment, no upregulation of cleaved PARP was observed in any cell line (Figure 2I), which may indicate that the observed cell death is not via induction of apoptosis. Since EZH2 has also been linked to the regulation of autophagy [38], the lysates of the three CM cell lines treated for 5 days with GSK503 or UNC1999 were investigated for expression of LC3B-II, a hallmark of autophagy [39]. Protein expression of LC3B-II was increased in CM cells upon GSK503 and UNC1999 treatment, although at different levels (Figure 2J), suggesting the induction of autophagy.

Table 2. Cell growth IC_{50} of EZH2 inhibitors in CM cell lines.

Cell line	GSK503 (μM)	UNC1999 (μM)
CRMM1	8.5±0.4	4.2±0.3
CRMM2	9.3±0.7	4.1±0.4
CM2005.1	15.9±1.4	4.4±0.3

Cell viability IC_{50} values of GSK503 (n=3) and UNC1999 (n=2) in CM cell lines (In-cell western assay) were determined based on relative 5-day survival.

Effect of *EZH2* knockdown in CM cells

Next, to genetically validate the findings of catalytic EZH2 inhibitors, we specifically depleted *EZH2* in melanoma cell lines using lentivirally-expressed short hairpin RNAs (shRNAs). Expression of EZH2 was significantly decreased in sh-*EZH2* expressing cells compared to control transduced cells (shc002, shc007), correlating with a global decrease of H3K27me3 (Figure 3A). This confirms that H3K27me3 is largely dependent on the presence of EZH2. Depletion of *EZH2* increased p21 protein levels in CRMM1, CRMM2 (shEZH2 20) and CM2005.1, suggesting that the cellular senescence marker *p21* participates in growth repression of CM cell lines. Activation of p21 transcription was detected in most *EZH2*-depleted cells, although some variation between cell lines and *EZH2* shRNAs was

observed (Figure 3B). We also investigated mRNA expression of *p16*, *p14ARF* and *p27*, but their expression was not affected by *EZH2* depletion (data not shown).

Importantly, the In-cell western assay indicated a lower proliferation of EZH2 shRNA-treated cells compared to control shRNA-treated cells (Figure 3C). Knockdown of *EZH2* also strongly decreased the ability of CM cells to form colonies (Supplementary Figure 4). Flow cytometry analyses showed that in CRMM1 and CRMM2, *EZH2* knockdown resulted in a S-phase depletion with G1 arrest (Figure 3D). Interestingly, in CM2005.1, *EZH2* depletion mainly caused an accumulation of cells in G2/M. In addition, an increased sub-G1 fraction was observed in all *EZH2*-depleted cells, suggesting that EZH2 protects CM cells from cell death.

Western blot showed that *EZH2* knockdown increased the amount of cleaved PARP in CM cell lines. It should be noticed that the full length PARP expression in CRMM2 cells upon *EZH2* depletion was strongly reduced, which may suggest that PARP is cleaved and that the cleaved product is unstable. In general, *EZH2* depletion induced some degree of apoptosis in CM cells, indicating its importance in cell survival. The results obtained upon *EZH2* depletion are strongly reminiscent of the data obtained with the GSK503 inhibitor (Figure 2D, 2E), suggesting that this inhibitor indeed mainly acts through inhibition of EZH2 activity, while UNC1999 might have additional activities [40].

Therapeutic effect of GSK503 in a zebrafish model

To confirm the findings obtained in cell culture, we established a zebrafish model to test the drug GSK503 *in vivo*. A well-tolerated concentration of GSK503 was determined as previously described [41]. Concentrations of GSK503 were nontoxic to the embryos till at least 8 days post-fertilization (dpf, Supplementary Figure 5), as over 80% of the embryos survived during the observation period, even at the highest concentration (24μM). Subsequently, three CM cell lines expressing tomato red were injected into the duct of Cuvier of (fli: GFP) Casper zebrafish embryos at 2dpf, and treatment with 24μM of GSK503 or DMSO diluted in egg water was initiated at 1-day post injection (dpi) and continued until 6dpi (5-day treatment). Next, cell growth

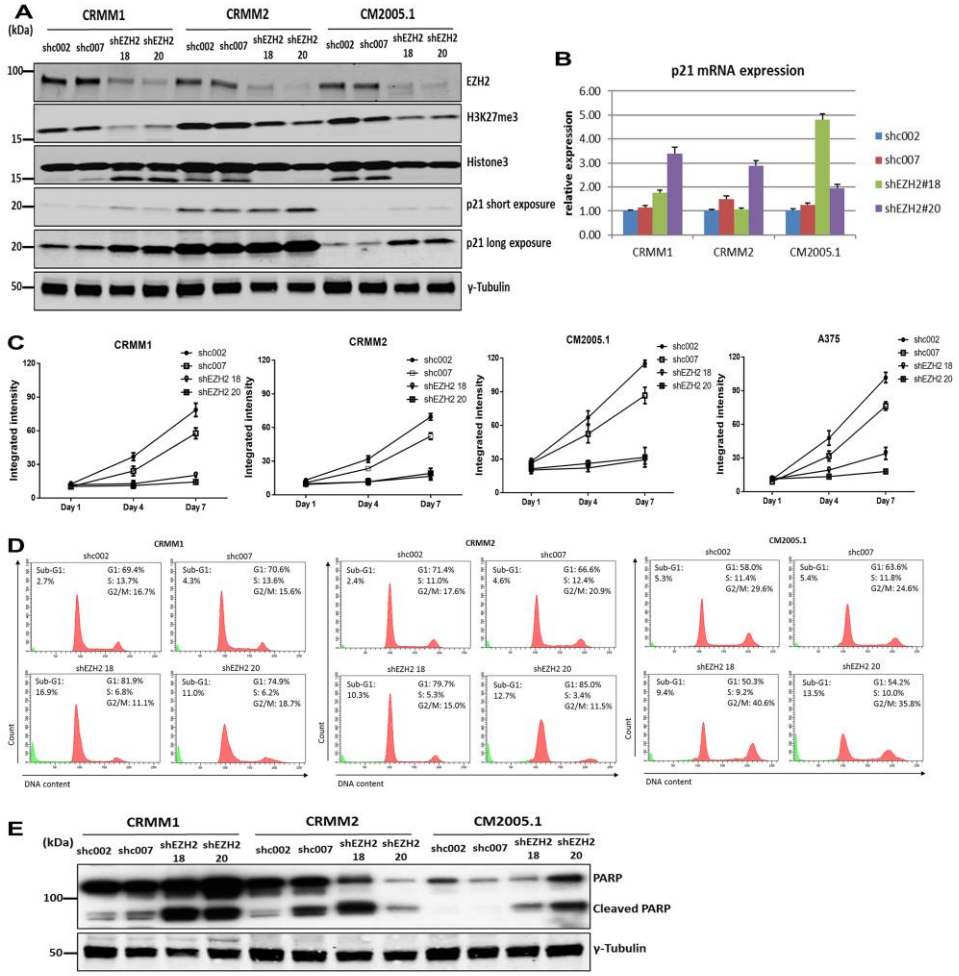

Figure 3. EZH2 knockdown reduces H3K27me3, elevates p21 expression, suppresses cell growth and induces cell cycle arrest and apoptosis in CM. (**A**) The expression of EZH2, H3K27me3, and cell cycle regulatory protein p21 was determined upon EZH2 depletion using (shEZH2 18, shEZH2 20) compared to control shRNAs (shc002 and shc007) 72h after puromycin selection. (**B**) The mRNA expression of p21 was elevated upon EZH2 knockdown. (**C**) Representative growth curves of CM cell lines and the A375 cell line after EZH2 knockdown by specific EZH2 shRNAs compared to control shRNAs. Error bars indicate the standard deviation. (**D**) Histograms show the percentages of CRMM1, CRMM2 and CM2005.1 cells in specific cell cycle phases, and western blot analysis (**E**) of (cleaved) PARP in CM cells upon EZH2 knockdown.

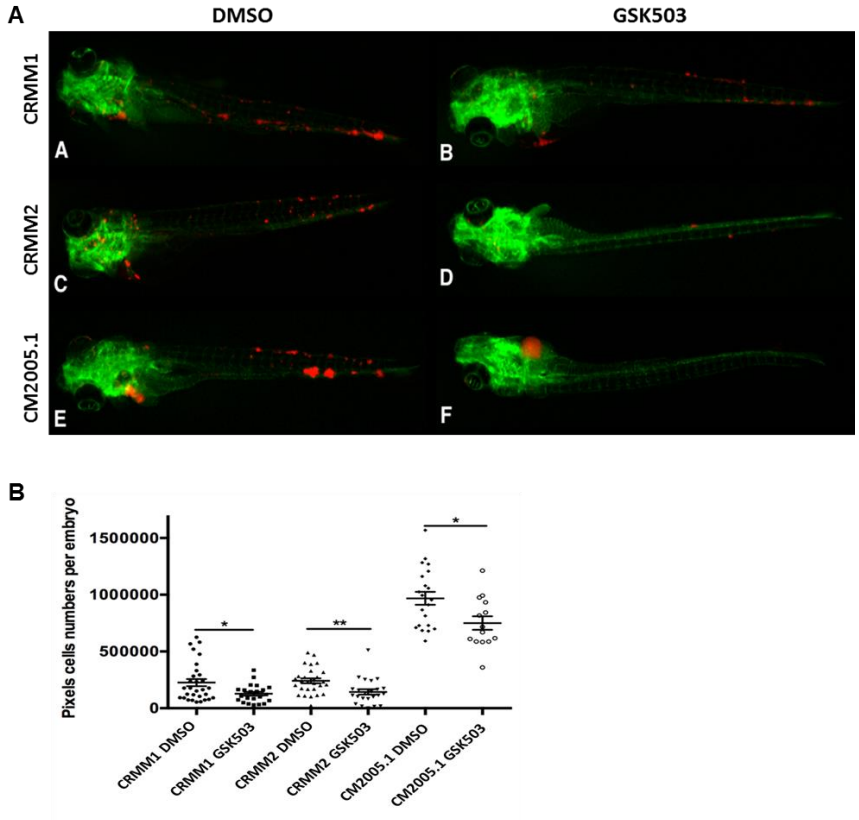

Figure 4. **GSK503 suppresses the cell growth of CM cell lines in the zebrafish model**. CM cells were labeled with tomato red (red) and injected into the duct of Cuvier at 2dpf in (fli: GFP) *Casper* zebrafish embryos which have a green vasculature. The images were taken at 6dpi. (**A**, black) Representative stereo fluorescent images (original magnification: 20x) show inhibition of tumour growth after exposure to 24μM GSK503. (**B**, black) Number of red pixels that represent tumour cells with DMSO or GSK503 treatment in CM xenografts. Each point indicates one embryo and its corresponding pixel count. Statistical significance was calculated by the generalized linear model and *p* values are indicated as follows: **p*< 0.05, ***p*< 0.01. $N_{CRMM1/DMSO}$= 30, $N_{CRMM1/GSK503}$= 22, $N_{CRMM2/DMSO}$= 28, $N_{CRMM2/GSK503}$= 23, $N_{CM2005.1/DMSO}$= 25, $N_{CM2005.1/GSK503}$= 18.

and dissemination were scored by counting the number of red pixels in the embryos. Figure 4 shows that tumor cells migrated to other areas through the blood circulation and proliferated. Importantly, the tumor burden of all three CM cell lines *in vivo* was significantly reduced after 5-day treatment with GSK503. We tested the difference

between the control and treated groups of the zebrafish embryos injected with three CM cell lines with a generalized linear model: the *p* values were 0.015 (CRMM1), 0.002 (CRMM2) and 0.028 (CM2005.1).

Discussion

To the best of our knowledge, this is the first study which demonstrates the importance of EZH2 in CM. Here we report the overexpression of EZH2 in CM. EZH2 was expressed on keratinocytes of normal conjunctiva, but not on cells of melanocytic lineage. This is consistent with studies of cutaneous melanoma, which similarly showed that EZH2 is present in epidermal keratinocytes, but absent or very low expressed in nevi and epidermal melanocytes [17,42]. Interestingly, although many CM develope in association with PAM [4], EZH2 was not expressed in PAM. Importantly, we demonstrate that EZH2 expression is detected in a significant proportion of CMs and is positively associated with one of the prognostic factors, tumor thickness [4]. Furthermore, EZH2 was highly expressed in most lymph node metastases. Taken together, our findings indicate that EZH2 protein levels are often increased in CM and metastases, and EZH2 may therefore be involved in the pathogenesis and progression of CM tumors.

Many small molecule inhibitors targeting EZH2 have been developed to block its catalytic activity, i.e. EZH2-mediated methylation of H3K27. A phase 1/2 clinical trial of Tazemetostat (EPZ-6438) is now ongoing against advanced solid tumors and B-cell lymphoma (NCT 01897571). In the present study, we applied two EZH2 inhibitors, GSK503 and UNC1999, on CM cell lines. In addition, we utilized genetic knockdown to confirm the findings of the pharmacologic depletion of *EZH2*. Interestingly, the tumor suppressor gene *p21* was more convincingly upregulated in *EZH2* knockdown CM cells than in inhibitor-treated cells, possibly suggesting that EZH2 has function(s) in transcription regulation independent of its catalytic activity. It is known that the mechanisms of EZH2 oncogenic activity are cancer type-dependent, including the canonical role of EZH2 in gene silencing in cutaneous

melanoma and colon cancer, and the non-canonical function of EZH2 that affects other pathways in a histone methylation-independent manner. For example, EZH2 can trigger NF-κB signaling in basal-like breast cancer, and can transcriptionally co-activate the androgen receptor in castration-resistant prostate cancer [43,44]. Further studies are warranted to elucidate the function(s) of EZH2 in CM. Regarding the cell cycle profile and apoptosis, drug treatment and RNA-interference (RNAi) similarly resulted in G1 arrest and S phase depletion in CRMM1 and CRMM2. GSK503 and UNC1999 appeared to induce cell death via partly different mechanisms. Similar to the genetic depletion of *EZH2*, the GSK503 inhibitor activated apoptosis and possibly some autophagy. However, increased caspase activity as monitored by PARP cleavage could not be detected upon UNC1999 treatment, but autophagy might be induced. Different patterns of cell death displayed by these treatments suggest that pharmaceutical inhibition cannot totally mimic the *EZH2* knockdown in this scenario. Discrepancies between genetic knockdown and enzymatic inhibitors of EZH2 on biological outcome have been described before: it was reported that catalytic inhibition of EZH2 using GSK343 and GSK126 induced no or modest expression of interferon gamma receptor 1 despite effective inhibition of H3K27me3 in a prostate cancer cell line, in contrast to depletion of EZH2 expression [45]. Similarly, it was found that SWI/SNF-mutant cancer lines are more sensitive to *EZH2* knockdown than catalytic inhibitors [46]. Regarding the autophagy context, the accumulation of LC3B-II may indicate that EZH2 inhibitors induce autophagy in CM cells. Although induction of autophagy may increase or repress cell survival depends on specific conditions, Hsieh et al. have shown that autophagy induced by GSK343 and UNC1999 occurred independently of EZH2 inhibition and promoted cell death in colorectal cancer cells [40]. This may explain why *EZH2* knockdown and UNC1999 treatment have partly distinct effects.

Our newly-developed zebrafish xenograft let tumor cells disseminate, and therefore served as an efficient metastatic model. After inoculation into the blood circulation, tumor cells spread to the head and tail of the zebrafish and proliferated, allowing further drug tests. GSK503 was not toxic to the fish, and like the results *in*

vitro, it profoundly reduced the growth of CM cells at a well-tolerated concentration. To the best of our knowledge, this is the first report using an animal model to test an epigenetic inhibitor in CM.

Overall, our results demonstrate that EZH2 is overexpressed in CM and lymph node metastases compared to normal conjunctival melanocytes and PAM, and high EZH2 protein levels are associated with tumor thickness. Both pharmaceutical compounds as well as RNAi targeting EZH2 repressed the growth of CM cells in culture and *in vivo*. Taken together, these data reveal that EZH2-targeted therapy may be a potential therapeutic strategy for patients with CM.

Acknowledgements

We thank Marja van Eggermond (IHB, LUMC, The Netherlands) for providing information regarding EZH2 and H3K27me3 antibodies, and Catalina Gomez Puerto (MCB, LUMC, The Netherlands) for sharing anti-p62 and anti-LC3B-II antibodies. And we appreciate that Robert M. Verdijk (Department of Pathology, Erasmas MC, The Netherlands) for providing metastases materials.

Abbreviations

Enhancer of zeste homolog 2 (EZH2), conjunctival melanoma (CM), polycomb repressive complex 2 (PRC2), trimethylation of lysine 27 in histone H3 (H3K27me3), immunohistochemistry (IHC), room temperature (RT), bovine serum albumin (BSA), phosphate buffered saline (PBS), staining index (SI), polyvinylidene difluoride (PVDF), horseradish peroxidase (HRP).

Conflict of interests

The authors declare no conflict of interest.

Grant support

This work was supported partly by grants from the China Scholarship Council (JC, 201206170141), the Dutch Cancer Society (UL 2013-5757), the LUMC MD/PhD programme grant (NJB), the Horizon2020 CURE UM 667787, and the National Council of Technological and Scientific Development CNPQ (Brazil, KCP).

Author contributions

MJJ initiated the idea, obtained funding and critically revised the article. AGJ participated in setting up, performing the experiments, and revising the manuscript. JC performed the *in vitro* experiments, analyzed the results and wrote the manuscript. KCP and AG established the animal model and did *in vivo* study. RCH and AFT was involved in *in vitro* experiments, and ESJ scored the slides. NJB collected clinical information and performed statistical analyses. MM and SD gave technical and material support.

References

1. Tuomaala S, Eskelin S, Tarkkanen A, *et al*. Population-based assessment of clinical characteristics predicting outcome of conjunctival melanoma in whites. *Invest Ophthalmol Vis Sci* 2002; 43: 3399-3408.

2. Yu GP, Hu DN, McCormick S, *et al*. Conjunctival melanoma: is it increasing in the United States? *Am J Ophthalmol* 2003; 135: 800-806.

3. Triay E, Bergman L, Nilsson B, *et al*. Time trends in the incidence of conjunctival melanoma in Sweden. *Br J Ophthalmol* 2009; 93: 1524-1528.

4. Shields CL, Shields JA, Gunduz K, *et al*. Conjunctival melanoma: risk factors for recurrence, exenteration, metastasis, and death in 150 consecutive patients. *Arch Ophthalmol* 2000; 118: 1497-1507.

5. Missotten GS, Keijser S, De Keizer RJ, *et al*. Conjunctival melanoma in the Netherlands: a nationwide study. *Invest Ophthalmol Vis Sci* 2005; 46: 75-82.

6. Werschnik C, Lommatzsch PK. Long-term follow-up of patients with conjunctival melanoma. *Am J Clin Oncol* 2002; 25: 248-255.

7. Griewank KG, Westekemper H, Murali R, *et al*. Conjunctival melanomas harbor BRAF and NRAS mutations and copy number changes similar to cutaneous and mucosal melanomas. *Clin Cancer Res* 2013; 19: 3143-3152.

8. Cao J, Heijkants RC, Jochemsen AG, *et al*. Targeting of the MAPK and AKT pathways in conjunctival melanoma shows potential synergy. *Oncotarget* 2016; 8: 58021-58036.

9. Pahlitzsch M, Bertelmann E, Mai C. Conjunctival melanoma and BRAF inhibitor therapy. *J Clin Exp Ophthalmol* 2014; 5: 322. doi: 10.4172/2155-9570.1000322.

10. Maleka A, Åström G, Byström P, *et al*. A case report of a patient with metastatic ocular melanoma who experienced a response to treatment with the BRAF inhibitor vemurafenib. *BMC Cancer* 2016; 16: 634.

11. Varambally S, Dhanasekaran SM, Zhou M, *et al*. The polycomb group protein EZH2 is involved in progression of prostate cancer. *Nature* 2002; 419: 624-629.

12. Bachmann IM, Halvorsen OJ, Collett K, *et al*. EZH2 expression is associated with high proliferation rate and aggressive tumor subgroups in cutaneous melanoma and cancers of the endometrium, prostate, and breast. *J Clin Oncol* 2006; 24: 268-273.

13. Ciferri C, Lander GC, Maiolica A, *et al*. Molecular architecture of human polycomb repressive compex 2. *eLife* 2012; 1: e00005. doi: 10.7554/eLife.00005.

14. Riquelme E, Behrens C, Lin HY, *et al*. Modulation of EZH2 expression by MEK-ERK or PI3K-AKT signaling in lung cancer is dictated by different KRAS oncogene mutations. *Cancer Res* 2016; 76: 675-685.

15. Konze KD, Ma A, Li F, *et al*. An orally bioavailable chemical probe of the Lysine Methyltransferases EZH2 and EZH1. *ACS Chem Biol* 2013; 8: 1324-1334.

16. Tiffen J, Gallagher SJ, Hersey P. EZH2: an emerging role in melanoma biology and strategies for targeted therapy. *Pigment Cell Melanoma Res* 2015; 28: 21-30.

17. Zingg D, Debbache J, Schaefer SM, *et al*. The epigenetic modifier EZH2 controls melanoma growth and metastasis through silencing of distinct tumor suppressors. *Nat Commun* 2015; 6: 6051. doi: 10.1038/ncomms7051.

18. Kim KH, Roberts CW. Targeting EZH2 in cancer. *Nat Med* 2016; 22: 128-133.

19. Knutson SK, Wigle TJ, Warholic NM, *et al*. A selective inhibitor of EZH2 blocks H3K27 methylation and kills mutant lymphoma cells. *Nat Chem Biol* 2012; 8: 890-896.

20. Bradley WD, Arora S, Busby J, *et al*. EZH2 inhibitor efficacy in non-Hodgkin's lymphoma does not require suppression of H3K27 monomethylation. *Chem Biol* 2014; 21: 1463-1475.

21. Edge SB, Byrd DR, Compton CC, *et al* (eds). Malignant melanoma of the conjunctiva. In AJCC Cancer Staging Manual 7th edn. 2010; pp 539–546. Springer: New York, NY.

22. Cao J, Brouwer NJ, Richards KE, *et al*. PD-L1/PD-1 expression and tumor-infiltrating lymphocytes in conjunctival melanoma. *Oncotarget* 2017; 8: 54722-54734.

23. Reijm EA, Timmermans AM, Look MP, *et al*. High protein expression of EZH2 is related to unfavorable outcome to tamoxifen in metastatic breast cancer. *Ann Oncol* 2014; 25: 2185-2190.

24. Nareyeck G, Wuestemeyer H, von der Haar D, *et al*. Establishment of two cell lines derived from conjunctival melanomas. *Exp Eye Res* 2005; 81: 361-362.

25. Keijser S, Maat W, Missotten GS, *et al*. A new cell line from a recurrent conjunctival melanoma. *Br J Ophthalmol* 2007; 91: 1566-1567.

26. Carlotti F, Bazuine M, Kekarainen T, *et al*. Lentiviral vectors efficiently transduce quiescent mature 3T3-L1 adipocytes. *Mol Ther* 2004; 9: 209-217.

27. Lawson ND, Weinstein BM. In vivo imaging of embryonic vascular development using transgenic zebrafish. *Dev Biol* 2002; 248: 307-318.

28. White RM, Sessa A, Burke C, *et al*. Transparent adult zebrafish as a tool for in vivo transplantation analysis. *Cell Stem Cell* 2008; 2: 183-189.

29. Schneider CA, Rasband WS, Eliceiri KW. NIH Image to ImageJ: 25 years of image analysis. *Nat Methods* 2012; 9: 671-675.

30. Pontes KC, Groenewoud A, Cao J, *et al.* Evaluation of (fli:GFP) Casper zebrafish embryos as a model for human conjunctival melanoma. *Invest Ophthalmol Vis Sci* 2017; in press.

31. R Core Team. R: A language and environment for statistical computing. 2013. R Foundation for Statistical Computing, Vienna, Austria. URL http://www.R-project.org/

32. Chou TC, Martine N. ComboSyn Inc Paramus NJ. 2005. CompuSyn for drug combinations. pc software and user's guide.

33. Barsotti AM, Ryskin M, Zhong W, *et al*. Epigenetic reprogramming by tumor-derived EZH2 gain-of-function mutations promotes aggressive 3D cell morphologies and enhances melanoma tumor growth. *Oncotarget* 2015; 6: 2928-2938.

34. Xu B, On DM, Ma A, *et al*. Selective inhibition of EZH2 and EZH1 enzymatic activity by a small molecule suppresses MLL-rearranged leukemia. *Blood* 2015; 125: 346-357.

35. Fan T, Jiang S, Chung N, *et al*. EZH2-dependent suppression of a cellular senescence phenotype in melanoma cells by inhibition of p21/CDKN1A expression. *Mol Cancer Res* 2011; 9: 418-429.

36. Xia H, Zhang W, Li Y, *et al*. EZH2 Silencing with RNA interference induces G2/M arrest in human lung cancer cells in vitro. *Biomed Res Int* 2014. doi: 10.1155/2014/348728.

37. Sha MQ, Zhao XL, Li L, *et al*. EZH2 mediates lidamycin-induced cellular senescence through regulating p21 expression in human colon cancer cells. *Cell Death Dis* 2016; 7: e2486.

38. Wei FZ, Cao Z, Wang X, *et al*. Epigenetic regulation of autophagy by the methyltransferase EZH2 through an MTOR-dependent pathway. *Autophagy* 2015; 11: 2309-2322.

39. Mizushima N, Yoshimori T. How to interpret LC3 immunoblotting. *Autophagy* 2007; 3: 542-545.

40. Hsieh YY, Lo HL, Yang PM. EZH2 inhibitors transcriptionally upregulate cytotoxic autophagy and cytoprotective unfolded protein response in human colorectal cancer cells. *Am J Cancer Res* 2016; 6: 1661-1680.

41. van der Ent W, Burrello C, Teunisse AF, *et al*. Modeling of human uveal melanoma in zebrafish xenograft embryos. *Invest Ophthalmol Vis Sci* 2014; 55: 6612-6622.

42. McHugh JB, Fullen DR, Ma L, *et al*. Expression of polycomb group protein EZH2 in nevi and melanoma. *J Cutan Pathol* 2007; 34: 597-600.

43. Lee ST, Li Z, Wu Z, *et al*. Context-specific regulation of NF-kB target gene expression by EZH2 in breast cancers. *Mol Cell* 2011; 43: 798-810.

44. Xu K, Wu ZJ, Groner AC, *et al*. EZH2 oncogenic activity in castration-resistant prostate cancer cells is Polycomb-independent. *Science* 2012; 338: 1465-1469.

45. Wee ZN, Li Z, Lee PL, *et al*. EZH2-mediated Inactivation of IFN-g-JAK-STAT1 signaling is an effective therapeutic target in MYC-driven prostate cancer. *Cell Rep* 2014; 8: 204-216.

46. Kim KH, Kim W, Howard TP, *et al*. SWI/SNF-mutant cancers depend on catalytic and non-catalytic activity of EZH2. *Nat Med* 2015; 21: 1491-1496.

Supplementary information

Supplementary Table 1. Primary antibodies for IHC.

Antibody	Specificity	Isotype	Company	Catalogue	Dilutions
EZH2	mouse	IgG1	BD Biosciences	612667	1:1000
H3K27me3	rabbit	IgG	Millipore	07-449	1:1000
Histone 3	mouse	IgG1	Cell signaling Technology (CST)	3638	1:1000
p21	mouse	IgG2bκ	Millipore	05-655	1:1000
PARP	rabbit	IgG	CST	9542	1:1000
LC3B	mouse	IgG1	NanoTools	0231-100	1:1000
USP7	mouse	IgG	Bethyl Laboratories	A300-033A	1:1000
γ-Tubulin	mouse	IgG1	Sigma-Aldrich	T6557	1:1000
Vinculin	mouse	IgG1	Sigma-Aldrich	V9131	1:1000

Supplementary Table 2. An overview of primers.

Primers	Forward	Reverse
p14ARF	TGATGCTACTGAGGAGCCAGC	ACCACCAGCGTGTCCAGGAA
p21	AGCAGAGGAAGACCATGTGGA	AATCTGTCATGCTGGTCTGCC
p16	AGCAGCATGGAGCCTTCGG	CGTAACTATTCGGTGCGTTGGG
p27	CAAATGCCGGTTCTGTGGAG	TCCATTCCATGAAGTCAGCGATA
CAPNS1	ATGGTTTTGGCATTGACACATG	GCTTGCCTGTGGTGTCGC
SRPR	CATTGCTTTTGCACGTAACCAA	ATTGTCTTGCATGCGGCC

Supplementary Table 3. Clinical information of patients.

Study number	Sex	Age at diagnosis (yr)	Follow-Up (months)	Local Recurrence	Time to recurrence (months)	Metastases	Time to metastasis (months)	Location of Metastases	Status	Location on Conjunctiva	Thickness (mm)	Largest Basal Diameter (mm)	cTNM (7th ed)	EZH2 score	EZH2 category
1	Female	59	43.6	No		No			Alive	Non-epibulbar	1.2	8	2	4	High
2	Female	47	246.8	Yes	48.9	No			Alive	Epibulbar	0.6	12	1	0	Low
3	Male	64	78.6	Yes	24.6	No			Alive	Epibulbar	0.3	7	1	4	High
4	Female	84	42.3	No		Yes	27	Distant skin	Death due to metastases	Non-epibulbar	6	20	2	6	High
5	Male	61	51.9	No		No			Alive	Non-epibulbar	1.4	17	2	1	Low
6	Female	21	50.5	No		No			Alive	Epibulbar	0.6	5	1	1	Low
7	Male	46	6.7	No		No			Alive	Non-epibulbar	2.5	30	2	2	Low
8	Male	33	107.6	Yes	37.8	No			Alive	Epibulbar	0.2	6	1	2	Low
9	Male	42	61.3	No		No			Alive	Epibulbar	Unknown	2	1	0	Low
10	Female	69	35	No		No			Alive	Non-epibulbar	16	16	2	9	High
11	Male	58	64.9	No		No			Alive	Epibulbar	4	13	1	4	High
12	Female	49	37.3	No		No			Alive	Non-epibulbar	4.2	10	2	4	High
13	Female	72	56.1	No		No			Alive	Epibulbar	0.3	15	1	2	Low
14	Female	84	3.3	No		No			Death due to unknown cause	Epibulbar	4	15	1	9	High
15	Female	73	37.2	No		No			Alive	Epibulbar	0.8	7	1	0	Low
16	Male	60	98.3	Yes	70.3	Yes	91.9	Brain. multiple visceral	Death due to metastases	Epibulbar	Unknown	5	1	1	Low
17	Female	67	45.7	No		No			Alive	Epibulbar	1.2	12	1	4	High
18	Female	56	23.8	No		No			Alive	Epibulbar	0.2	5	1	6	High
19	Male	56	34.2	Yes	32.7	No			Alive	Epibulbar	0.2	12	1	1	Low
20	Female	56	27.1	Yes	8.5	No			Alive	Epibulbar	2.5	Unknown	1	6	High
21	Female	75	41.9	Yes	8.4	No			Death due to unknown cause	Epibulbar	5	Unknown	1	4	High
22	Female	40	58.1	Yes	34.8	No			Alive	Epibulbar	1	9	1	2	Low
23	Female	86	12.8	No		No			Alive	Epibulbar	0.1	6	1	6	High
24	Male	68	46.4	Yes	17.8	No			Alive	Epibulbar	0.2	2	1	2	Low
25	Male	68	29.5	No		No			Alive	Epibulbar	0.2	12	1	2	Low
26	Male	80	52.4	Yes	42.1	Yes	51.4	Unknown	Death due to metastases	Non-epibulbar	Unknown	Unknown	2	6	High

Supplementary Table 4. EZH2 score of PAM.

Study number	Atypia	EZH2 score	EZH2 category
PAM1	Mild	0	low
PAM2	Unknown	0	low
PAM3	Mild	0	low
PAM4	Mild	0	low
PAM5	Mild	0	low
PAM6	Mild	0	low
PAM7	Severe	0	low
PAM8	Moderate	0	low
PAM9	Mild	0	low

PAM: Primary acquired melanosis.

Supplementary Table 5. EZH2 score of lymph node metastases.

Study number	EZH2 score	EZH2 category
M1	3	low
M2	4	high
M3	6	high
M4	9	high
M5	4	high
M6	6	high
M7	9	high
M8	6	high

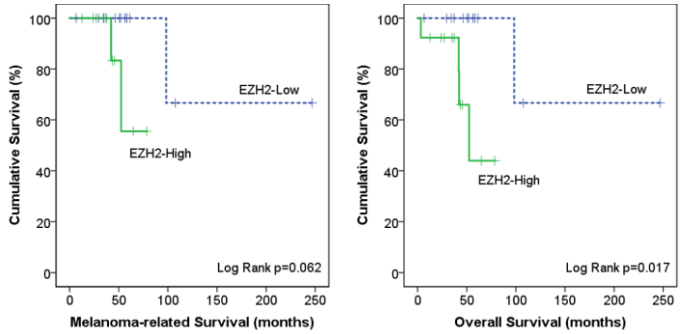

Supplementary Figure 1. Kaplan-Meier survival curves based on low and high EZH2 expression in CM groups of 26 patients. Left: melanoma-related survival. Right: overall survival.

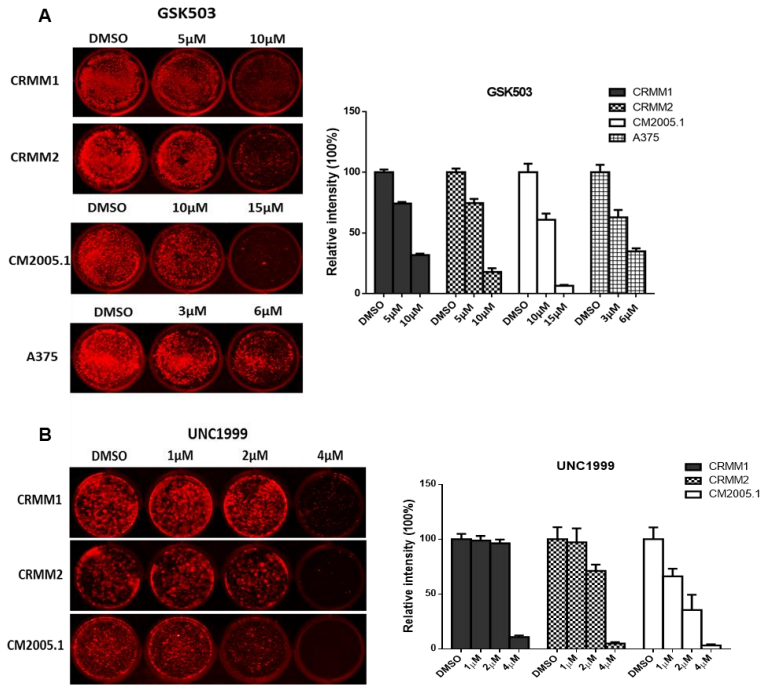

Supplementary Figure 2. GSK503 and UNC1999 inhibit colony formation in melanoma cell lines. Left: Representative images of cells exposed to drugs for 2 weeks. Right: Corresponding statistical analysis of colony formation. Error bars represent SEM. Data are presented as means ± SEM, from one representative experiment.

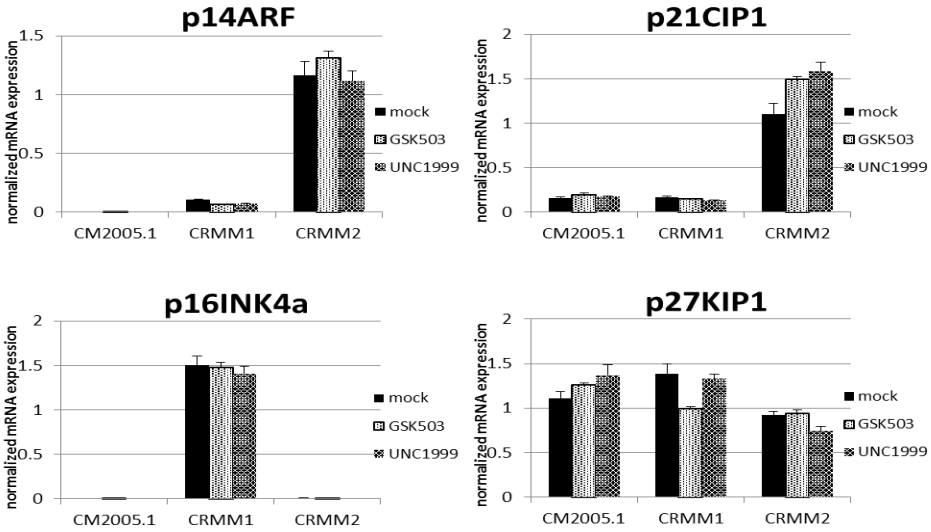

Supplementary Figure 3. GSK503 and UNC1999 don't alter the mRNA levels of p14ARF, p16, p21 or p27 in CM cell lines. Three CM cell lines were treated with GSK503 or UNC1999, and the relative expression was obtained by normalizing to housekeeping genes CAPNS1 and SRPR.

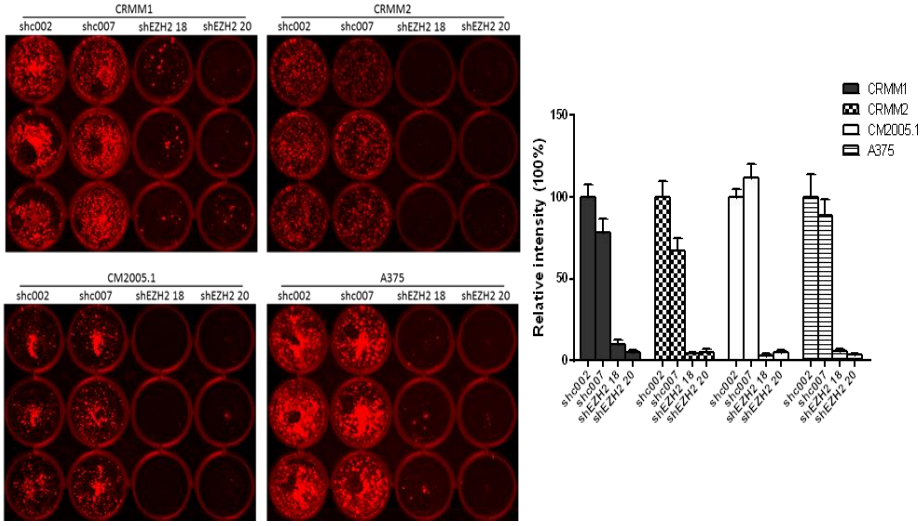

Supplementary Figure 4. EZH2 depletion inhibits colony-formation of three CM cell lines and A375. Cells were seeded in triplicate in 12-well plates. After 2-week incubation with siRNA, the plates were scanned. The intensity (Y axis) was normalized to shc002 control cells in each experiment. Data represent means ± SEM.

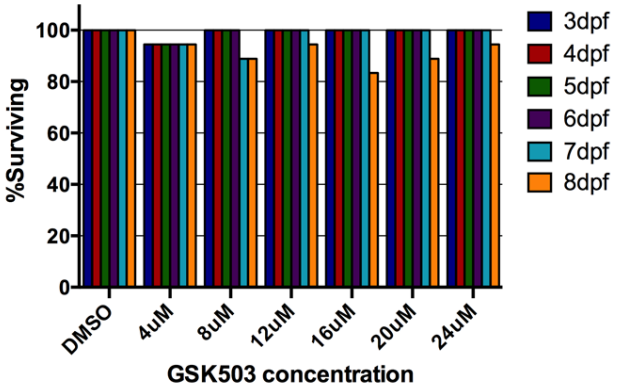

Supplementary Figure 5. Toxicity test of GSK503 in zebrafish. Toxicity test performed in non-injected (fli: GFP) Casper zebrafish embryos from 3 dpf until 8dpf, using different concentrations of GSK503. A concentration with a survival equal or higher than 80% was considered nontoxic to the embryos.

Chapter 4

A murine model for metastatic conjunctival melanoma

Nadine E. de Waard, Jinfeng Cao, Sean P. McGuire, Paraskevi E. Kolovou, Ekaterina S. Jordanova, Bruce R. Ksander, Martine J. Jager

NEdW and JC contributed equally to the paper, and are both considered first authors.

Published: Invest Ophthalmol Vis Sci. 2015; 56:2325–2333.

DOI: 10.1167/iovs.14-152

Abstract

Purpose. Conjunctival melanoma (CM) is an ocular malignancy with a high rate of local recurrences after treatment, and can give rise to deadly metastases. The establishment of a murine model will help to further our understanding of this disease and allows in vivo testing of new therapies. We therefore analyzed the ability of three CM cell lines to grow orthotopically and spread to distant sites. Furthermore, we determined the characteristics of the xenografts and their metastases.

Methods. Orthotopic xenografts of human CM were established by subconjunctival injection of three different CM cell lines into NOD/SCID IL2 rγ^{null} mice. Singe cell suspensions were generated from the primary tumors and placed subconjunctivally in another set of mice, which were then screened for metastases. The presence of melanoma markers was determined on the cell lines and during tumor development.

Results. Subconjunctival injection of cultured CM cells into immunodeficient NOD/SCID IL2 rγ^{null} mice led to excellent subconjunctival tumor growth in all inoculated mice (n=101) within two weeks; however, no metastases were found at the time of autopsy. Serial in vivo passage of primary tumor cells resulted in metastatic tumors in the draining lymph nodes (n=21). The CM cell lines, as well as the tumor xenografts and their metastases were positive for the melanoma markers HMB-45, S100B, and MART-1. Two cell lines and their corresponding xenografts carried a BRAF mutation, the third showed an NRAS mutation.

Conclusions. We established a murine model for CM that shows excellent formation of metastases in a pattern that accurately resembles metastatic human CM following in vivo passaging.

Key words: conjunctiva, melanoma, metastatic, mouse model.

Introduction

Conjunctival melanoma (CM) is an ocular malignancy that originates from conjunctival melanocytes. Although it is a rare form of cancer, CM has a high rate of local recurrence after treatment, and recurs in more than one in three cases [1]. Tumor-related mortality following the diagnosis of CM is 15% after five years and 30% after 10 years, with metastatic spread as the main cause of death [2].

Current therapies focus on radical excision of the tumor, and are frequently supplemented with cryotherapy or local therapy [3, 4]. The type of additional local treatment is a matter of discussion, although some studies support the use of adjuvant therapy regardless of clinical staging due to the high risk of local recurrence [5-7]. However, the rarity of this disease limits the ability to develop randomized clinical trials to determine which adjuvant chemotherapy or new treatment will improve prognosis [8]. To overcome these limitations, the use of a murine model is a good alternative; several studies have recently shown evidence that immunodeficient mice can be used successfully for hosting xenogeneic tumor cells [9-14]. Hence, the development of a mouse model that follows the natural progression from primary to metastatic disease will provide a unique opportunity to examine in vivo tumor growth and progression. Although several animal models have been developed to study uveal melanoma, very few models are available for CM. There is one report which describes the induction of conjunctival primary acquired melanosis by using topical 7,12-dimethylbenz[a]anthracene in rabbit eyes. The pigmented conjunctival lesions are intraepithelial precursors of melanoma and recapitulate the human local conjunctival disease, but metastases were not detected in this model [15].

Conjunctival melanoma exhibits a high rate of local recurrence and metastases, therefore more effective treatments directed against the local and distant recurrences are needed. Recent findings have demonstrated that immunotherapy targeting specific tumor-associated antigens may reduce recurrences in cutaneous melanoma. [16, 17]. The presence of melanoma markers during different stages of CM tumor growth may provide an opportunity for the development of adequate immunotherapy.

Conjunctival melanomas exhibit BRAF and NRAS mutations similar to cutaneous and mucosal melanomas [18-21]. A large cohort study demonstrated that 29% of CMs harbor a BRAF mutation, and 18% an NRAS mutation, in a mutually exclusive pattern [22]. The presence of these mutations may allow specific targeted therapy, as is already used for the treatment of metastases from cutaneous melanoma carrying these mutations [23, 24].

The establishment of a murine model for human CM would help to further our understanding of the disease and provide us with a strategy to test new treatments, thereby increasing the efficiency of therapeutic modalities and reduce recurrences. So we examined the possibility of CM growing orthotopically in nonobese diabetic (NOD)/severe combined immunodeficiency (SCID) IL-2 $r\gamma^{null}$ mice, and to create a model in which metastatic spread resembles human disease.

Materials and Methods

Cell Culture

Three CM cell lines, all derived from locally recurrent tumors, were used. The cell lines CRMM-1 and CRMM-2 were created by Gordan Nareyeck (Essen, Germany) [8], and kindly provided by Michele Madigan (Sydney, Australia). The cell line CM2005.1 was created in our lab by Sander Keijser (Leiden University Medical Center, Leiden, The Netherlands) [25]. In Boston, CRMM-1 and CRMM-2 cells were grown in F-12K Nutrient Mixture, Kaighn's Modification (1x) supplemented with 10% fetal bovine serum (FBS) (both from Invitrogen, Grand Island, NY), 1% 200mM L-Glutamine and 1% Penicillin/Streptomycin/Amphotericin-B mixture (both from Lonza, Walkersville, MD) at a 5% CO_2 atmosphere. The CM2005.1 cells were grown in RPMI-1640 (Lonza) supplemented with 10% FBS, 1% 200mM L-Glutamine, with 20mM Hepes and 1g/L $NaHCO_3$ (Gibco, Grand Island, NY) 1% Penicillin/Streptomycin/Amphotericin-B mixture, in 5% CO_2 atmosphere. In Leiden, the F-12K Nutrient Mixture, Kaighn's Modification (1x) was provided by Gibco (Life Technologies, UK), supplemented with 10% FBS (Greiner Bio-one, the

Netherlands), and Amphotericin-B was not used. Photographs of the cultured cells were taken with a microscope (Zeiss AX10; Carl Zeiss Meditec, Jena, Germany) equipped with a camera (Axiocam MRm).

Short Tandem Repeat (STR) Profiles

Short tandem analysis was carried out using the AmpFLSTR® Identifiler™ PCR Amplification Kit (Life Technologies, UK) based on the procedure recommended by The International Cell Line Authentication Committee (ICLAC) in Baseclear (Baseclear, Leiden, The Netherlands) [26] (See Table 1).

Cell Line Growth Kinetics

Proliferation of the CM cell lines was measured by mitochondrial function using the water-soluble tetrazolium salt (WST-1) assay (Roche Diagnostics, Indianapolis, IN). After culturing, cells were transferred into 96-well micro-culture plates (Costar 3596, Corning, NY) at four different concentrations and placed in an incubator at 37°C. Growth was measured daily for four days: first 10µl of WST-1 (Roche) was added to each well, followed by a 2-hour incubation at 37°C; analysis was performed using a microplate spectrophotometer (µQuant, MQX200, BioTek, Winooski, VT, USA).

Isolation of DNA and Sanger Sequencing

DNA material from the three CM cell lines as well as paraffin-embedded tumors of CM xenografts were extracted with, respectively, the QIAamp DNA mini kit (Qiagen, Venlo, The Netherlands) and the ReliaPrep FFPE gDNA miniprep System (Promega, Fitchburg, WI, USA). Polymerase chain reaction (PCR) analysis was performed to amplify BRAF exon 15, NRAS exon 2 and NRAS exon 3, as previously described [27, 28]. Following the PCR, the reverse primer was added to the purified PCR products. Sequencing was examined (Baseclear), and mutations were identified using Mutation Surveyor software (SoftGenetics, State College, PA, USA).

Table 1. Short Tandem Repeat Profiles of In Vitro Grown CM cells.

	Locus																
Cell line	**D8S1179**	**D21S11**	**D7S820**	**CSF1PO**	**D3S1358**	**TH01**	**D13S317**	**D16S539**	**D2S1338**	**D19S433**	**vWA**	**TPOX**	**D18S51**	**AM**	**D5S818**	**FGA**
CRMM-1	14	29;32.2	8;11	10;13	15;18	7	12	11	17;20	13;14	15	8;11	12;17	x	12;13	21;23
CRMM-2	12;14	28;31.2	8;11	12	15	7;9.3	8;11	9;13	17;23	13;14	16	8	14;17	x;y	11	24
CM2005.1	14;15	29;30	12;14	10;12	17	9	11;14	12;13	17;25	16,2	17	8;11	14;16	x	11;12	20;23

We used all three cell lines described above. Short tandem analysis was carried out using the AmpFLSTR® Identifiler™ PCR Amplification Kit (Life Technologies, UK) based on the procedure recommended by ICLAC in Baseclear [26].

Antibodies

The following primary antibodies were used: mouse anti-HMB45 mAb (1:100 dilution; ab787; Abcam, Cambridge, UK), rabbit anti-S100B pAb (1:3200 dilution; Code Z0311; Dako, Glostrup, Denmark) and mouse anti-MART-1 mAb (1:80 dilution; Clone M2-7C10; Covance, Denver, PA, USA). As secondary antibodies, we used a goat anti-mouse IgG pAb (1:200 dilution, Code E0433; Dako) and a biotinylated goat anti-rabbit antibody (1:300 dilution, BA-1000; Vector, Burlingame, CA, USA).

Immunocytochemistry

Expression of HMB-45, S100B, and MART-1 was determined on cytospins of the three CM cell lines. Cytospins were made from a cell suspension of 0.3×10^6 cells/ml cell suspension of 2% BSA/ PBS using a Shandon Cytospin 4 cytocentrifuge (Thermo Fisher Scientific, Waltham, USA). Cytospins were made from the three different cell lines at different times. Air-dried cytospin preparations were fixed in acetone for 10 minutes. The slides were washed in PBS and blocked with normal goat serum in 1% BSA/PBS (1:50 dilution, Code X0907; Dako)

at room temperature for 30 minutes. Excess serum was removed before overnight incubation at 4°C with the primary antibodies at the required concentrations, diluted in 1% BSA/PBS. Thereafter, cells were washed three times in PBS followed by incubation with either one or two secondary antibodies for 60 minutes, and washed again. Staining was visualized with nuclear Fast Red (Vectastain ABC-AP kit; Vector). Sections were then counterstained with Mayer's haematoxylin (Klinipath, Duiven, The Netherlands) and embedded in Kaiser's glycerin. Evaluation of the staining was done by light microscopy; two independent observers determined scores and the average result was reported. In case of a difference, consensus was reached during a simultaneous grading session.

Eyes were fixed in 4% paraformaldehyde and embedded in paraffin. Paraffin-embedded whole eye sections were used for immunohistochemistry to investigate the expression of HMB-45, S100B and MART-1. Tissue sections were baked at 60°C overnight. After sections were deparaffinized and rehydrated in a graded series of alcohol, they underwent antigen retrieval with citrate buffer for 20 minutes and were rinsed in PBS. Slides were blocked with normal goat serum in 1%BSA/PBS at room temperature for 30 minutes. The rest of the staining method was performed as described above. Control sections were incubated with secondary antibody alone, and did not show staining.

In Vivo

Animals. Non-obese diabetic/SCID IL-2 receptor gamma chain null mice were purchased from The Jackson Laboratory (Bar Harbor, ME, USA). The animals were maintained under defined conditions in accordance with institutional guidelines of The Schepens Eye Research Institute and experiments were performed according to approved experimental protocols, following the guidelines for the use of animals in research of the Association for Research in Vision and Ophthalmology. Mice were anesthetized by intraperitoneal (IP) injection of ketamine (100 mg/kg) and xylazine (9 mg/kg). Mice were euthanized using CO_2 asphyxia, followed by cervical dislocation. All internal organs were inspected macroscopically at the time of

autopsy with special attention given to the regional lymph nodes, heart, lung, and liver.

Conjunctival Melanoma Xenografts and Follow-up. Orthotopic xenografts of human CM were established by subconjunctival injection of the cell lines CRMM-1, CRMM-2, and CM2005.1. The cells were harvested from an in vitro cell culture, and, after counting, resuspended in media. Mice were anesthetized as described and injections were delivered under a microscope using a 33-gauge needle, inserted into the nasal subconjunctival space. Each injection contained 0.4×10^6 cells in a total volume of 5µl. Tumor formation and growth were monitored weekly, at least up to the endpoint of 10 weeks, unless excessive tumor growth required euthanasia earlier. For preparation of whole eye sections, the eyes were enucleated and tissue was fixed in 4% paraformaldehyde, embedded in paraffin and sectioned. Staining with haematoxylin and eosin was used for histopathologic analysis. At the time mice were euthanized, all mice were autopsied and screened for visible metastases. When metastases were found, some of them were removed and fixed in 4% paraformaldehyde for quantification and histopathological analysis.

In Vivo Passaging. In vivo passaging of the primary tumor xenografts was carried out by surgical dissection of the xenograft, and its processing into a single cell suspension. Cells were counted, washed, and resuspended in media. Orthotopic xenografts of the in vitro cultured melanoma cells were then established as described above.

Results

Morphology and Growth of Human CM Cells

Three cell lines derived from three different CMs were cultured in vitro and their growth characteristics were determined. The CRMM-1 had been obtained from a nodular tumor located in the bulbar conjunctiva, which was the third local recurrence of a mainly epithelioid CM [8]. CRMM-2 also originated from a recurrent melanoma

located at the bulbar part of the conjunctiva, with a predominantly epithelioid cell type [8]. We observed that, in culture, both cell lines displayed a spindle-cell type appearance with large nuclei, mostly mononucleated, containing prominent nucleoli (Fig. 1A, a-d). The third cell line, CM2005.1, had also been established from a recurrent CM, located at the palpebral part of the conjunctiva with extension into the nasal cavity [25]. In vitro, this cell line had a spindle-cell appearance with dendritic extensions, abundant cytoplasm, and large round nuclei with prominent nucleoli (Fig. 1A, e-f). All three cell lines showed a slow but steady proliferation rate at four different seeding densities in the WST-1 proliferation assay (Fig. 1B). Immunocytochemistry was performed on cytospin preparations at three different moments, and the percentage of positive cells and the intensity of the staining were determined. All three cell lines showed a high expression of HMB-45. Staining for S100B revealed a weak expression pattern on most of the cells from cell line CRMM-1 (80%), and strong expression on a lower percentage of cells from cell lines CRMM-2 and CM2005.1 (10% of CRMM-2; 35% of CM2005.1). MART-1 was moderately expressed on cell lines CRMM-1 and CRMM-2 (on 62% of CRMM-1 and 77% of CRMM-2), with a strong expression on cell line CM2005.1 on almost all cells (90%) (Fig. 1C).

BRAF and NRAS Mutations

We determined the presence of specific mutations in CM by using all three cell lines, and material obtained from the primary and in vivo passaged tumor xenografts of CRMM-1 and CM2005.1. We detected the BRAF c.1799T>A (V600E) mutation in both the cell lines CRMM-1 and CM2005.1, as well as their established xenografts and in vivo passaged tumors. Also, the metastasis derived from cell line CRMM-1 exhibit the BRAF mutation (Table 2). The cell line CRMM-2 and the corresponding xenografts harbors the NRAS c.182A>T mutation. There was no tissue of in vivo passaged tumors available for this cell line.

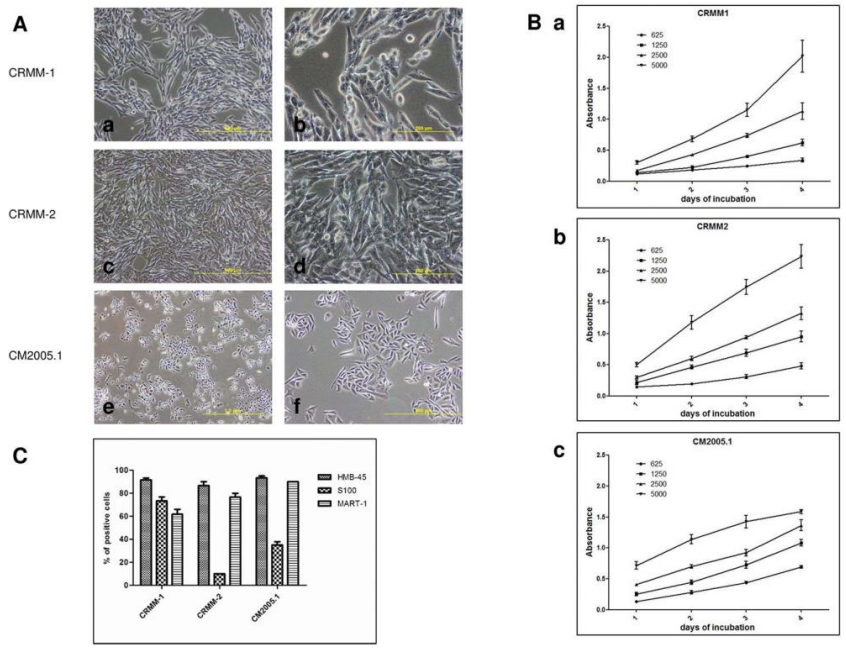

Figure 1. Characteristics of the CM cell lines. (**A**) Representative light microscopic images of the cultured cell lines CRMM-1, CRMM-2 and CM2005.1. Photographs were taken 72 hours after seeding. Images at original magnification of ×4 (**a, c, e**) and ×10 (**b, d, f**) respectively. (**B**) Growth kinetics of the CM cell lines (**a**) CRMM-1, (**b**) CRMM-2, and (**c**) CM2005.1, determined with a WST cell proliferation assay. Measurements were taken daily for 4 days. (**C**) Representative *bar graph* showing immunocytochemistry analysis on cytospins of the expression of HMB-45, S100B and MART-1 in the CM cell lines.

In Vivo Growth of CM Cells

Since the availability of an animal model will create the opportunity to test new therapies, we set out to establish orthotopic xenografts of human CM by injecting the cell lines CRMM-1, CRMM-2, and CM2005.1 subconjunctivally in NOD/SCID IL2 rγ^{null} mice. Of the 101 inoculated mice, 100% developed a detectable tumor within two weeks of the subconjunctival injection (CRMM-1 n = 33, CRMM-*2* n = 34, CM2005.1 n = 35). Tumor formation was closely monitored and a difference was observed in the in vivo growth rate of the cell lines. However, obtaining accurate

Table 2. BRAF and NRAS Mutations in Three CM Cell Lines and Their Corresponding Tumor Primary Subconjunctival Xenografts, and Passaged Tumors

Material	Type of mutations	
	BRAF (T1799A)	NRAS (A182T)
CRMM-1		
Cell line	+	-
Primary tumor	+	-
In vivo-passaged tumor	+	-
CRMM-2		
Cell line	-	+
Primary tumor	-	+
CM2005.1		
Cell line	+	-
Primary tumor	+	-
In vivo-passaged tumor	+	-

There was not enough material to study mutations in metastases. +, presence of mutation; -, absence of mutation.

in vivo measurements of tumor volume was difficult, and therefore typical examples of clinical tumor behavior are shown in Figure 2A. The degree of in vivo pigmentation varied, with CRMM-1-derived tumors being non-pigmented, tumors from CRMM-2 being slightly pigmented, and those from cell line CM2005.1 being heavily pigmented (Fig. 2A). Histological analysis of more than 50 tumor xenografts showed that all the tumors generated from the three cell lines had comparable morphological characteristics: the subconjunctival grafts grew on the ocular surface and into the sclera, with an epithelioid cell morphology with large nuclei and prominent nucleoli. The tumor cells had large cytoplasmic compartments with vacuoles (Figure 2B). In all specimens, mitoses were observed. Histologically, tumor xenografts derived from the cell lines CRMM-1 and CRMM-2 did not contain pigment, in contrast to xenografts from cell line CM2005.1, which were pigmented. Only CRMM-2-derived tumors showed some necrotic areas, whereas in the xeno-

grafts from cell line CM2005.1 some sclerosis was observed (Fig. 2B).

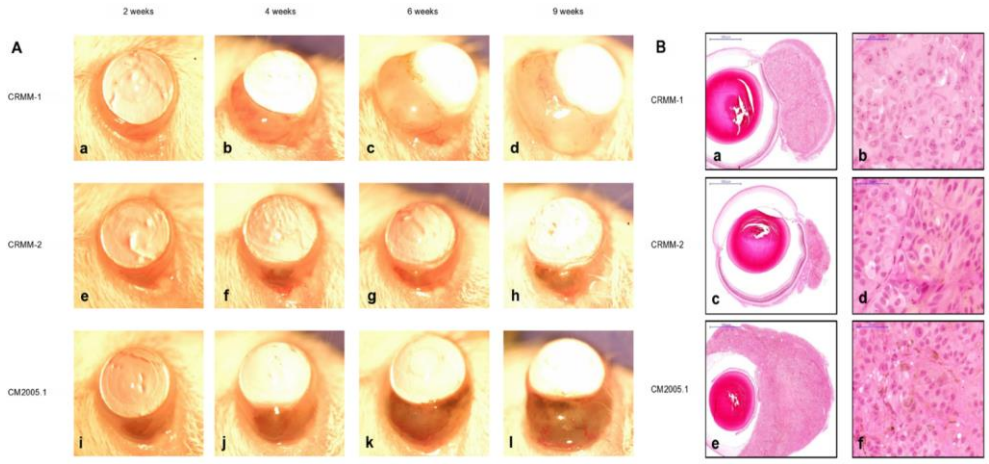

Figure 2. Assessment of tumor development and histological analysis of the xenografts. (**A**) Tumor development after subconjunctival injection of 0.4×10^6 human CM cell lines into NOD/SCID IL2 rγ^{null} mice. Tumors developed after injection with cell line CRMM-1 (**a-d**), CRMM-2 (**e-h**), and CM2005.1 (**i-l**). Day 0 is the time of injection; photos were taken 2, 4, 6 and 9 weeks post-injection. (**B**) Histological analysis of whole eye sections derived from mice previously injected with CM cells. Haematoxylin/eosin staining shows a non-invasive growth pattern in the tumor xenografts when harvested nine weeks post injection (**a, c, e**). Image at original magnification of ×10 (**a, c, e**) and ×400 (**b, d, f**).

A total of 44 mice (CRMM-1 *n* = 14, CRMM-2 *n* = 15, CM2005.1 *n* = 15) was examined for systemic spread at six weeks post-injection, and another 22 mice were inspected at nine weeks post-injection (CRMM-1 *n* = 6, CRMM-2 *n* = 10, CM2005.1 *n* = 6*)*. Although subconjunctival injection of cultured CM cells into immunodeficient mice led to excellent local growth, at the time of autopsy, no metastatic sites were found in any of the mice, showing that this model does not mimic human disease.

To select for more aggressive cancer cells, we decided to try in vivo passaging. A single cell suspension was generated from an established conjunctival tumor xenograft, and subsequently transplanted into the subconjunctival space of another set of immunodeficient NOD/SCID IL2 rγ^{null} mice (Fig. 3A). We choose to use two

cell lines (CRMM-1 and CM2005.1) as they displayed a high and similar in vivo growth rate (Fig. 2A). Exactly the same number of cells was injected each time (0.4×10^6 cells in a total volume of 5µl). All 21 inoculated mice developed a visible subconjunctival tumor within two weeks (CRMM-1 $n = 9$, CM2005.1 $n = 12$). Tumor formation was monitored closely, and growth pattern and degree of pigmentation of these in vivo-passaged tumors was similar to their original tumor xenografts. During tumor growth, there was no indication of necrosis. We consistently observed that the mice who had received an in vivo transfer of tumor cells lost weight and developed symptoms of pain. Subsequently, the mice were killed nine weeks after injection, after which an autopsy was performed (Fig. 3B). Metastases were present in all mice that had received a subconjunctival transfer and were mainly found in the cervical lymph node region, the heart and lungs.

To verify the melanocytic origin of the tumor material, we examined the tumor xenografts and metastases immunohistochemically for the presence of pigment cell makers. Most cells in the primary xenografts derived from cell line CRMM-1 were strongly positive for the melanoma marker HMB-45 (80% of the cells), whereas S100B and MART-1 were moderately expressed on a low number of cells (33% and 20%, respectively). Most cells in the primary xenografts from cell line CRMM-2 stained strongly with all three antibodies (83% with anti-HMB-45, $n = 3$; 92% with anti-S100B, $n = 3$; and 73% with anti-MART-1, $n = 3$). The primary tumors derived from the third cell line, CM2005.1, showed similarly high expression levels (83% with anti-HMB-45, 90% with anti-S100B, and 78% with anti-MART-1 (Figs. 4E-H). Examination of xenografts derived from an in vivo-passaged tumor from cell line CM2005.1 showed a high expression of HMB-45 (70%) and S100B (70%), with a lower expression of MART-1 (30%) (Figs. 4I-L). We also examined a lung metastasis from cell line CM2005.1: it showed a high expression of all three antigens (80% with anti-HMB-45; 90% with anti-S100B; 80% for anti-MART-1) (Figs. 4M-P). CRMM-1 metastases seen in lung tissue were strongly positive for all three markers. Altogether, these findings show that we established a murine CM model that leads to metastatic disease.

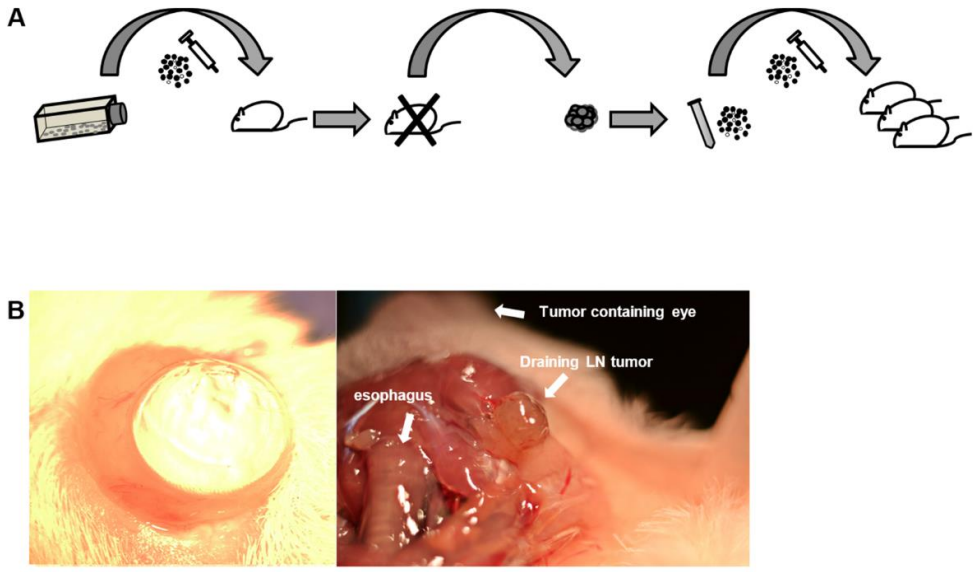

Figure 3. Serial passaging of human CM cells in immunodeficient mice. Tumor development after in vivo passaging. (**A**) Orthotopic xenografts were first established as described previously; tumor growth was monitored up to 9 weeks. Subsequently, mice were euthanized and surgical dissection of the primary tumor was performed to generate a single cell suspension. Cells were washed, counted and resuspended before reinjection into the subconjunctival space of a new set of NOD/SCID IL2 rγ^{null} mice. (**B**) Primary tumor 8 weeks after subconjunctival injection of 0.4×10^6 xenograft-derived human CM cells (cell line CRMM-1) into NOD/SCID IL2 rγ^{null} mice (*left*) and metastasis found at time of autopsy (*right*). The cells have been passaged in vivo once. Day 0 is the time of injection.

Discussion

Although it has long been known that CM exhibits a high rate of local recurrence and can lead to death due to metastatic spread, the lack of a reliable animal model has hampered thorough investigation of new therapies [14, 29-31]. In this study, we report the establishment of a murine CM model in which metastatic spread follows human disease.

Recurrences of human CMs stem from failure to eradicate a part of the tumor, either the "in situ" (i.e. the intraepithelial) or the invasive component. A difference between our model and human CM is that, in our murine model, the tumor cells are

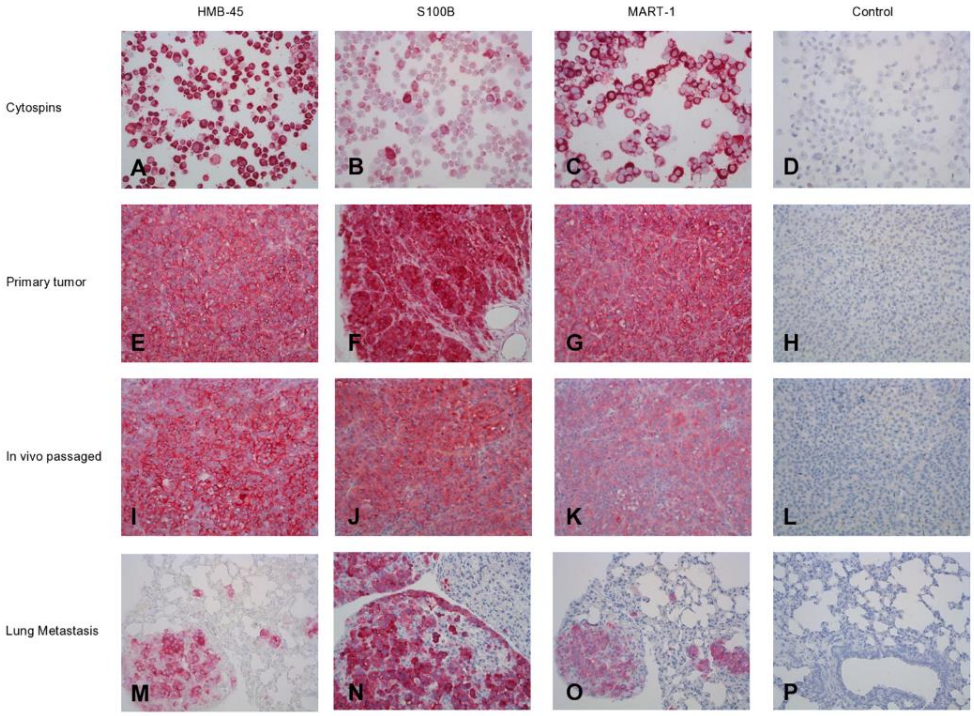

Figure 4. Immunohistochemical analysis to determine the expression of melanocytic markers during tumor development. Immunohistochemical staining of cytospins, tumor xenografts, and metastasis for the melanocyte markers HMB-45, S100B and MART-1; all tumor material was derived from cell line CM2005.1. (**A-D)** Staining of cytospins (original magnification ×200). (**E-H)** Primary CM. (**I-L)** In vivo passaged orthotopic tumor xenograft. (**M-P)** Lung metastasis (original magnification ×200). Negative controls were stained with secondary antibody alone.

injected into the subconjunctival space. However, in the human eye, melanomas develop in the epithelium and enter the vertical growth phase at a later stage. Transition to the vertical growth phase is the critical step in conversion to malignant CM. In conjunctival melanocytic intraepithelial neoplasia with atypia, the atypical melanocytes are confined within the conjunctival epithelium by the conjunctival basement membrane; in contrast, in CM the atypical melanocytes have broken through the epithelial basement membrane and invaded the underlying stroma, which contains lymph and blood vessels. [32,33] We injected the tumor cells directly below

the conjunctiva, thereby placing them at a site from where the malignant cells could spread to regional lymph nodes.

To assess the potential of using these tumors for immunotherapy and to confirm the melanocytic nature of the tumor cells, we determined the presence of melanoma markers. Conjunctival melanoma can be quite heterogeneous in its clinical and histological features and can lack pigmentation; therefore, monoclonal antibodies are being used to investigate the melanocytic nature of conjunctival lesions, for instance to examine the expression of the markers HMB-45, S100B, and MART-1. A previous study on CM compared the expression of MART-1/Melan-A with the expression of HMB-45, which identifies gp100, and of S100B. Expression of the melanoma markers HMB-45 and S100B were usually strong on CM, whereas MART-1 staining intensity was mostly weak or moderate. [34]. In this study, tissues were fixed in 4% buffered formaldehyde and embedded in paraffin. A different antibody was used for MART-1/Melan-A: they used NCL-Melan-A (Clone A103, code no. 4450, NovoCastra, Newcastle, UK), whereas we used a mouse anti-Mart-1 mAb (Clone 2-7C10, Covance). In another study, the expression of HMB-45 and S100B in different types of conjunctival melanocytic lesions was compared, including conjunctival naevi and melanomas arising in the context of primary acquired melanosis with and without atypia. An association was observed between increased malignancy and a higher expression of HMB-45, whereas S100B was expressed to the same extent in all different groups. In this study, formalin-fixed tissues were used [35]. A similar study was performed using monoclonal antibodies against three different S100 antigens: S100A1, S100A6 and S100B, and against MART-1. On average, conjunctival naevi often had a high expression of S100B and MART-1, whereas CMs were strongly positive for S100A and S100B, but not for MART-1 [36]. We found a more comparable staining intensity for all three antigens HMB-45, S100B, and MART-1. Tumor xenografts derived from cell line CRMM-1 were strongly positive for the melanoma marker HMB-45, whereas S100B and MART-1 were only moderately expressed. Tumors derived from cell lines CRMM-2 and CM2005.1 showed strong staining with all three different antibodies. The high

expression levels of HMB-45 agree with the fact that all tumors were derived from a malignant melanoma. We did not find a clear association between increased malignancy and the expression levels of HMB-45, as staining of in vivo passaged tumors and metastases did not show a further increase in expression of HMB-45. Nonetheless, the presence of these three melanocyte markers on the cells indicates that we are indeed dealing with pigment cells.

To grow the human CM cell lines in a murine model, we used the severely immunodeficient NOD/SCID IL2 IL2 rγ^{null} mice, as recent studies have shown that these mice are highly susceptible to the establishment of metastasis when compared with less immunodeficient mice [13, 37-39]. Nonetheless, formation of metastases was observed only after applying the method of in vivo passaging, indicating that the in vivo environment plays a crucial role in enhancing tumorigenicity when compared with the in vitro environment.

In fact, previous studies have indeed shown that the in vivo passage of tumorigenic cells resulted in more aggressively growing tumor cells, thereby suggesting that the in vivo environment exerts selective pressure and favors malignant transformation. [40, 41] It was noticed that stromal activation and an increase in the expression of hematopoietic growth factors occur due to a switch from paracrine to autocrine growth control. Independence of growth-regulatory mechanisms, together with an improved adaptation of cells for growth in the in vivo environment and an increase in angiogenesis, leads to accelerated enlargement of tumors after in vivo passaging. [40] Together, these data suggest that in vivo passaging will lead to tumor cells with a higher metastatic ability than exhibited by the original cell line, as a result of better adaptation to their microenvironment [40-42]. Moreover, in vivo passaging also helped to overcome one problem frequently associated with the formation of metastasis: the long latency that is often required [29, 43].

At this point we do not know which molecular changes have occurred in the CM cells, causing the in vivo passaged cells to be more malignant. To date, it has not been shown that the subconjunctival space is immunosuppressive as is the

intraocular environment, and we do not know which molecular changes have occurred in the CM cells, causing in vivo-passaged cells to be more malignant. However, we speculate that epigenetic regulation might be one of the options, as has been described in other tumors, in highly specialized environments. An example of epigenetic regulation of metastases comes from an intraocular study: LS174T colon cancer cells were placed in the eye of immunodeficient mice, and subsequently removed and grown in vitro [44]. Analysis showed a downregulation of the expression of CXCR4, a chemokine which plays an important role in tumor cell migration. The cells derived from the anterior chamber showed a higher methyltransferase and deacetylase activity, and the decreased CXCR4 expression was reversed by addition of 5-Aza-2-deoxycytidine, a demethylating agent. We are investigating this option.

Additionally, considering the identification of specific mutations in cutaneous melanoma that has led to the development of new and targeted chemotherapy treatments, we sought to define the mutational status of the cell lines as well as their established xenografts before and after the in vivo passaging. It is of great interest that we detected the BRAF c.1799T>A (V600E) mutation in both the cell lines and tumor xenografts from CRMM-1 and CM2005.1, and the NRAS c.182A>T mutation in cell line CRMM-2 and the corresponding xenografts. This highlights the important of our murine model, as it facilitates further research to investigate treatments that specifically target these different mutations. Also, it allows the testing of multiple drugs, with or without the use of, for instance, additional MEK inhibitors [23].

Although we show that the use of NOD/SCID IL2 rγ^{null} mice offers the opportunity to establish a mouse model for human CM, the mice's lack of a functional immune system limits the possibility for effective studies to investigate therapeutic advances of, for instance, natural immunological treatments. On the other hand, our model provides the ability to test the antitumor effect of specific T cells following direct transfer, from mice with a functional immune system. Furthermore, this model may be used to determine the expression of various immunologically

relevant factors, such as those of major histocompatibility complex and adhesion molecules during tumor progression.

In conclusion, we established a mouse model for human CM in which metastatic spread follows and recapitulates the clinical disease. This model will provide opportunities for finding new and more effective treatments to prevent the development of metastasis, as well as the ability to analyze the changes in tumor cell biology that coincide with disease progression and metastatic dissemination.

Acknowledgement

We thank Aat A. Mulder, BASc, for technical assistance.

Supported by Stichting Leids Oogheelkundig Ondersteunings Fonds, Stichting Dondersfonds, Nelly Reef Fund, Alcon BV, Stichting Blindenhulp, and China Scholarship Council.

Disclosure: **N.E. de Waard**, None; **J. Cao**, None; **S.P. McGuire**, None; **P.E. Kolovou**, None; **E.S. Jordanova**, None; **B.R. Ksander**, None; **M.J. Jager**, None

References

[1] Shields, C.L., Markowitz, J.S., Belinsky, I., et al. Conjunctival melanoma: outcomes based on tumor origin in 382 consecutive cases. *Ophthalmology*. 2011;118:389-395. e1-e2.

[2] Errington, J.A., Conway, R.M., Walsh-Conway, N., et al. Expression of cancer-testis antigens (MAGE-A1, MAGE-A3/6, MAGE-A4, MAGE-C1 and NY-ESO-1) in primary human uveal and conjunctival melanoma. *Br J Ophthalmol*. 2012;96:451-458.

[3] Shields, J.A., Shields, C.L., and De Potter, P. Surgical management of circumscribed conjunctival melanomas. *Ophthal Plast Reconstr Surg.* 1998;14:208-15.

[4] Westekemper, H., Freistuehler, M., Anastassiou, G., et al. Chemosensitivity of conjunctival melanoma cell lines to chemotherapeutic agents. *Int J Clin Pharmacol Ther*. 2011;49:78-80.

[5] Lim, L.A., Madigan, M.C., and Conway, R.M. Conjunctival melanoma: a review of conceptual and treatment advances. *Clin Ophthalmol.* 2013;6:521-531.

[6] Damato, B. and Coupland, S.E. Management of conjunctival melanoma. *Expert Rev Anticancer Ther.* 2009;9:1227-1239.

[7] Karim, R. and Conway, R.M. Conservative resection and adjuvant plaque brachytherapy for early-stage conjunctival melanoma. *Clin Experiment Ophthalmol.* 2011;39:293-298.

[8] Nareyeck, G., Wuestemeyer, H., von der Haar, D., Anastassiou, G. Establishment of two cell lines derived from conjunctival melanomas. *Exp Eye Res.* 2005;81:361-362.

[9] Li, M., Zhou, M., Gong, M., et al. A novel animal model for bone metastasis in human lung cancer. *Oncol Lett.* 2012;3:802-806.

[10] Greiner, D.L., Hesselton, R.A., and Shultz, L.D. SCID mouse models of human stem cell engraftment. *Stem Cells.* 1998;16:166-177.

[11] Quintana, E., Shackleton, M., Sabel, M.S., et al. Efficient tumour formation by single human melanoma cells. *Nature.* 2008;456:593-598.

[12] Schatton, T., Murphy, G.F., Frank, N.Y., et al. Identification of cells initiating human melanomas. *Nature.* 2008;451:345-349.

[13] Shtivelman, E., Namikawa, R. Species-specific metastasis of human tumor cells in the severe combined immunodeficiency mouse engrafted with human tissue. *Proc Natl Acad Sci U S A.* 1995;92:4661-4665.

[14] Iorns, E., Drews-Elger, K., Ward, T.M., et al. A new mouse model for the study of human breast cancer metastasis. *PLoS One.* 2012;7:e47995.

[15] Folberg, R., Baron, J., Reeves, R.D., Stevens, R.H., Bogh, L.D. Animal model of conjunctival primary acquired melanosis. *Ophthalmology.* 1989;96:1006-1013.

[16] Alexandrescu, D.T., Ichim, T.E., Riordan, N.H., et al. Immunotherapy for melanoma: current status and perspectives. *J Immunother.* 2010;33:570-590.

[17] Jandus, C., Speiser, D., Romero, P. Recent advances and hurdles in melanoma immunotherapy. *Pigment Cell Melanoma Res.* 2009;22:711-723.

[18] Gear, H., Williams, H., Kemp, E.G., Roberts, F. BRAF mutations in conjunctival melanoma. *Invest Ophthalmol Vis Sci.* 2004;45:2484-2488.

[19] Spendlove, H.E., Damato, B.E., Humphreys, J., et al. BRAF mutations are detectable in conjunctival but not uveal melanomas. *Melanoma Res.* 2004;14:449-452.

[20] Goldenberg-Cohen, N., Cohen, Y., Rosenbaum, E., et al. T1799A BRAF mutations in conjunctival melanocytic lesions. *Invest Ophthalmol Vis Sci.* 2005;46:3027-3030.

[21] Lake, S.L., Damato, B.E., Dopierala, J., et al. Multiplex ligation-dependent probe amplification analysis of uveal melanoma with extraocular extension demonstrates heterogeneity of gross chromosomal abnormalities. *Invest Ophthalmol Vis Sci.* 2011;52:5559-5564.

[22] Griewank, K.G., Westekemper, H., Murali, R., et al. Conjunctival melanomas harbor BRAF and NRAS mutations and copy number changes similar to cutaneous and mucosal melanomas. *Clin Cancer Res.* 2013;19:3143-3152.

[23] Flaherty, K.T., Infante, J.R., Daud, A., et al. Combined BRAF and MEK inhibition in melanoma with BRAF V600 mutations. *N Engl J Med.* 2012;367:1694-1703.

[24] Flaherty, K.T., Puzanov, I., Kim, K.B., et al. Inhibition of mutated, activated BRAF in metastatic melanoma. *N Engl J Med.* 2010;363:809-819.

[25] Keijser, S., Maat, W., Missotten, G.S., de Keizer, R.J. A new cell line from a recurrent conjunctival melanoma. *Br J Ophthalmol.* 2007;91:1566-1567.

[26] Capes-Davis, A., Reid, Y.A., Kline, M.C., et al. Match criteria for human cell line authentication: where do we draw the line? *Int J Cancer.* 2013;132:2510-2519.

[27] Maat, W., Kilic, E., Luyten, G.P., et al. Pyrophosphorolysis detects B-RAF mutations in primary uveal melanoma. *Invest Ophthalmol Vis Sci.* 2008;49:23-27.

[28] Wong, C.W., Fan, Y.S., Chan, T.L., et al. BRAF and NRAS mutations are uncommon in melanomas arising in diverse internal organs. *J Clin Pathol.* 2005;58:640-644.

[29] Francia, G., Cruz-Munoz, W., Man, S., Xu, P., Kerbel, R.S. Mouse models of advanced spontaneous metastasis for experimental therapeutics. *Nat Rev Cancer.* 2011;11:135-141.

[30] Missotten, G.S., Keijser, S., De Keizer, R.J., De Wolff-Rouendaal, D. Conjunctival melanoma in the Netherlands: a nationwide study. *Invest Ophthalmol Vis Sci.* 2005;46:75-82.

[31] Paridaens, A.D., Minassian, D.C., McCartney, A.C., Hungerford, J.L. Prognostic factors in primary malignant melanoma of the conjunctiva: a clinicopathological study of 256 cases. *Br J Ophthalmol.* 1994;78:252-259.

[32] Damato B, Coupland SE. Conjunctival melanoma and melanosis: a reappraisal of terminology, classification and staging. *Clin Experiment Ophthalmol.* 2008;36:786–795.

[33] Eagle RC. *Eye Pathology: An Atlas and Text. Philadelphia:Williams & Wilkins*; 2011.

[34] Heegaard, S., Jensen, O.A., Prause, J.U. Immunohistochemical diagnosis of malignant melanoma of the conjunctiva and uvea: comparison of the novel antibody against melan-A with S100 protein and HMB-45. *Melanoma Res.* 2000;10:350-354.

[35] Sharara, N.A., Alexander, R.A., Luthert, P.J., Hungerford, J.L., Cree, I.A. Differential immunoreactivity of melanocytic lesions of the conjunctiva. *Histopathology.* 2001;39:426-431.

[36] Keijser, S., Missotten, G.S., Bonfrer, J.M., et al. Immunophenotypic markers to differentiate between benign and malignant melanocytic lesions. *Br J Ophthalmol.* 2006;90:213-217.

[37] Nemeth, J.A., Harb, J.F., Barroso, U., Jr., et al. Severe combined immunodeficient-hu model of human prostate cancer metastasis to human bone. *Cancer Res.* 1999;59:1987-1993.

[38] Yonou, H., Yokose, T., Kamijo, T., et al. Establishment of a novel species- and tissue-specific metastasis model of human prostate cancer in humanized non-obese diabetic/severe combined immunodeficient mice engrafted with human adult lung and bone. *Cancer Res.* 2001;61:2177-

2182.

[39] Kuperwasser, C., Dessain, S., Bierbaum, B.E., et al. A mouse model of human breast cancer metastasis to human bone. *Cancer Res.* 2005;65:6130-6138.

[40] Mueller, M.M., Fusenig, N.E. Constitutive expression of G-CSF and GM-CSF in human skin carcinoma cells with functional consequence for tumor progression. *Int J Cancer.* 1999;83:780-789.

[41] Mueller, M.M., Peter, W., Mappes, M., et al. Tumor progression of skin carcinoma cells in vivo promoted by clonal selection, mutagenesis, and autocrine growth regulation by granulocyte colony-stimulating factor and granulocyte-macrophage colony-stimulating factor. *Am J Pathol.* 2001;159:1567-1579.

[42] Bruns, C.J., Harbison, M.T., Kuniyasu, H., Eue, I., Fidler, I.J. In vivo selection and characterization of metastatic variants from human pancreatic adenocarcinoma by using orthotopic implantation in nude mice. *Neoplasia.* 1999;1:50-62.

[43] Khanna, C., Hunter, K. Modeling metastasis in vivo. *Carcinogenesis.* 2005;26:513-523.

[44] Li, H., Niederkorn, J.Y., Sadegh, L., Mellon, J., Chen, P.W. Epigenetic regulation of CXCR4 expression by the ocular microenvironment. *Invest Ophthalmol Vis Sci.* 2013;54:234-243.

Chapter 5

PD-L1/PD-1 expression and tumor-infiltrating lymphocytes in conjunctival melanoma

Jinfeng Cao*, Niels J. Brouwer*, Kate E. Richards, Marina Marinkovic, Sjoerd van Duinen, Daan Hurkmans, Els M. E. Verdegaal, Ekaterina S. Jordanova, Martine J. Jager

*: Both authors contribute equally to this work.

Pubplished: Oncotarget. 2017; 8: 54722-54734.

DOI: 10.18632/oncotarget.18039.

Abstract

Conjunctival melanoma (CM) is an infrequent but potentially lethal malignancy, with limited therapeutic options for metastases. Recent inhibitors of the interaction of programmed cell death protein 1 (PD-1) and its ligand PD-L1 are associated with good clinical responses in many malignancies. To investigate the therapeutic potential of targeting the PD-1/PD-L1 axis in CM, we analyzed the expression of PD-1 and PD-L1 and the density of various types of tumor-infiltrating lymphocytes (TILs) in primary CM (*n*=27), using immunofluorescence staining. Results were compared with clinical parameters and outcome. Flow cytometry was exploited to determine the PD-L1 and PD-1 protein expression in conjunctival and cutaneous melanoma cell lines. PD-L1 expression was identified on tumor cells in five (19%) primary CM and on stromal cells (mainly $CD68^{+}CD163^{+}$ M2 macrophages) in 16 (59%) cases. PD-L1 expression on tumor cells was associated with the presence of distant metastases and a worse melanoma-related survival. PD-1 expression was seen in 17 (63%) cases, all of which were T2 stage tumors. Small tumors had a higher density of TILs than large tumors. The density of TILs was not correlated with survival, tumoral/stromal PD-L1 or PD-1 expression. *In vitro* results showed that most CM and cutaneous melanoma cell lines do not constitutively express PD-L1. However, expression could be upregulated after interferon gamma stimulation. Our findings suggest that blocking the PD-1/PD-L1 axis should be evaluated as a treatment for CM.

Key words: conjunctiva, melanoma, metastatic, mouse model.

Introduction

Conjunctival melanoma (CM) is a rare ocular malignancy, accounting for 5% of all ocular melanoma [1]. CM is a subtype of mucosal melanoma, which is possibly associated with ultraviolet light exposure [2]. The incidence in Caucasians has risen in the last few decades to 0.8/million [3]. CM arises from melanocytes in the conjunctiva, often presenting as a brownish lesion on the eye. Most frequently, CM develops in primary acquired melanosis (PAM) (up to 74%), and less frequently in a nevus (7%) or de novo (19%) [4]. Treatment of primary CM generally consists of wide local excision followed by adjuvant treatment with either cryotherapy, brachytherapy, or topical chemotherapy [5]. Radical surgical procedures like exenteration are reserved for the most advanced stages [5]. The local recurrence rate is high, and may reach 60% in patients after 5 years, with a 5-year melanoma-related death rate of 14% [6]. Treatment options for metastasis of conjunctival melanoma are currently limited.

Recently, immunotherapies aiming at immune checkpoint pathways, such as cytotoxic T lymphocyte antigen 4 (CTLA-4) and programmed death 1 (PD-1), have been successfully exploited in the treatment of metastases of different malignancies and have led to long-lasting clinical responses [7]. Both CTLA-4 and PD-1 are upregulated on the surface of activated T cells and can bind to their respective ligands: CTLA-4 binds to B7 on antigen-presenting cells (APCs), and subsequently prevents the delivery of co-stimulatory signals and therefore the activation of T cells. PD-1 on T cells binds to the programmed death ligand 1 (PD-L1), a major PD-1 ligand which is present on the cell surface of tumor cells and macrophages, and functionally impairs the activated T cell, thereby preventing it from mounting an effective immune response against tumor antigens. Monoclonal antibodies that inhibit the interaction between PD-1 and PD-L1 block this inhibitory function and have led to improved survival in patients with metastases of cutaneous melanoma, colorectal cancer and non-small cell lung cancer [8-10].

CM in many ways resembles cutaneous melanoma, suggesting that patients with CM metastases might also benefit from treatment with anti-PD-1/PD-L1 agents. PD-L1 expression determined by immunohistochemistry (IHC) on tumor cells is thought to be a potential biomarker predicting the sensitivity of anti-PD-1/PD-L1 treatment [11-13]. Whether blocking the PD-1/PD-L1 axis will be an effective therapy for CM may therefore depend on the PD-1/PD-L1 expression status of CM. To further elucidate the role of the PD-1/PD-L1 axis in CM, and its potential interrelationship with the tumor microenvironment, we studied PD-1/PD-L1 expression and the presence of tumor-infiltrating lymphocytes (TILs) in a cohort of primary CM, and compared expression and (co)localization of these factors to clinical and histological characteristics.

Results

Patient characteristics

We studied primary CM from 27 patients who had been treated at the LUMC between 1996 and 2014 (Table 1). Fifteen (56%) patients were female, and 14 (52%) were over 60 years old. The epibulbar localization (*n*=20) is comprised of limbal (*n*=16) and bulbar conjunctiva (*n*=4). The non-epibulbar localization (*n*=7) includes tarsal, forniceal and caruncular conjunctiva. The clinical TNM stage was T1 in 20 (74%) and T2 in 7 (26%) cases. Two (7%) of the patients underwent surgical excision alone as primary treatment, three (11%) excision with cryotherapy, one (4%) excision and mitomycin C, 16 (59%) excision and subsequent brachytherapy, one (4%) external beam radiation, and four (15%) were treated by exenteration. The median follow-up time was 46 months (range 3-247 months). Eleven (41%) cases developed local recurrences. At the end of the follow-up period, four patients had died from CM metastases, two from unknown diseases without any signs of metastases, and 21 patients were alive.

Table 1. Clinicopathological characteristics and correlation with PD-L1 and PD-1 expression.

Characteristic	All cases	Tumoral PDL1			Stromal PDL1			Stromal PD1		
		Negative	Positive		Negative	Positive		Negative	Positive	
	Cases (%)	*Cases (%)*	*Cases (%)*	*p*	*Cases (%)*	*Cases (%)*	*p*	*Cases (%)*	*Cases (%)*	*p*
Overall	**27 (100)**	**22 (81)**	**5 (19)**		**11 (41)**	**16 (59)**		**10 (37)**	**17 (63)**	
Sex										
Male	12 (44)	10 (45)	2 (40)	1.00*	4 (36)	8 (50)	0.70*	4 (40)	8 (47)	1.00*
Female	15 (56)	12 (55)	3 (60)		7 (64)	8 (50)		6 (60)	9 (53)	
Age at diagnosis										
Age ⩽60 year	13 (48)	12 (55)	1 (20)	0.33*	8 (73)	5 (31)	0.03**	5 (50)	8 (47)	1.00*
Age >60 year	14 (52)	10 (45)	4 (80)		3 (27)	11 (69)		5 (50)	9 (53)	
Tumor size, thickness	***N=23***	***N=20***	***N=3***		***N=10***	***N=13***		***N=9***	***N=14***	
Median [range], mm	1.0 [0.1-16.0]	0.9 [0.2-5.0]	6.0 [0.1-16.0]	0.40[&]	0.8 [0.2-5.0]	1.4 [0.1-16.0]	0.65[&]	0.6 [0.2-5.0]	1.2 [0.1-16.0]	0.56[&]
Tumor size, LBD	***N=24***	***N=19***	***N=5***		***N=10***	***N=14***		***N=9***	***N=15***	
Median [range], mm	9.5 [2.0-30.0]	10.0 [2.0-30.0]	6.0 [5.0-20.0]	0.89[&]	9.5 [2.0-12.0]	10.0 [2.0-30.0]	0.44[&]	7.0 [2.0-15.0]	10.0 [2.0-30.0]	0.48[&]
Location										
Epibulbar	20 (74)	17 (77)	3 (60)	0.58*	9 (82)	11 (69)	0.66*	10 (100)	10 (59)	*0.03**
Non-epibulbar	7 (26)	5 (23)	2 (40)		2 (18)	5 (31)		0 (0)	7 (41)	
cTNM										
T1	20 (74)	17 (77)	3 (60)	0.58*	10 (82)	11 (69)	0.66*	10 (100)	10 (59)	*0.03**
T2	7 (26)	5 (23)	2 (40)		2 (18)	5 (31)		0 (0)	7 (41)	
Local recurrence										
No	16 (59)	13 (59)	3 (60)	1.00*	6 (55)	10 (63)	0.71*	8 (80)	8 (47)	0.12*
Yes	11 (41)	9 (41)	2 (40)		5 (45)	6 (38)		2 (20)	9 (53)	
Distant metastasis										
No	23 (85)	21 (95)	2 (40)	*0.01**	11 (100)	12 (75)	0.12*	10 (100)	13 (76)	0.27*
Yes	4 (15)	1 (5)	3 (60)		0 (0)	4 (25)		0 (0)	4 (24)	

LBD = largest basal diameter. cTNM = clinical TNM stage, based on the first occurring conjunctival melanoma. *P* value calculation: * = Fischer exact test; ** = Pearson's chi-square; [&] = Mann Whitney U test. Italic *P* values are ≤ 0.05.

Expression of PD-L1/PD-1 and TILs in CM

We determined PD-L1 expression on sections of 27 CM that were co-stained with HMB45/MART-1 antibody. The combination allowed us to distinguish between PD-L1 expressing tumor cells versus non-tumor cells. The PD-L1 positive non-tumor cells were mainly comprised of macrophages, similar to what has been described previously [14].

Using a cut-off value of 5%, tumoral and stromal PD-L1 membranous expression was identified in five (19%) and 16 (59%) CM sections, respectively, as illustrated in Figure 1 and Table 1. One tumor showed 30% tumoral PD-L1 expression, while the other four cases had between 5-10% of the tumor cells expressing PD-L1. Published cut-off points used to define PD-L1 positivity vary from 1% to 50% [13]. As only one sample had sporadic PD-L1 positive tumor cells (1% to 5%) in our cohort, we decided to use 5% as cut-off point for comparisons.
PD-L1 expression in stroma was seen more often in patients over 60 (p=0.03), while positive PD-L1 staining in tumor areas was associated with the development of distant metastases (p=0.01). Kaplan-Meier analysis and log rank testing similarly showed that PD-L1 positive staining in the tumor was associated with a worse melanoma-related survival (p=0.045; Figure 4). Furthermore, to better understand the nature of PD-L1 positive cells in stroma, we stained sections from seven CM that contained PD-L1 positive stromal cells with anti-PD-L1, CD68 and CD163 antibodies. We observed that PD-L1 positive stromal cells were mainly$CD68^{+}CD163^{+}$ cells (Figure 2).

PD-1 expression was localized on the membrane of T cells (Figure 3), and was seen in 17 (63%) CM samples. All tumors at T2 stage were PD-1 positive (p=0.03). Absence of PD-1 tended to correlate with less local recurrence (p=0.12). A prior study on cutaneous melanoma showed that those melanomas often harbor intrinsically PD-1-positive tumor cell subpopulations [15]; however, we did not find positive PD-1 staining on the tumor cells themselves.

In order to see whether specific types of infiltrating leukocytes contributed to PD-L1 and PD-1 expression on tumor cells, we determined the presence of different

subsets of T cells and myeloid cells in the same CM, by performing immunofluorescence (IF) staining according to previously described techniques [16]: we measured the numbers of CD3, $CD3^+CD8^+$, $CD3^+CD8^-$, $CD3^+CD8^-Foxp3^+$ and $CD3^+CD8^-Foxp3^-$ T cells, and CD68 (macrophages) and $CD68^+CD163^+$ (M2 macrophages) within tumor areas of 26 primary CM sections. Figure 5 shows an example of a tumor with a high number of infiltrating lymphocytes. In general, all tumors presented a wide variety of different types of TILs (Table 2). T2 tumors showed less infiltration with $CD3^+CD8^-$ and $CD3^+CD8^-Foxp3^-$ positive cells than non-T2 tumors (p=0.048 and 0.02, respectively, Table 2).

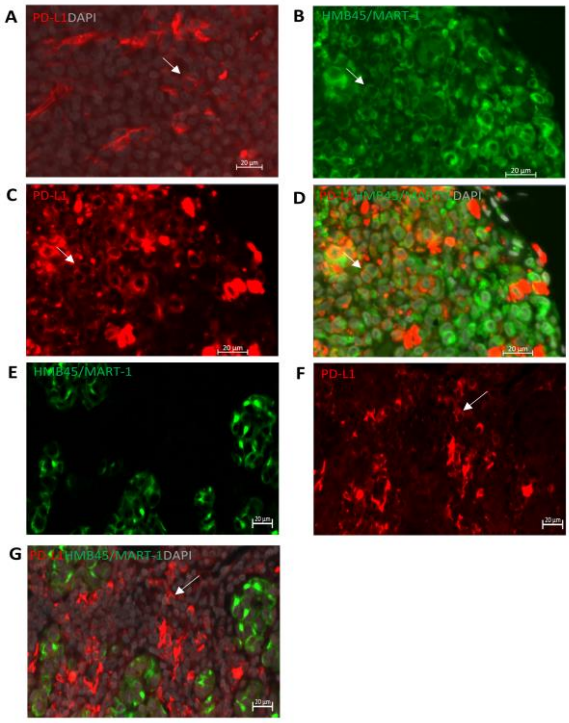

Fig. 1: PD-L1 expression in primary CM as determined by IF analysis. (**A**) Positive membranous PD-L1 (red) staining in the positive control, human tonsil tissue. (**B-D**) Representative images of HMB45/MART-1 (**B**, green, cytoplasmic/membranous), PD-L1 (**C**, red, membranous) and double staining (**D**) with DAPI (grey), show that PD-L1 is expressed on CM cells. (**E-G**) PD-L1 is expressed on HMB45/Mart-1 negative stromal cells. Scale bar is 20µm. White arrows indicate the positive cells.

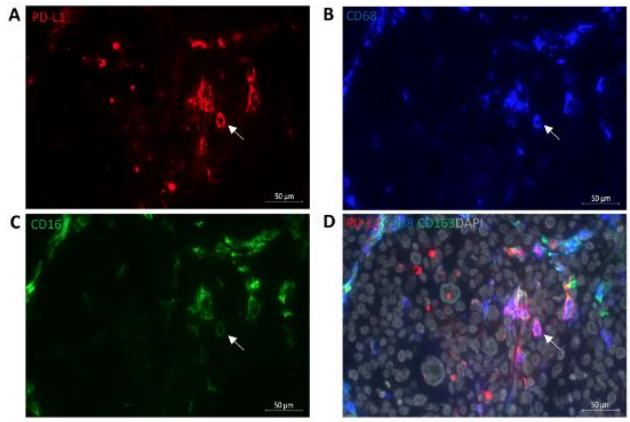

Fig. 2: PD-L1 positive stromal cells are primarily CD68^{+}CD163^{+} macrophages. (**A**) PD-L1 (red, membranous), (**B**) CD68 (blue, cytoplasmic/membranous), (**C**) CD163 (green, cytoplasm/membrane) and merged image (**D**) with DAPI (grey) show that PD-L1 positive stromal cells are also CD68+CD163+ positive cells. White arrow indicates the positive staining. Scale bar is 50µm.

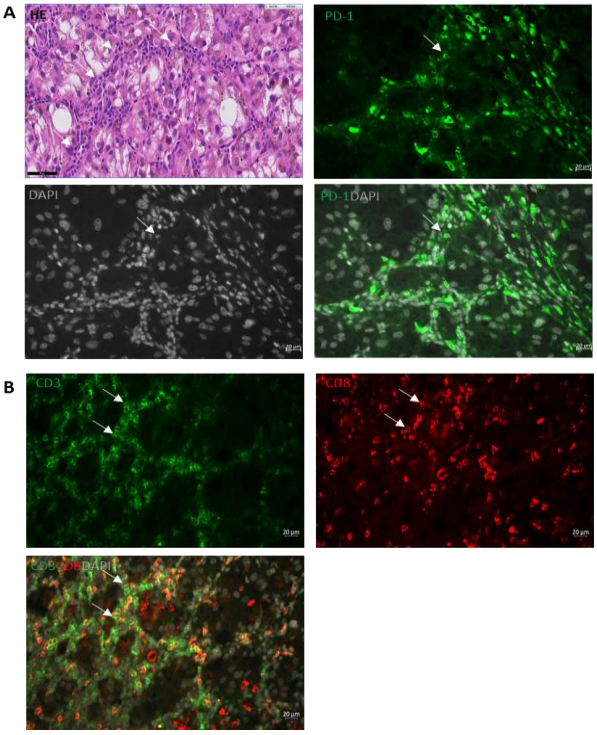

Fig. 3: PD-1 expression in CM. Representative immunohistological staining shows that: (**A**) PD-1 (green, membrane) is expressed on stromal cells surrounding the primary tumor areas (white arrows); (**B**) staining of CD3 (green) and CD8 (red) demonstrates these stromal cells are T cells (white arrows). Scale bar of IF is 20µm, and of HE is 50µm.

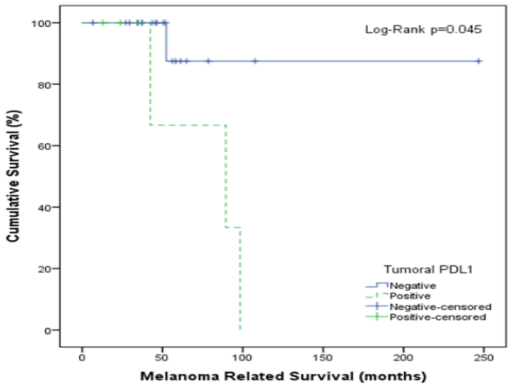

Fig. 4: Survival analysis according to PD-L1 status in CM. Kaplan-Meier plot shows disease-specific survival of patients with PD-L1-positive tumors (green, dotted) and negative tumors (blue, continuous) (cut-off at 5%). *P*-value has been calculated using the log-rank test.

Although the $CD3^+CD8^-Foxp3^+$ regulatory T cells may function as suppressors of effector T cells, Spearman rank analysis showed significantly positive associations between the density of $CD3^+CD8^-Foxp3^+$ and of CD3, $CD3^+CD8^+$, $CD3^+CD8^-$ as well as of $CD3^+CD8^-Foxp3^-$ T cells (Supplementary Table 1). The different subsets of T cells frequently co-infiltrate CM. As tumor thickness is a known prognostic risk factor for CM [17], we correlated the density of TILs with tumor thickness, and observed that thicker tumors had less $CD3^+CD8^+$ T cells (p=0.03) and tumor-infiltrating M2 macrophages (p=0.02; Table 3). Tumors with larger basal diameters contained fewer infiltrating CD3 (p=0.01), $CD3^+CD8^+$(p=0.02), $CD3^+CD8^-$ (p=0.01), $CD3^+CD8^-Foxp3^-$ (p=0.02) and $CD3^+CD8^-Foxp3^+$(p=0.03) T cells within their tumor areas than tumors with smaller basal diameters (Table 3). The density of all types of TILs mentioned above was not correlated with tumoral/stromal PD-L1 expression (p>0.05) or with melanoma-related survival. IF staining of CD68 and $CD68^+CD163^+$ showed that the majority of macrophages belong to the M2 phenotype, suggesting a potential tumor-favorable environment created by macrophages in CM. As high cytotoxic T lymphocyte (CTL)/regulatory T cell (Treg) and high M1 ($CD68^+CD163^-$)/M2 macrophage ratios have been found to be associated with improved survival in breast cancer and cutaneous melanoma, respectively [14,18], we evaluated these ratios in our study. No significant difference in survival or association with clinical parameters was observed (p>0.05). However, higher CTL/Treg ratio tended to correlate with local

recurrence (p=0.13). Correlation coefficients are shown in Table 3 and Supplementary Table 1.

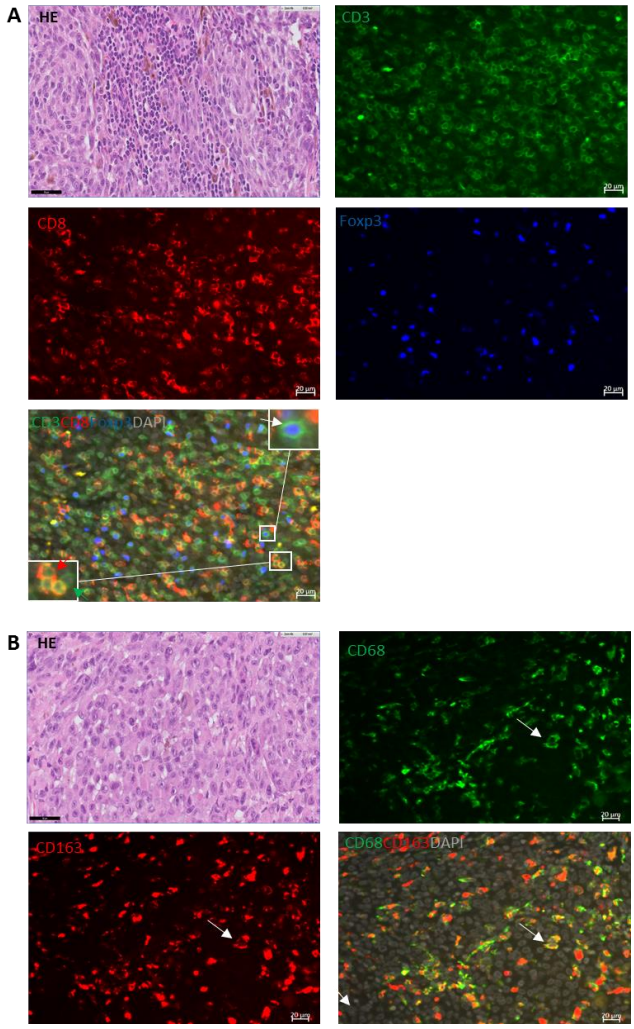

Fig. 5: T cell and macrophage subset analysis in the tumor area of CM. **A**. HE, CD3 (green, membrane), CD8 (red, membrane), Foxp3 (blue, nucleus) and the merged image; the combination of nuclear blue Foxp3 and surface green CD3 staining (white arrow) indicates the presence of $CD3^+CD8^-$ $Foxp3^+$ T cells. The green arrow indicates a $CD3^+CD8^-Foxp3^-$ T cell, and the red arrow points at $CD3^+CD8^+$ T cells. **B**. HE, CD68 (green, cytoplasm/membrane), CD163 (red, cytoplasm/membrane) and merged image shows double-positive M2 macrophages cells. Scale bar of IF is 20µm, and of HE is 50µm.

Table 2. Baseline clinicopathological characteristics and correlation with tumor-infiltrating lymphocytes.

Categorical variables	***Cases (%)***	**CD3**		**$CD3^+CD8^+$**		**$CD3^+CD8^-$**		**$CD3^+CD8^-Foxp3^-$**		**$CD3^+CD8^-Foxp3^+$**		**CD68**		**$CD68^+CD163^+$**	
		Median [range]	*p*	Median [range]	*p*	Median [range]	*p*	Median [range]	*p*	Median [range]	*p*	Median [range]	*p*	Median [range]	*p*
Overall	26 (100)	151 [71-637]		68 [26-335]		70 [26-314]		44 [13-202]		30 [10-124]		59 [19-248]		39 [8-220]	
Sex															
Male	11 (42)	130 [71-637]	0.33	65 [26-335]	0.51	65[26-302]	0.33	39 [13-202]	0.22	32 [11-100]	0.72	39 [19-248]	0.1	30 [8-220]	0.54
Female	15 (58)	159 [85-617]		80 [43-303]		83 [30-314]		53 [13-190]		26[10-124]		63 [22-189]		41 [11-161]	
Age at diagnosis, yr															
⩽60	12 (46)	137 [85-299]	0.86	66 [28-170]	0.86	73 [26-173]	0.98	48 [15-100]	1	30 [11-80]	0.86	40 [19-76]	0.08	29 [8-59]	0.09
>60	14 (54)	158 [71-637]		74 [26-335]		69 [30-314]		42 [13-202]		30 [10-124]		63 [19-248]		43 [18-220]	
Location															
Epibulbar	19 (73)	171 [71-637]	0.08	82 [26-335]	0.15	83 [26-314]	*0.048*	53 [15-202]	*0.02*	34 [10-124]	0.53	63 [19-248]	0.12	41 [8-220]	0.23
Non-epibulbar	7 (27)	121 [110-144]		58 [50-80]		63 [30-76]		35 [13-51]		25 [17-48]		47 [19-63]		22 [11-59]	
cTNM															
T1	19 (73)	171 [71-637]	0.08	82 [26-335]	0.15	83 [26-314]	*0.048*	53 [15-202]	*0.02*	34 [10-124]	0.53	63 [19-248]	0.12	41 [8-220]	0.23
T2	7 (27)	121 [110-144]		58 [50-80]		63 [30-76]		35 [13-51]		25 [17-48]		47 [19-63]		22 [11-59]	
Local recurrence															
No	15 (58)	125[71-617]	0.61	58 [26-303]	0.28	68 [30-314]	0.88	42 [13-189]	0.88	27 [10-124]	0.84	57 [19-189]	1	41 [8-161]	1
Yes	11 (42)	161 [85-637]		74 [43-335]		79 [26-302]		45 [13-202]		32 [11-100]		63 [22-248]		38 [11-220]	
Distant metastasis															
No	22 (85)	151 [71-637]	0.86	66 [26-335]	0.76	70 [26-314]	0.52	46 [15-202]	0.2	27 [10-124]	0.76	63 [19-248]	0.17	43 [8-220]	0.28
Yes	4 (15)	142 [110-207]		77 [62-82]		70 [30-133]		27 [13-92]		39 [17-48]		40 [27-47]		26 [19-39]	

cTNM = clinical TNM stage, based on the first occurring conjunctival melanoma. P values were calculated by Mann Whitney U test. $P \leq 0.05$ are in italics.

Human CM cell lines express various levels of PD-L1

Infiltration lymphocytes may be a source of interferon gamma (IFN-γ), which has been reported to enhance PD-L1 and PD-1 expression [19,20]. To examine how PD-L1 and PD-1 are expressed on the cell surface of CM cell lines, and to determine whether expression is sensitive to environmental cytokines, we performed flow cytometry on three human cutaneous melanoma and three CM cell lines. The cutaneous melanoma cell line MEL13.03 served as PD-L1 and PD-1 positive control. Figure 6 shows that compared to MEL13.03, the other five cell lines were PD-L1 negative, while only one other cell line, CRMM2, expressed PD-1. Next, to mimic the immune environment *in vivo*, we stimulated these cells with IFN-γ. As a control, we determined the upregulation of IFN-γ pathway by analyzing HLA Class I expression, using an anti-HLA class I antibody (Supplementary Figure 1). HLA Class I expression of all cell lines was upregulated upon IFN-γ stimulation. After 48h incubation with IFN-γ, PD-L1 expression was upregulated at different levels on two of the three cutaneous melanoma cell lines (MEL13.03, MEL93.05) and on two of the three CM cell lines tested (CRMM2 and CM2005.1), while PD-1 was only slightly increased on one cell line (CRMM2) (Figure 6).

Table 3. Correlation between different types of infiltrating immune cells and tumor size.

	Tumor thickness		Tumor LBD	
	r	*p*	*r*	*p*
CD3	-0.4	0.06	-0.56	*0.01*
$CD3^+CD8^+$	-0.45	*0.03*	-0.5	*0.02*
$CD3^+CD8^-$	-0.36	0.09	-0.54	*0.01*
$CD3^+CD8^-Foxp3^-$	-0.39	0.07	-0.5	*0.02*
$CD3^+CD8^-Foxp3^+$	-0.32	0.19	-0.46	*0.03*
CD68	-0.38	0.07	-0.26	0.24
$CD68^+CD163^+$	-0.49	*0.02*	-0.23	0.3
Tumor thickness	-	-	0.65	*0.001*

r =two-tailed Spearman correlation coefficient, with 26 observations. LBD = largest basal diameter. $P \leq 0.05$ are in italics.

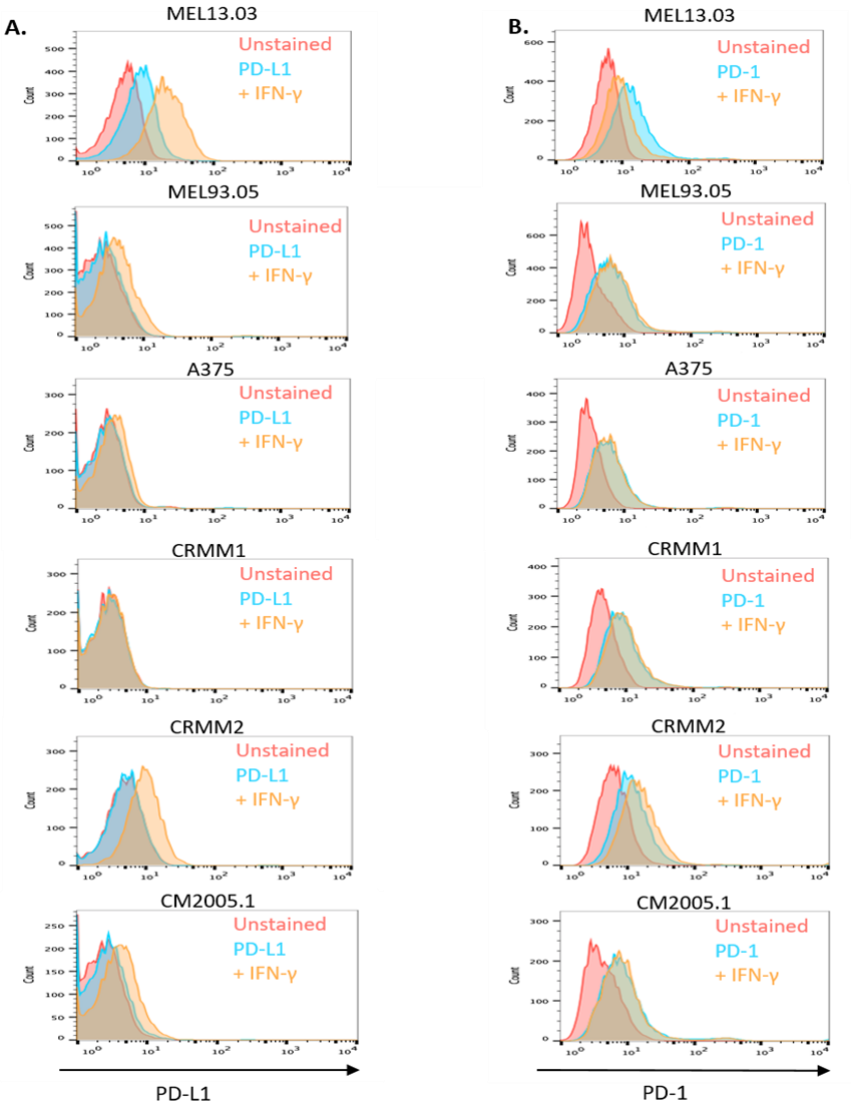

Fig. 6: Cutaneous (MEL13.03, MEL93.05 and A375) and conjunctival melanoma (CRMM1, CRMM2 and CM2005.1) cell lines express various levels of PD-L1 and PD-1. MEL13.03 is the positive control cell line for both PD-L1 and PD-1. Representative histograms show (**A**) PD-L1 and PD-1 (**B**) expression in cell lines with or without IFN-γ (100IU/ml) exposure for 48h. Pink, blue and brown shaded histograms represent unstained, PD-L1 (PD-1) staining, and the effect of IFN-γ stimulation on PD-L1 and PD-1, respectively.

Discussion

Immunotherapies that work through inhibiting the PD-L1/PD-1 axis have been successful in inducing clinical responses in patients with different malignancies, including cutaneous melanoma, non-small cell lung cancer, and bladder cancer [21-23]. However, there are no data yet on the expression of immune checkpoint molecules in CM, a rare malignancy. As far as we know, one ongoing clinical trial testing the efficacy and safety of Ipilimumab in metastatic melanoma patients is currently recruiting CM patients (NCT01355120). Very recently, a CM patient with a breast metastasis was successfully treated with Nivolumab, a monoclonal antibody directly against PD-1 [24]. However, the PD-L1 expression of the primary or metastatic tumor of the patient was not described. Although the accuracy and reproducibility of PD-L1 staining is disputable, and the clinical responses may occur in PD-L1 negative tumors and not all PD-L1 positive tumors respond [23], immunostaining is the best attempt to predict the potential of immune-based therapies [25]. Since most CM are small and heterogenous, and some are pigmented, we decided to use the anti-PD-L1 SP142 clone as it has been shown to work in IF staining on paraffin-embedded sections [14,23]. In addition, it has recently been approved by the FDA as a complementary diagnostic to help make treatment decisions for the use of Atezolizumab in patients with non-small cell lung cancer. We determined whether PD-L1 expression was located on tumor cells or cells of the tumor microenvironment by simultaneous staining with a melanoma marker.

PD-L1 expression is a potential biomarker for prognosis in different types of cancer [26-29]. Expression of PD-L1 has been investigated in varies malignancies with most researchers using either a 1% or 5% cut-off for positivity [30]. Cytoplasmic staining of PD-L1 has often been neglected because the significance of intracellular expression of PD-L1 remains unclear and does not seem functional [31]. In the present study of a human CM cohort, we found that 19% of the tumors expressed PD-L1 (cut-off 5%), and that this expression was correlated with the presence of distant metastases and a worse melanoma-related survival. The incidence of tumor PD-L1 expression is lower than cutaneous melanoma, as reported

previously [32]. However, our finding should be interpreted with caution as our cohort has a limited size. More patients are needed for further analysis of the prognostic value of PD-L1 expression in CM in order to confirm our findings. Although one study shows positive PD-L1 expression in 13% (3/23) of mucosal malignant melanoma of head and neck [33], another study [34] did not find any clinical response by application of PD-1 inhibitors in a group of patients with advanced recurrent mucosal melanoma of head and neck. However, the cohort is rather small (n=5).

Not only expression of PD-L1 on tumor cells may be important, also PD-L1 expressed by myeloid cells in the tumor microenvironment may play an essential role in suppression of the host's immune response, even when the malignant cells lack PD-L1 [14, 35]. Stromal PD-L1 expression can predict poor prognosis in adult T-cell leukemia or lymphoma and gastric carcinoma [9, 29]. Here, we observe that 59% of CM contained PD-L1 positive stromal cells, but expression did not correlate with survival. The PD-L1 positive stromal cells were mainly comprised of $CD68^{+}CD163^{+}$ M2 macrophages, similar to what has been described previously [14]. *In vitro* experiment showed that all CM cell lines expressed low levels of membranous PD-L1, and a variable but clear increase of PD-L1 expression was seen in two out of three CM cell lines following IFN-γ stimulation. These findings suggest that in CM, initially PD-L1 negative or weakly positive tumors may display enhanced PD-L1 expression after exposure to IFN-γ produced by TILs.

Cancer exploits multiple mechanisms to avoid antitumor immune responses. Based on the "cancer immunogram" depicted by Blank, et al. [36], the general immune status and immune cell infiltration needs to be addressed to facilitate the understanding of immune-based treatments. Unlike another type of ocular melanoma, uveal melanoma (UM), the immunology of CM has hardly been studied. Although the unique conjunctiva-associated lymphoid tissue (CALT) system in conjunctiva especially contains B lymphocytes [37], we mainly focus on T lymphocytes because the PD-L1/PD-1 axis inactivates T-cell function. When we compare expression with the cell counts of TILs in UM, using the same antibodies and techniques as in our

prior study on UM, we notice that CM contain higher densities of CD4 ($CD3^+CD8^-$), CD4 helper ($CD3^+CD8^-Foxp3^-$) and Foxp3 ($CD3^+CD8^-Foxp3^+$) cells than UM. However, the densities of CD8 ($CD3^+CD8^+$), CD68 and CD68CD163 cells were lower than those in UM. Compared to one study of cutaneous melanoma metastasis [38], the density of CD3 and CD68CD163 was similar, with a higher density of CD4 and Foxp3, and lower density of CD8 cells. Some studies have shown that PD-L1 expression inversely correlates with TILs [32, 39]. We find no association between tumoral or stromal PD-L1 positivity and the density of TILs. However, the density of TILs was inversely correlated with tumor size, with larger tumors containing fewer immune cells, suggesting that in the absence of infiltrating immune cells, including cytotoxic T cells, the tumor could grow unrestrained.

A major limitation of the present study is the small size of the cohort, coming from a single institute, due to the rarity of CM. We need more patients and tumor material, especially metastases, to carry out further studies and draw solid conclusions. In addition, we should be aware that CM samples are generally quite small, and that a representative section accounts for a small volume of tumor, and may not represent the PD-L1 expression of the whole tumor, as it is known that PD-L1 expression may be quite heterogeneous [35].

In general, we provide a comprehensive view of PD-L1 and PD-1 protein expression, and immune infiltration status in CM. These findings deepen our understanding of the immunology of CM. We believe that these results support the rationale of PD-L1/PD-1 checkpoint immunotherapy for patients with metastatic CM and recommend to include these patients in future immunotherapy clinical trials inhibiting the PD-L1/PD-L1 pathway.

Materials and Methods

Patient data

Twenty-seven patients with histologically-proven primary CM were included in this study. All patients were seen at the Leiden University Medical Center, The

Netherlands, and diagnosed with CM between 1996 and 2014. The medical files were reviewed for clinical and histopathological data. Information regarding the localisation and size of the primary tumors was obtained from the patient files, histology reports, and pre-excision color photographs. All tumors were evaluated by an experienced ophthalmic pathologist. Tumor stage was determined according to the 7th edition of the AJCC TNM cancer staging manual [40]. Treatment was defined as the initial treatment applied immediately or directly after histologic confirmation of CM. Local recurrence was defined as recurrence of histologically-proven CM. Metastasis was proven by histology or imaging. Total follow up time was defined as the time from diagnosis to the last known moment of survival or death. The study adhered to the tenets of the declaration of Helsinki, and the institutional Medical Ethical Committee of LUMC did not object to this retrospective analysis.

Immunofluorescence staining

Formalin-fixed, paraffin-embedded blocks containing tumor material were cut in 4 µm sections, and mounted on slides. After deparaffinization with Xylene, rehydration with alcohol (100%, 90%, 80%, 70%), and Tris-EDTA (pH 9.0) heat-based antigen retrieval, the tissues were incubated with primary antibodies at 4°C overnight. On the second day, after washing with phosphate-buffered saline (PBS), the samples were incubated with AlexaFluor (Invitrogen, Breda, The Netherlands) secondary antibodies for 1 hour at room temperature, followed by washing steps. The slides were counterstained and mounted with VECTASHIELD mounting medium with DAPI (4',6-diamidino-2-phenylindole; H-1200; Vector Laboratories, USA). Tonsil tissues were used as positive control. Incubation with 1% bovine serum albumin (BSA)/PBS instead of primary antibodies served as negative control. One tumor contained only enough material for PD-L1 and PD-1 staining, and not for additional staining. The primary antibodies are listed below: HMB45/Mart-1 (mouse, clone HMB45 + DT101 + BC199, ab732, 1:200; Abcam, UK), anti-PD-L1 (rabbit, clone SP142, 1:100; Spring Bioscience, CA, USA), anti-PD1 (goat, AF1086, 1:100; R&D Systems, UK), CD3 (rabbit, ab828, 1:100; Abcam), anti-CD8 (mouse IgG2b, 4B11, 1:75; Novocastra, Valkenswaard, The Netherlands), anti-FoxP3 (mouse IgG1,

clone 236A/E7, 1:100; Abcam), anti-CD68 (mouse IgG2a, ab49777, 1:75; Abcam) and anti-CD163 (mouse IgG1, clone 10D6, 1:100; Novocastra). The secondary antibodies are in Supplementary Table 2.

Imaging, scoring and analysis

The images of hematoxylin and eosin (HE) stained tumor sections were captured using Philips Image Management System 2.2. Images of IF staining were captured using either a Leica TCS SP8 X or Zeiss LSM 700 confocal laser scanning microscope. Depending on the tumor size, one to seven representative images at high power (250X) in different areas were randomly selected. Tumor areas were morphologically recognized by DAPI nuclear staining. Two investigators, without prior knowledge of clinicopathological data, scored membranous PD-L1 and PD1 expression. Expression of PD-L1 and PD-1 was designated as positive, when ≥5% of the tumor/stromal cells were positive [32,41]. For evaluation of the number of tumor-infiltrating lymphocytes within the tumor sites, tumor regions (mm^2) were evaluated using Leica Application Suite X or Zeiss Zen 2.1 software. Positive cells were counted manually by two observers, as previously described [16]. Results were presented as cell numbers/mm^2.

Cell lines

Three conjunctival melanoma cell lines (CRMM1, CRMM2 and CM2005.1) [42, 43] and three cutaneous melanoma cell lines (A375 (ATCC), and MEL93.05 and MEL13.03, established in the Department of Medical Oncology, LUMC, Leiden) were used in our experiments. To determine the expression of PD-L1 and PD-1 on the cell lines, cells were first seeded in 6-well plates. On the second day, media were refreshed or replaced with culture media containing 100 international units (IU)/ml of IFN-γ (ImmunoTools, Germany) and incubated for 48h. Cells were subsequently prepared for fluorescence-activated cell sorting (FACS).

Flow cytometry

Cells were incubated with the previously determined optimal dilution of mouse

monoclonal PD-L1 (17-5983, APC; Bioscience), PD-1 (329935, FITC; BioLegend) or HLA class I antibodies (W6/32, 311414, Alexa Fluor 647; BioLegend). Cells were collected (10000-20000 per live gate) using the FACSCalibur cytometer (Becton Dickinson), and results were analyzed using FlowJo software (V10.0.7, Flowjo LLC).

Statistical analysis

Data were analyzed with SPSS software version 23.0 (SPSS, Inc., Chigaco, IL, USA). Data were considered statistically significant if $p \leq 0.05$. Pearson's chi square and Fisher's exact test were applied for categorical data; Mann Whitney U test was used for numerical data. Spearman's rank correlation analysis (two-tailed) was performed to compare correlations between different TILs and tumor size. Survival analysis was performed using Kaplan-Meier with log rank tests.

Acknowledgements

We thank Nick Landman for performing flow cytometry, Mieke Versluis for cutting sections, and Brendy EWM van den Akker and Joop Wiegant for assistance using the confocal microscope. We thank Sjoerd van der Burg for critical comments.

Abbreviations

programmed cell death protein 1 (PD-1), programmed death-ligand 1 (PD-L1), conjunctival melanoma (CM), tumor-infiltrating lymphocytes (TIL), cytotoxic T lymphocyte antigen 4 (CTLA-4), antigen-presenting cells (APCs), immunohistochemistry (IHC), immunofluorescence (IF), cytotoxic T lymphocyte (CTL), regulatory T cell (Treg), Interferon-gamma (IFN-γ), conjunctiva-associated lymphoid tissue (CALT).

Conflicts of interests

The authors declare no conflict of interest.

Grant support

This work was supported partly by grants from the China Scholarship Council (JC), the Dutch Cancer Society funding (UL 2013-5757), Horizon 2020 CURE UM grant, The Leiden Ophthalmological Support Fund, The Uveal Melanoma Bontius Fund, and a LUMC MD/PhD programme grant (NJB).

Author contributions

MJJ initiated the idea, supervised the study, obtained funding and critically revised the article. EJ was involved in setting up, conducting and analyzing the experiments, and improving the manuscript. JC performed the experiments, analyzed the data and wrote the manuscript. NB collected materials and clinical information, interpreted data, and wrote the manuscript. KER and DH collected material and clinical data, and KER performed the experiments and interpreted the data. EMV was involved in the experiment and critically reviewed the manuscript. MM and SD gave technical and material support.

References

[1] Isager P, Engholm G, Overgaard J, Storm H. Uveal and conjunctival malignant melanoma in Denmark 1943–97: Observed and relative survival of patients followed through 2002. Ophthalmic Epidemiology. 2006; 13: 85-96.

[2] Triay E, Bergman L, Nilsson B, All-Ericsson C, Seregard S. Time trends in the incidence of conjunctival melanoma in Sweden. Br J Ophthalmol. 2009; 93:1524–1528.

[3] Tuomaala S, Eskelin S, Tarkkanen A, Kivelä T. Populationbased assessment of clinical characteristics predicting outcome of conjunctival melanoma in whites. Invest Ophthalmol Vis Sci. 2002; 43:3399-3408.

[4] Shields CL, Markowitz JS, Belinsky I, Schwartzstein H, George NS, Lally SE, Mashayekhi A, Shields JA: Conjunctival melanoma, outcome based on tumor origin in 382 consecutive cases. Ophthalmology. 2011; 118:389-395.

[5] Wong JR, Nanji AA, Galor A, Karp CL. Management of conjunctival melanoma: a review and update. Expert Rev Ophthalmol. 2014; 9:185-204.

[6] Missotten GS, Keijser S, De Keizer RJ, De Wolff-Rouendaal D. Conjunctival melanoma in the Netherlands: a nationwide study. Invest Ophthalmol Vis Sci. 2005; 46:75-82.

[7] Sharma P, Allison JP. The future of immune checkpoint therapy. Science. 2015; 348:56–61.

[8] Weber JS, D'Angelo SP, Minor D, Hodi FS, Gutzmer R, Neyns B, Hoeller C, Khushalani NI, Miller WH Jr, Lao CD, Linette GP, Thomas L, Lorigan P, et al.: Nivolumab versus chemotherapy in patients with advanced melanoma who progressed after anti-CTLA-4 treatment (CheckMate 037): a randomised, controlled, open-label, phase 3 trial. Lancet Oncol. 2015; 16:375-84.

[9] Miyoshi H, Kiyasu J, Kato T, Yoshida N, Shimono J, Yokoyama S, Taniguchi H, Sasaki Y, Kurita D, Kawamoto K, Kato K, Imaizumi Y, Seto M, Ohshima K. PD-L1 expression on neoplastic or stromal cells is respectively a poor or good prognostic factor for adult T-cell leukemia/lymphoma. Blood. 2016; 128:1374-1381.

[10] Li Y, Liang L, Dai W, Cai G, Xu Y, Li X, Li Q, Cai S. Prognostic impact of programed cell death-1 (PD-1) and PD-ligand 1 (PD-L1) expression in cancer cells and tumor infiltrating lymphocytes in colorectal cancer. Mol Cancer. 2016; 15:55. doi: 10.1186/s12943-016-0539-x.

[11] Taube JM, Anders RA, Young GD, Xu H, Sharma R, McMiller TL, Chen S, Klein AP, Pardoll DM, Topalian SL, Chen L. Colocalization of inflammatory response with B7-h1 expression in human melanocytic lesions supports an adaptive resistance mechanism of immune escape. Sci Transl Med. 2012; 4:127ra37.

[12] Mahoney KM, Freeman GJ, McDermott DF. The next immune checkpoint inhibitors: PD-1/PD-L1 blockade in melanoma. Clinical Ther. 2015; 37:765-782.

[13] Patel SP, Kurzrock R. PD-L1 Expression as a Predictive Biomarker in Cancer Immunotherapy. Mol Cancer Ther. 2015; 14:847-856.

[14] Heeren AM, Punt S, Bleeker MC, Gaarenstroom KN, van der Velden J, Kenter GG, de Gruijl TD, Jordanova ES. Prognostic effect of different PD-L1 expression patterns in squamous cell carcinoma and adenocarcinoma of the cervix. Mod Pathol. 2016; 29:753-763.

[15] Kleffel S, Posch C, Barthel SR, Mueller H, Schlapbach C, Guenova E, Elco CP, Lee N, Juneja VR, Zhan Q, Lian CG, Thomi R, Hoetzenecker W, et al. Melanoma cell-intrinsic PD-1

receptor functions promote tumor growth. Cell. 2015; 162:1242-1256.

[16] Bronkhorst IH, Vu TH, Jordanova ES, Luyten GP, van der Burg SH, Jager MJ. Different subsets of tumor-infiltrating lymphocytes correlate with macrophage influx and monosomy 3 in uveal melanoma. Invest Ophthalmol Vis Sci. 2012; 53:5370-5378.

[17] Tuomaala S, Toivonen P, Al-Jamal R, Kivelä T. Prognostic significance of histopathology of primary conjunctival melanoma in Caucasians. Curr Eye Res. 2007; 32:939-952.

[18] Melief SM, Visconti VV, Visser M, van Diepen M, Kapiteijn EH, van den Berg JH, Haanen JB, Smit VT, Oosting J, van der Burg SH, Verdegaal EM. Long-term survival and clinical benefit from adoptive T-cell transfer in stage IV melanoma patients is determined by a four-parameter tumor immune signature. Cancer Immunol Res. 2017; 5:170-179.

[19] Terawaki S, Chikuma S, Shibayama S, Hayashi T, Yoshida T, Okazaki T, Honjo T. IFN-α directly promotes programmed cell death-1 transcription and limits the duration of T cell-mediated immunity. J Immunol. 2011; 186:2772-2779.

[20] Abiko K, Matsumura N, Hamanishi J, Horikawa N, Murakami R, Yamaguchi K, Yoshioka Y, Baba T, Konishi I, Mandai M. IFN-γ from lymphocytes induces PD-L1 expression and promotes progression of ovarian cancer. Br J Cancer. 2015; 112:1501-1509.

[21] Topalian SL, Hodi FS, Brahmer JR, Gettinger SN, Smith DC, McDermott DF, Powderly JD, Carvajal RD, Sosman JA, Atkins MB, Leming PD, Spigel DR, Antonia SJ, et al. Safety, activity, and immune correlates of anti-PD-1 antibody in cancer. N Engl J Med. 2012; 366:2443–2454.

[22] Powles T, Eder JP, Fine GD, Braiteh FS, Loriot Y, Cruz C, Bellmunt J, Burris HA, Petrylak DP, Teng SL, Shen X, Boyd Z, Hegde PS, et al. MPDL3280A (anti-PD-L1) treatment leads to clinical activity in metastatic bladder cancer. Nature. 2014; 515:558-562.

[23] Herbst RS, Soria JC, Kowanetz M, Fine G, Hamid O, Gordon MS, Sosman JA, McDermott DF, Powderly JD, Gettinger SN, Kohrt HE, Horn L, Lawrence DP, et al. Predictive correlates of response to the anti-PD-L1 antibody MPDL3280A in cancer patients. Nature. 2014; 515:563-567.

[24] Ford J, Thuro BA, Thakar S, Hwu WJ, Richani K, Esmaeli B. Immune checkpoint inhibitors for treatment of metastatic melanoma of the orbit and ocular adnexa. Ophthal Plast Reconstr Surg. 2016. DOI: 10.1097/IOP.0000000000000790.

[25] Bhaijee F, Anders RA. PD-L1 Expression as a Predictive Biomarker: Is absence of proof the same as proof of absence? JAMA Oncol. 2016; 2:54-55.

[26] Sabatier R, Finetti P, Mamessier E, Adelaide J, Chaffanet M, Ali HR, Viens P, Caldas C, Birnbaum D, Bertucci F. Prognostic and predictive value of PDL1 expression in breast cancer. Oncotarget. 2015; 6: 5449-5464.

[27] Böger C, Behrens HM, Mathiak M, Krüger S, Kalthoff H, Röcken C. PD-L1 is an independent prognostic predictor in gastric cancer of Western patients. Oncotarget. 2016; 7:24269-24283.

[28] Ottenhof SR, Djajadiningrat RS, de Jong J, Thygesen HH, Horenblas S, Jordanova ES. Expression of programmed death ligand 1 in penile cancer is of prognostic value and associated with HPV Status. J Urol. 2017; 197:690-697.

[29] Cho J, Lee J, Bang H, Kim ST, Park SH, An JY, Choi MG, Lee JH, Sohn TS, Bae JM, Kang WK, Kim S, Kim KM. Programmed cell death-ligand 1 expression predicts survival in patients with gastric carcinoma with microsatellite instability. Oncotarget. 2017; doi: 10.18632/oncotarget.14519.

[30] Ilie M, Hofman V, Dietel M, Soria JC, Hofman P. Assessment of the PD-L1 status by

immunohistochemistry: challenges and perspectives for therapeutic strategies in lung cancer patients. Virchows Arch 2016; 268:511-525.

[31] Mahoney KM, Sun H, Liao X, et al. PD-L1 antibodies to its cytoplasmic domain most clearly delineate cell membranes in immunohistochemical staining of tumor cells. Cancer Immunol Res. 2015; 3:1308-1315.

[32] Taube JM, Klein A, Brahmer JR, Xu H, Pan X, Kim JH, Chen L, Pardoll DM, Topalian SL, Anders RA. Association of PD-1, PD-1 ligands, and other features of the tumor immune microenvironment with response to anti-PD-1 therapy. Clin Cancer Res. 2014; 20:5064-5074.

[33] Thierauf J, Veit JA, Affolter A, Bergmann C, Grünow J, Laban S, Lennerz JK, Grünmüller L, Mauch C, Plinkert PK, Hess J, Hoffmann TK. Identification and clinical relevance of PD-L1 expression in primary mucosal malignant melanoma of the head and neck. Melanoma Research. 2015; 25:503–509.

[34] Thierauf J, Veit JA, Hess J, Treiber N, Lisson C, Weissinger SE, Bommer M, Hoffmann TK. Checkpoint inhibition for advanced mucosal melanoma. Eur J Dermatol. 2017; 27:160-165.

[35] McLaughlin J, Han G, Schalper KA, Carvajal-Hausdorf D, Pelekanou V, Rehman J, Velcheti V, Herbst R, LoRusso P, Rimm DL. Quantitative assessment of the heterogeneity of PD-L1 expression in non–small-cell lung cancer. JAMA Oncol. 2016; 2:46-54.

[36] Blank CU, Haanen JB, Ribas A, Schumacher TN. Cancer immunology. The "cancer immunogram". Science. 2016; 352:658-660.

[37] Knop N, Knop E. Conjunctiva-associated lymphoid tissue in the human eye. Invest Ophthalmol Vis Sci. 2000; 41:1270-1279.

[38] Erdag G, Schaefer JT, Smolkin ME, Deacon DH, Shea SM, Dengel LT, Patterson JW, Slingluff CL Jr. Immunotype and immunohistologic characteristics of tumor-infiltrating immune cells are associated with clinical outcome in metastatic melanoma. Cancer Res. 2012; 72:1070-1080.

[39] Inman BA, Sebo TJ, Frigola, Dong H, Bergstralh EJ, Frank I, Fradet Y, Lacombe L, Kwon ED. XPD-L1 (B7-H1) expression by urothelial carcinoma of the bladder and BCG-induced granulomata: associations with localized stage progression. Cancer. 2007; 109:1499-1505.

[40] Edge SB, Byrd DR, Comptom CC, editors. AJCC Cancer Staging Manual. 7th ed. New York, NY: Springer; 2010; 539-546.

[41] D'Incecco A, Andreozzi M, Ludovini V, Rossi E, Capodanno A, Landi L, Tibaldi C, Minuti G, Salvini J, Coppi E, Chella A, Fontanini G, Filice ME. PD-1 and PD-L1 expression in molecularly selected non-small-cell lung cancer patients. Br J Cancer. 2015; 112:95-102.

[42] Nareyeck G, Wuestemeyer H, von der Haar D, Anastassiou G. Establishment of two cell lines derived from conjunctival melanomas. Exp Eye Res. 2005; 81:361-362.

[43] Keijser S, Maat W, Missotten GS, de Keizer RJ. A new cell line from a recurrent conjunctival melanoma. Br J Ophthalmol. 2007; 91:1566-1567.

Supplementary files

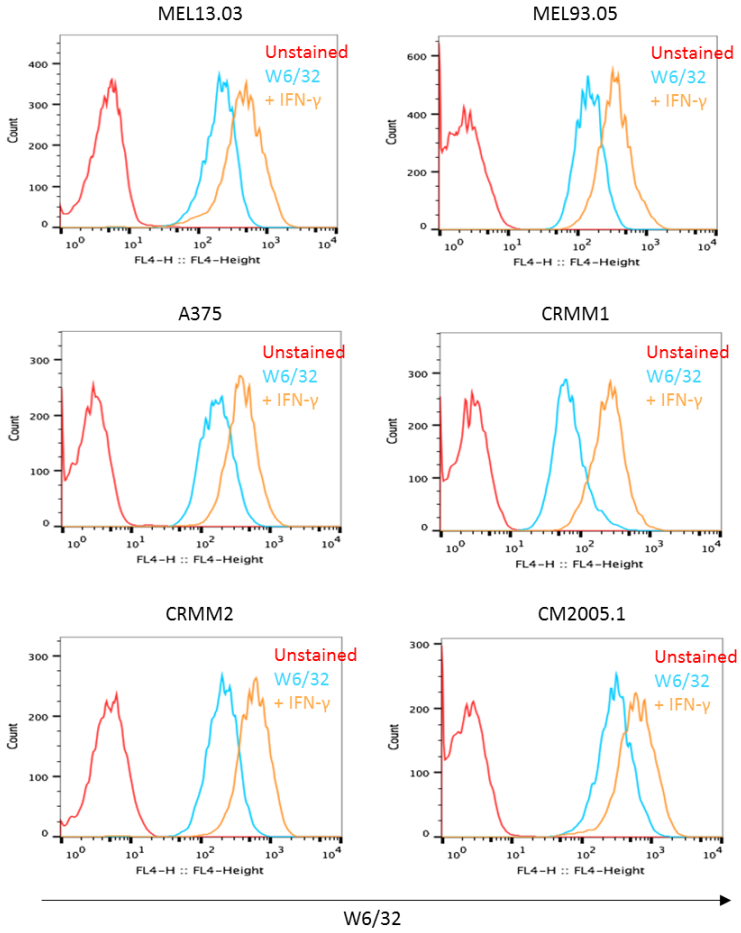

Supplementary Fig. 1. The confirmation of IFN-γ effect on cutaneous (MEL13.03, MEL93.05 and A375) and conjunctival melanoma (CRMM1, CRMM2 and CM2005.1) cell lines using the anti-human HLA-A, B, C antibody (W6/32). The cells were treated with IFN-γ (100IU/ml) for 48h. Histograms with red, blue and brown line represent unstained, W6/32 expression, and the effect of IFN-γ stimulation on W6/32, respectively.

Supplementary Table 1. Correlation between different infiltrating immune Cells (T Cells and Macrophages)

		$CD3^+CD8^+$	**$CD3^+CD8^-$**	**$CD3^+CD8^-$ $Foxp3^-$**	**$CD3^+CD8^-$ $Foxp3^+$**	**CD68**	**$CD68^+CD163^+$**
CD3	*r*	0.84	0.95	0.88	0.84	0.63	0.48
	P	*<0.001*	*<0.001*	*<0.001*	*<0.001*	*0.001*	*0.01*
$CD3^+CD8^+$	*r*		0.69	0.63	0.57	0.59	0.46
	P		*<0.001*	*0.001*	*0.002*	*0.001*	*0.02*
$CD3^+CD8^-$	*r*			0.93	0.84	0.53	0.38
	P			*<0.001*	*<0.001*	*0.005*	0.053
$Foxp3^-$	*r*				0.65	0.51	0.34
	P				*<0.001*	*0.01*	0.09
$Foxp3^+$	*r*					0.49	0.46
	P					*0.01*	*0.02*
CD68	*r*						0.87
	P						*<0.001*

r =two-tailed Spearman correlation coefficient, with 26 observations. $P \leq 0.05$ are in italics.

Supplementary Table 2. Secondary antibodies used in IF

Antibody	Specificity	Isotype	Company	Catalogue number	Dilutions
AlexaFluor 488	mouse	IgG	Life Technologies	A-11001	1:300
AlexaFluor 546	rabbit	IgG	Life Technologies	A-11010	1:300
AlexaFluor 488	goat	IgG	Life Technologies	A-11055	1:300
AlexaFluor 488	rabbit	IgG	Life Technologies	A-11034	1:300
AlexaFluor 546	mouse	IgG2b	Life Technologies	A-21143	1:300
AlexaFluor 647	mouse	IgG1	Life Technologies	A-21240	1:300
AlexaFluor 488	mouse	IgG2a	Life Technologies	A-21131	1:300
AlexaFluor 546	mouse	IgG1	Life Technologies	A-21123	1:300
AlexaFluor 647	mouse	IgG2a	Life Technologies	A-21241	1:300
AlexaFluor 488	mouse	IgG1	Life Technologies	A-21121	1:300

Chapter 6

HLA class I antigen expression in conjunctival melanoma is not associated with PD-L1/PD-1 status

Jinfeng Cao, Niels J. Brouwer, Ekaterina S. Jordanova, Marina Marinkovic, Sjoerd van Duinen, Nadine E. de Waard, Bruce R. Ksander, Arend Mulder, Frans H.J. Claas, Mirjam H.M. Heemskerk, Martine J. Jager

Submitted for publication

Abstract

Purpose: Anti-tumor T cells need expression of human leukocyte antigen (HLA) class I molecules, but can be inhibited by ligands such as PD-L1. We determined expression and regulation of these molecules in human conjunctival melanoma (CM) samples, cell lines, and murine xenografts.

Methods: Immunofluorescence staining was performed to examine the expression of HLA-A, HLA-B/C and beta-2-microglobulin (B2M) in 23 primary CM samples. HLA class I expression was compared with clinicopathological characteristics, the presence of tumor-infiltrating leukocytes and PD-L1/PD-1 status. The effect of interferon gamma (IFN-γ) on HLA class I expression was tested on three CM cell lines using qPCR and flow cytometry. Furthermore, HLA class I expression was determined in CM cell line-derived murine xenografts.

Results: One third of tumors had positive HLA-A, HLA-B/C and B2M expression. A positive expression was especially seen in thin and epibulbar tumors, but not associated with recurrences. HLA class I expression was correlated with M2 macrophage density, and tended to associate with $CD8^+$ T cell density, but was independent of PD-L1 or PD-1 expression. IFN-γ upregulated HLA class I expression and genes involved in HLA transcription and transportation on CM cell lines. Murine xenografts showed a comparable HLA class I expression as their respective cell lines.

Conclusions: Our data indicate that subsets of CM have positive HLA class I expression, and HLA class I and PD-L1/PD-1 are expressed independently. When one considers immunotherapy to a CM patient, one should keep the variable HLA class I expression in mind.

Key words: conjunctival melanoma, HLA class I, immune escape, animal model, tumor infiltrating lymphocytes.

Introduction

Currently, a lot of attention is given to the role of the immune system in tumor growth, control and treatment. The theory of immune surveillance, which states that the immune system can recognize and destroy tumor cells, has been widely accepted and provides targets for therapy[1]. The discovery of immune checkpoint regulators has transformed the treatment of many malignancies: cancer often protects itself from T cell attack by blocking T cell signals. Binding of programmed death ligand 1 (PD-L1) on the cancer cell to PD-1 on the T cell will suppress the T cell's function, impair cytokine production, and induce T cell apoptosis. To reverse this immunologically-tolerant state, antibodies against these immune checkpoints have been developed, which target e.g. PD-1 or cytotoxic T-lymphocyte-associated protein 4 (CTL-A4). The results in cutaneous melanoma, bladder cancer, non-small cell lung cancer and mucosal melanoma are promising, but restricted to subsets of patients[2-5].

Expression of the human leukocyte antigen (HLA) class I molecules is needed to recognize and lyse tumor cells by cytotoxic T cells: cytotoxic T cells (CTL) can destruct cells which express the appropriate peptide/MHC class I complex[6]. HLA class I molecules consist of a glycoprotein heavy chain (coded in the HLA region on chromosome 6p21) and a beta-2-microglobulin (B2M) light chain (gene located on chromosome 15)[7]. Defects in HLA class I antigen-processing machinery (APM) components impair effective immune responses to cancer, although tumor-infiltrating lymphocytes may still present. A lack of HLA class I expression which may be associated with a worse survival[8], has been described in many malignancies, and can either be "soft" (reversible) or "hard" (irreversible), due to various mechanisms[9]. A low HLA expression can often be corrected by interferon-gamma (IFN-γ), thereby restoring a tumor cell's susceptibility to be lysed by T cells.

Although a lot of immunological research in melanoma has focused on cutaneous lesions, little is known about melanoma of the conjunctiva. Conjunctival melanoma (CM) is a rare type of mucosal melanoma that originates in the melanocytes of the basal layer of the conjunctiva and accounts for 5% of all ocular

melanoma[10]. The incidence in Caucasians is 0.8/million[11], and in recent years has been increasing in Western countries[12,13]. The appearance of CM ranges from amelanotic to heavily pigmented and CM can occur in any part of the epibulbar or non-epibulbar conjunctiva. Wide local excision with adjuvant treatment (cryotherapy, chemotherapy, brachytherapy) is the most common therapy, while more extensive surgical procedures are reserved as a last resort therapy[14]. Despite treatment, recurrence rates of 26-61% 5-year post treatment have been reported[15-18], with metastases occurring in 11-16% of patients[15,19]. Since limited chemotherapeutic options are available for extended or metastasized CM, these patients may benefit from the new T-cell-mediated treatments. We recently described that PD-1 and PD-L1 positive cells are present in CM[20], making treatment with PD-L1/PD-1 inhibitors potentially interesting. Very recently, Nivolumab (PD-1 inhibitor) led to a successful clinical response in a CM patient with breast metastases[21].

However, effective T cell immune responses also need a proper expression of the HLA class I antigens. Currently, very little is known regarding the expression of the HLA class I antigens in CM. We studied the degree of HLA class I expression in human CM samples, CM cell lines and animal xenografts. We found out that HLA class I expression was not associated with PD-L1/PD-1 status, and detected positive HLA class I expression in only one third of primary CM.

Methods

Patient data and selection

Patients were treated at the Leiden University Medical Center, Leiden, The Netherlands, between 1996 and 2014. The tumour cohort included 23 primary CM for which sufficient material was available (Table 1). Tumors were examined by an experienced ophthalmic pathologist (SD). Tumor stage was assessed according to the 7th edition of the AJCC TNM cancer staging manual[22]. Local recurrence was defined as a histologically-proven recurrence. Metastasis was verified by histological examination or imaging analysis. Total follow-up time was from the

time of diagnosis to the last known status. The study adhered to the tenets of the Declaration of Helsinki, and the Medical Ethical Committee of LUMC agreed with this retrospective study.

Immunohistological staining and scoring

Immunofluorescence (IF) staining of HLA-A, HLA-B/C and B2M on human paraffin-embedded CM sections was performed as previously described[19,23]. For immunohistochemistry (IHC) on mouse xenografts, the procedures were performed as described[24]. In short, primary antibodies HCA2 (mouse, anti-HLA-A, IgG1, MUB2036P, 1:50; Nordic Mubio), HC10 (mouse, anti-HLA-B/C, IgG2a, MUB2037P, 1:100; Nordic Mubio) and B2M (rabbit, Z0311, 1:2000 (IHC), 1:1000 (IF); DAKO) were used for both IF and IHC staining. Isotype control staining was obtained by replacing primary antibodies with control antibodies with respective isotypes antibodies. The detailed information of secondary antibodies is in Supplementary Table 1. IF images were taken using a Zeiss LSM 700 confocal scanning microscope. Based on the tumor size, one to five representative images at high power (250X) were randomly selected from different areas for scoring. Tumor areas were distinguishable from normal tissue by DAPI (4',6-diamidino-2-phenylindole; H-1200; Vector Laboratories, USA) staining. Two independent observers (JC and NB or EJ), blinded to the clinicopathological data, evaluated the intensity and percentage of HC10, HCA2 and B2M expression separately. In case of discrepancies, a consensus was reached by simultaneous analysis. The semi-quantitative scoring system was obtained from prior studies[23,25-27]: intensity was scored as 0 (absent), 1 (weak), 2 (moderate) and 3 (strong), and the percentage of positive cells as 0 (0%), 1 (1-5%), 2 (6-25%), 3 (26-50%), 4 (51-75%) and 5 (76-100%). A single value was reached by adding intensity and percentage, and was used to create three categories: negative (0-2), weak (3-6) and positive expression (7-8). Stromal cells served as an internal positive control. The B2M staining of one tumor was not scorable, and was therefore excluded. The images of hematoxylin and eosin (HE) staining were captured using the Philips Image Management System 2.2. The staining and scoring method of tumor-infiltrating lymphocytes (CD3, $CD3^+CD8^+$,

$CD3^+CD8^-$, $CD3^+CD8^-Foxp3^+$ and $CD3^+CD8^-Foxp3^-$ T cells, and CD68 and $CD68^+CD163^+$ macrophages) was performed as previously described[20]. Expression of PD-L1 on tumor or stromal cells and of PD-1 was determined as described[20].

HLA typing

HLA typing was performed at the Laboratory of the Department of Immunohematology and Blood Transfusion (IHB, LUMC) using the Gen-Probe LIFECODES HLA-SSO HLA Typing assay for HLA class I typing.

Cell lines and treatment

Three CM cell lines (CRMM1, CRMM2 and CM2005.1) derived from primary tumors, kindly provided by Michele Madigan (Sydney, Australia) and Sander Keijser (Leiden University Medical Center, Leiden, The Netherlands) were used[28,29]. To examine the influence of IFN-γ on HLA class I expression, CM cells were cultured with or without 100 international units (IU)/ml of IFN-γ (ImmunoTools, Germany) for 48h[30].

RNA isolation and quantitative real-time polymerase chain reaction (qPCR)

The isolation of total cellular RNA, complementary DNA conversion and qPCR was performed based on a standard protocol of our laboratory, as described previously[31]. Primer sequences are in Supplementary Table 2. CFX Manager 3.1 (Bio-Rad) software was used to analyse the data: the Ct values of each sample were normalized against the geometric mean Ct values of housekeeping genes (RPS11 and RPL13).

Flow cytometry

Cells were incubated with anti-HLA class I antibody (W6/32, 311414, Alexa Fluor 647; BioLegend) to detect total HLA class I expression. HLA-allele specific monoclonal antibodies were obtained from the IHB Department, LUMC (Supplementary Table 3)[32,33], and were applied for detecting HLA allele-specific expression. Appropriate FITC (F0315, DAKO) or RPE (R5111, DAKO) secondary antibodies were selected. Cells were collected (10,000-50,000 cells per live gate)

using Accuri C6 or FACSCalibur cytometer (Beckton Dickinson). Results were analysed with FlowJo software (V10.0.7, Flowjo LLC).

In vivo xenografts

Mice were used to grow xenografts of CM cell lines[24]. Briefly, non-obese diabetic (NOD)/severe combined immunodeficiency (SCID) IL-2 receptor gamma chain null mice were subconjunctivally injected with one of three CM cell lines. Subsequently, cells (CRMM1 and CM2005.1) obtained from established CM tumor xenografts were reinjected into the subconjunctival space of the second set of NOD/SCID mice. This *in vivo*-passaging technique led to lung metastases. The animal experiment was maintained under the guidelines of the Schepens Eye Research Institute, Boston, USA, and experiments were carried out based on the guidelines for the use of animals in research of the Association for Research in Vision and Ophthalmology.

Statistical analysis

Data were analyzed with SPSS software version 22.0 (SPSS, Inc., Chigaco, IL, USA). Statistical significance was defined as $p \leq 0.05$. Fisher-Freeman-Halton test and Kruskal-Wallis test were used.

Results

Frequent downregulation of HLA class I expression in primary CM

HCA2 and HC10 recognize HLA-A and HLA-B/C, respectively[34]. B2M is a component of the HLA class I complex[35]. We used triple immuno-fluorescence staining to determine the percentage of positively-staining tumor cells and the intensity of staining on formalin-fixed, paraffin-embedded sections of 23 human primary CM (Figure 1). Expression of HLA-A, HLA-B/C and B2M correlated strongly (Table 2). Four (17%) cases showed no staining of HLA-A, three (13%) cases no expression of HLA-B/C, and three cases (14%) no staining of B2M (Table 1). Twelve (52%), 13 (57%) and 11 (50%) cases exhibited weak expression (scores 3-6) of HLA-A, HLA-B/C, and B2M, respectively, with the remaining tumors

showing a positive expression of B2M, HLA-A and HLA-B/C. Heterogenous HLA class I expression was seen in three cases, as presented in Figure 2.

Patient characteristics

We correlated expression levels of HLA-A, HLA-B/C, and B2M with clinical and histopathological data (Table 1, supplementary Table 4). The mean age of the patients at diagnosis was 62.6 (SD 14.3) years, and 13 of the 23 patients (57%) were women. The median follow-up time was 42 months (range 3-249 months). At the end of the follow-up, 10 (43%) patients had developed local recurrences, three (13%) had died from CM metastases, two (9%) from unknown causes, while 18 (78%) patients were alive. Local recurrence was only related to tumor largest basal diameter (p=0.046), not to tumor thickness (p=0.24), or TNM stage (p=0.089). HLA-A, HLA-B/C or B2M expression was not correlated with largest basal diameter, local recurrence, metastasis formation, or melanoma-related survival. Epibulbar/T1 tumors had a higher HLA class I expression than non-epibulbar/T2 tumors (p=0.03 HCA2, p=0.046 B2M, Table 1). Thicker tumors showed a lower HLA-A as well as B2M expression than the thinner tumors (p=0.03 and 0.046, respectively), with a trend for downregulation of HLA-B/C (p=0.08). Additionally, thick tumors had fewer $CD68^+CD163^+$ macrophages (r=-0.56, p=0.01). Expression of HLA class I was associated with the number of $CD68^+CD163^+$ macrophages in the tumor area (p=0.03 HCA2, p=0.07 HC10, p=0.02 B2M, Table 2) and tended to correlate with $CD8^+$ T cell density (p=0.09 HCA2, p=0.10 HC10, p=0.14 B2M, Table 2). These data suggest that macrophages and T cells play a role in stimulating HLA class I expression in CM (Table 2). Expression of PD-L1 on tumor or stromal cells, and of PD-1 occurred independently of HLA class I expression (Table 1 and Cao et al.[20]). Figure 2.

mRNA and membrane expression of HLA class I in CM cell lines

To better understand the regulation of HLA class I expression in CM, we studied

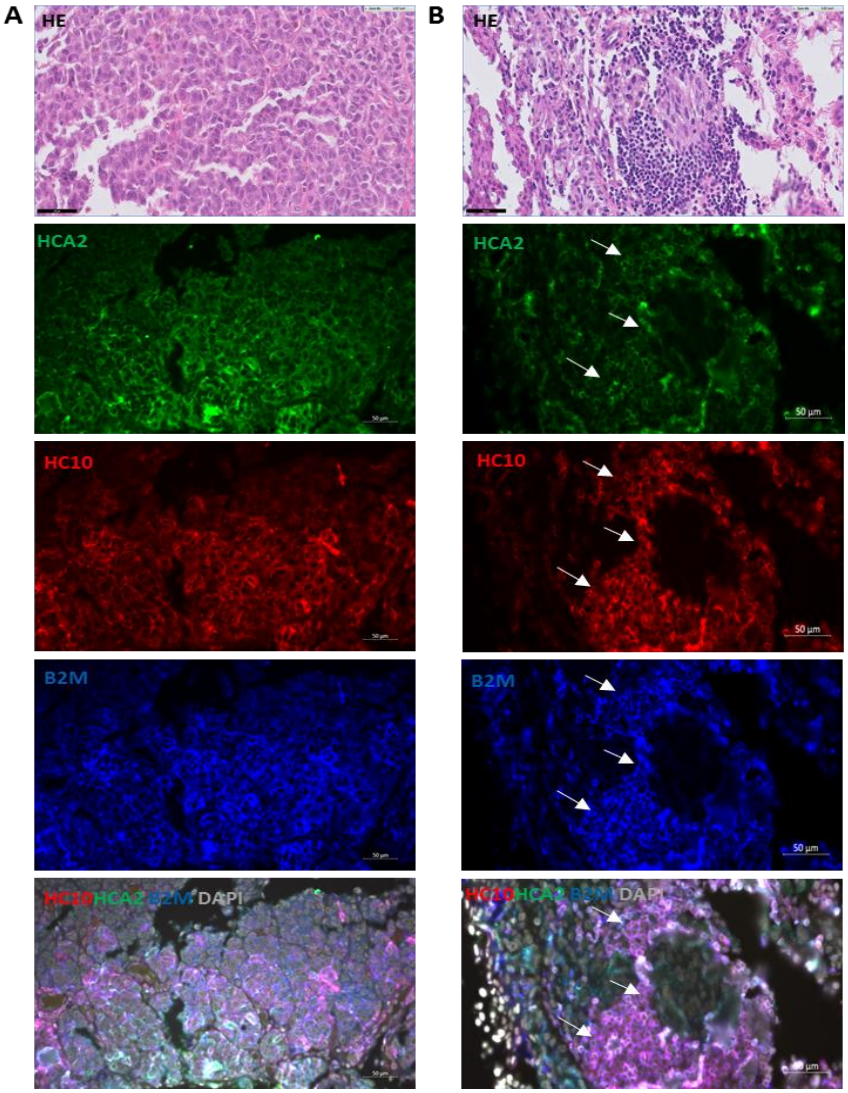

Figure 1. **Immunofluorescence analysis of HLA class I expression**. Representative pictures of triple staining show expression on CM cells in one tumor (**A**) and on T cells in another (**B**): similar membrane expression patterns are seen for the antibodies HCA2 (HLA-A, green), HC10 (HLA-B/C, red), and B2M (HLA class I, blue), respectively. White arrows indicate T cells surrounding the tumor area. Scale bar is 50µm.

Table 1. Clinicopathological characteristics and correlation with HLA-A, HLA-B/C and B2M expression.

Characteristic	All cases	HLA-A (HCA2)				HLA-B/C (HC10)				B2M			
		negative	weak	positive		negative	weak	positive		negative	weak	positive	
	Cases (%)	*Cases (%)*	*Cases (%)*	*Cases (%)*	*p*	*Cases (%)*	*Cases (%)*	*Cases (%)*	*p*	*Cases (%)*	*Cases (%)*	*Cases (%)*	*p*
Overall	23 (100)	4 (17)	12 (52)	7 (30)		3 (13)	13 (57)	7 (30)		3 (14)	11 (50)	8 (36)	
Sex													
Male	10 (43)	1 (25)	4 (33)	5 (71)	0.28*	1 (33)	4 (31)	5 (71)	0.25*	1 (33)	3 (27)	5 (63)	0.30*
Female	13 (57)	3 (75)	8 (67)	2 (29)		2 (67)	9 (69)	2 (29)		2 (67)	8 (73)	3 (38)	
Age at diagnosis, yr													
⩽60	11 (48)	2 (50)	6 (50)	3 (43)	1.00*	1 (33)	8 (62)	2 (29)	0.42*	1 (33)	7 (64)	3 (38)	0.51*
>60	12 (52)	2 (50)	6 (50)	4 (57)		2 (67)	5 (38)	5 (71)		2 (67)	4 (36)	5 (63)	
Tumor thickness	***N=21***	***N=4***	***N=11***	***N=6***		***N=3***	***N=13***	***N=5***		***N=3***	***N=11***	***N=7***	
Median [range], mm	1.2 [0.1-16.0]	1.9 [0.8-16.0]	1.4 [0.2-6.0]	0.2 [0.1-2.5]	*0.03*†	2.5 [0.8-16.0]	1.2[0.2-6.0]	0.2 [0.1-2.5]	0.08†	2.5 [0.8-16.0]	1.4 [0.2-6.0]	0.2 [0.1-2.5]	*0.046*†
Tumor LBD	***N=20***	***N=4***	***N=10***	***N=6***		***N=3***	***N=12***	***N=5***		***N=3***	***N=10***	***N=7***	
Median [range], mm	11.0 [2.0-30.0]	12.0 [7.0-30.0]	12.0 [5.0-20.0]	6.5 [2.0-12.0]	0.14†	16.0 [7.0-30.0]	12.0 [5.0-20.0]	6.0 [2.0-12.0]	0.06†	16.0 [7.0-30.0]	11.0 [5.0-20.0]	7.0 [2.0-12.0]	0.17†
Location													
Epibulbar	16 (70)	1 (25)	8 (67)	7 (100)	*0.03* *	1 (33)	9 (69)	6 (86)	0.30*	1 (33)	7 (64)	8 (100)	*0.046* *
Non-epibulbar	7 (30)	3 (75)	4 (33)	0 (0)		2 (67)	4 (31)	1 (14)		2 (67)	4 (36)	0 (0)	
cTNM													
T1	16 (70)	1 (25)	8 (67)	7 (100)	*0.03* *	1 (33)	9 (69)	6 (86)	0.30*	1 (33)	7 (64)	8 (100)	*0.046* *
T2	7 (30)	3 (75)	4 (33)	0 (0)		2 (67)	4 (31)	1 (14)		2 (67)	4 (36)	0 (0)	
Local recurrence													
No	13 (57)	4 (100)	7 (58)	2 (29)	0.08*	3 (100)	8 (62)	2 (29)	0.18*	3 (100)	7 (64)	3 (38)	0.20*
Yes	10 (43)	0 (0)	5 (42)	5 (71)		0 (0)	5 (38)	5 (71)		0 (00)	4 (36)	5 (63)	
Distant metastasis													
No	20 (87)	4 (100)	10 (83)	6 (86)	1.00*	3 (100)	12 (92)	5 (71)	0.53*	3 (100)	10 (91)	7 (88)	1.00*
Yes	3 (13)	0 (0)	2 (17)	1 (14)		0 (0)	1 (8)	2 (29)		0 (0)	1 (9)	1 (13)	
Tumoral PD-L1													
No	19 (83)	3 (75)	11 (92)	5 (71)	0.46*	2 (66)	12 (92)	5 (71)	0.31*	2 (66)	10 (91)	6 (75)	0.43*
Yes	4 (17)	1 (25)	1 (8)	2 (29)		1 (33)	1 (8)	2 (29)		1 (33)	1 (9)	2 (25)	
Stromal PD-L1													
No	9 (39)	1 (25)	6 (50)	2 (29)	0.62*	0 (0)	8 (62)	1 (14)	0.051*	0 (0)	6 (55)	3 (38)	0.25*
Yes	14 (61)	3 (75)	6 (50)	5 (71)		3 (100)	5 (38)	6 (86)		3 (100)	5 (45)	5 (63)	
PD-L1													
No	7 (30)	1 (25)	5 (42)	1 (14)	0.59*	1 (66)	5 (38)	1 (14)	0.69*	1 (66)	5 (45)	1 (13)	0.27*
Yes	16 (70)	3 (75)	7 (58)	6 (86)		2 (33)	8 (62)	6 (86)		2 (33)	6 (55)	7 (88)	

LBD = largest basal diameter. cTNM = clinical TNM stage, based on the first occurring conjunctival melanoma. * = Fisher-Freeman-Halton test; † = Kruskal-Wallis test. Italic *p* values are ≤ 0.05. Some columns/rows do not add up to 100 due to rounding. HLA scoring system is based on previous studies[23]: intensity was scored as 0 (absent), 1 (weak), 2 (moderate) and 3 (strong), and the percentage of positive cells as 0 (0%), 1 (1-5%), 2 (6-25%), 3 (26-50%), 4 (51-75%) and 5 (76-100%). A single value was given by adding intensity and percentage, and was used to evaluate HLA class I expression in three categories: negative (0-2), weak (3-6) and positive (7-8). B2M: beta-2-microglobulin.

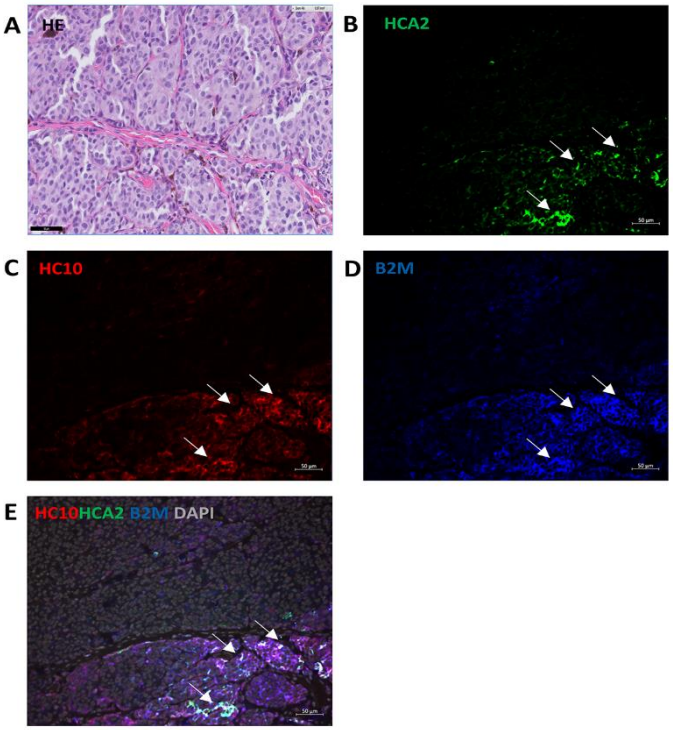

Figure 2. Heterogeneous expression of HLA class I antigens in a CM. Representative IF staining shows membranous HCA2 (HLA-A, green), HC10 (HLA-B/C, red), and B2M (HLA class I, blue) expression only in the lower part of the tumor area. White arrows indicate areas of positive expression. Scale bar is 50μm.

Table 2. Correlation between thickness, HLA expression and different types of infiltrating immune cells.

		HLA-A (HCA2)	HLA-B/C (HC10)	B2M	CD3	$CD3^+CD8^+$	$CD3^+CD8^-$	$CD3^+CD8^-$ $Foxp3^-$	$CD3^+CD8^-$ $Foxp3^+$	CD68	$CD68^+C$ $D163^+$
Thickness	*r*	-0.49	-0.5	-0.53	-0.35	-0.39	-0.32	-0.33	-0.27	-0.35	-0.5
	P	*0.02*	*0.02*	*0.01*	0.12	0.08	0.16	0.15	0.23	0.12	*0.02*
HLA-A (HCA2)	*r*	-	0.94	0.97	0.25	0.36	0.17	0.18	0.22	0.4	0.45
	P	-	*<0.01*	*<0.01*	0.25	0.09	0.45	0.41	0.31	0.06	*0.03*
HLA-B/C (HC10)	*r*	-	-	0.97	0.29	0.36	0.18	0.15	0.33	0.3	0.38
	P	-	-	*<0.01*	0.18	0.1	0.4	0.51	0.13	0.16	0.07
B2M	*r*	-	-	-	0.31	0.33	0.24	0.25	0.28	0.43	0.49
	P	-	-	-	0.17	0.14	0.27	0.25	0.21	*0.04*	*0.02*

r =two-tailed Spearman correlation coefficient, with 23 observations. $P \leq 0.05$ are in italics. The staining and scoring method is previously described16. B2M: beta-2-microglobulin.

three CM cell lines. For this, we first performed HLA-DNA typing (Table 3). CRMM1 genetically carries the HLA-A*02:01 allele, which is a very attractive genotype, because so far, most of the clinical T-cell receptor (TCR) cancer therapies are HLA-A*02:01 restricted.

Table 3. Results of HLA typing in three CM cell lines.

Cell line	HLA alleles
CRMM1	A*02:01/02:07/02:09+, A*02:01/02:07/02:09+, B*44:03/44:07/44:13+, B*44:03/44:07/44:13+, C*04:01/04:07/04:09N+, C*04:01/04:07/04:09N+, DRB1*07:01/07:03/07:04+, DRB1*07:01/07:03/07:04+ DQB1*02:01/02:02/02:04+, DQB1*02:01/02:02/02:04+
CRMM2	A*03:01/03:37/03:03N+, A*30:01/30:14L/30:15+, B*40:01/40:22N/40:54+, B*44:02/44:23N/44:27+, C*03:04/03:24/03:35+, C*05:01/05:05/05:07N+, DRB1*11:01/11:04/11:02+, DRB1*13:01/13:02/13:05+, DQB1*06:03/06:07/06:14+, DQB1*06:03/06:07/06:14+
CM2005.1	A*11:01/11:05/11:07+, A*24:02/24:06/24:09N+, B*14:02/14:09/14:16+, B*35:01/35:41/35:07+, C*02:02/02:09/02:11+, C*04:01/04:09N/04:28+, DRB1*01:01/01:07/01:04+, DRB1*14:54/14:01/14:07+, DQB1*05:01/05:03/05:02, DQB1*05:03/05:02/05:07+

Next, we determined expression of HLA-A, HLA-B, B2M on the three cell lines and analyzed the effect of IFN-γ, which is a known HLA stimulator. HLA allele-specific antibodies were selected according to the results of the HLA DNA typing. Flow cytometry analysis showed that most genetically-determined HLA class I antigens were expressed, except for HLA-A2 and HLA-B44 on CRMM1, and HLA-B44 on CRMM2 (Figure 3A). IFN-γ treatment increased the expression of most alleles, except for HLA-A2 on CRMM1 and HLA-B44 on CRMM2, indicating a hard loss of HLA antigens.

When loss of expression was observed, we set out to determine whether there was a normal activity of the transcriptional regulators (CIITA, IRF1, NLRC5) and

genes encoding the peptide-loading machinery (TAP1, TAP2), using specific primers and qPCR. NLRC5 is essential for HLA class I transcription, whereas CIITA and IRF1 are involved in HLA class I as well as class II transcriptional regulation. TAP1 and TAP2 transport peptides from the cytoplasm to the endoplasmic reticulum and present these peptides to MHC class I molecules[35]. Figure 3B shows that the three CM cell lines presented various baseline mRNA levels of the regulator genes. mRNA expression of not only HLA-A, HLA-B, B2M, but also of CIITA, IRF1, NLRC5, TAP1, and TAP2 was increased after IFN-γ stimulation, indicating that these molecules were normally responsive.

HLA class I expression was maintained in animal xenografts

We previously established a CM metastasis model using *in vivo* passaging[24], and wondered whether *in vivo* placement of the tumor cell lines affected HLA expression. Because immunodeficient mice were used, the HLA class I expression on xenografts would not be influenced by local infiltration with T lymphocytes and environmental cytokines, thus showing the tumor's "natural" expression. IHC staining using HCA2, HC10, and B2M antibodies showed that HLA class I expression of CM cells was maintained in the murine models in the same manner as on the cell lines *in vitro* (Figure 4 and Table 4). There seemed a trend towards a decrease of HLA class I expression during tumor progression (primary-in vivo passaged-metastasis, Figure 4); however, HLA class I was expressed at all stages.

Discussion

We investigated expression of HLA class I molecules in primary CM and compared HLA class I expression with clinical parameters. In only a third of CM did we observe a positive expression of HLA-A (~30%), HLA-B/C (~30%), and B2M (~36%). The presence of a negative or weak HLA class I antigen expression in about 70% of CM is similar to that of bladder cancer, but higher than of cutaneous mela-

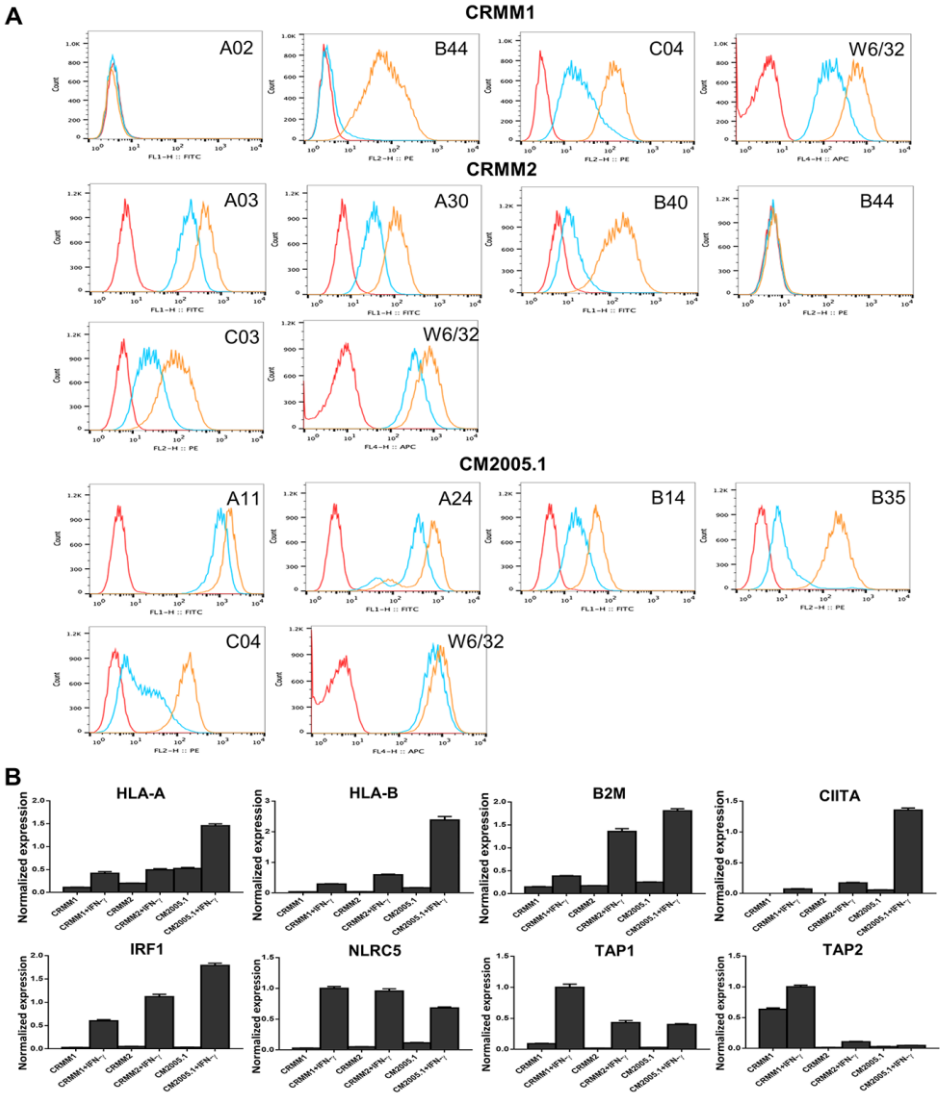

Figure 3. IFN-γ upregulates protein and gene expression of HLA class I, and increases mRNA levels of several HLA regulators in CM cell lines. Cells were treated with or without IFN-γ (100IU/ml) exposure for 48h. (**A**) Representative histograms show the surface expression of HLA class I (W6/32) and specific HLA allele antigens of CRMM1, CRMM2 and CM2005.1 cell lines. Histograms with red, blue and brown line represent unstained, baseline expression, and expression after IFN-γ stimulation, respectively. (**B**) The mRNA expression of HLA genes (HLA-A, HLA-B, B2M), HLA transcriptional regulators (CIITA, IRF1, NLRC5) and genes encoding the peptide-loading machinery (TAP1, TAP2) were variably increased, after IFN-γ stimulation.

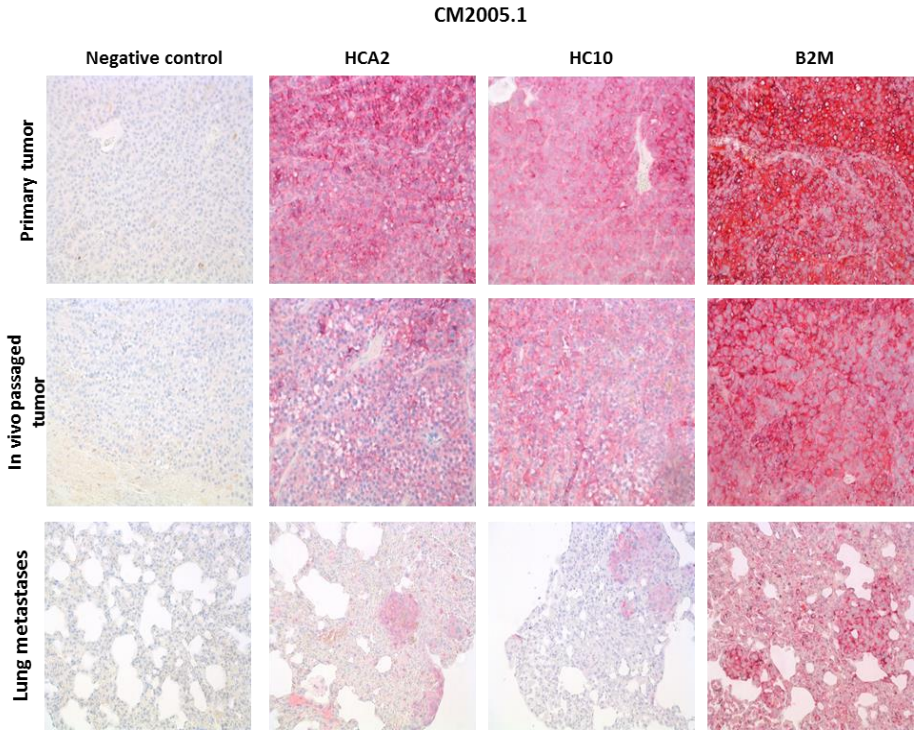

Figure 4. Murine xenografts maintain their HLA class I expression. Representative images present the membranous expression of HLA-A (HCA2), HLA-B/C (HC10) and B2M in a CM2005.1 murine model. Cells from cell line CM2005.1 were first placed subconjunctivally, transferred to the subconjunctival space of a second set of mice, and spread systemically, giving rise to lung metastases. Images were taken at ×200 magnification.

noma and intrahepatic cholangiocarcinoma[37,38]. Several factors may contribute to this observed lack of HLA class I antigen expression: mutations or loss of heterozygosity (LOH) in chromosomes 6 or 15 (where B2M is located), or prior immune selection, leaving only HLA class I negative tumor cells[39]. We did indeed find some tumors that lacked B2M, but do not have information on mutations in this gene. An absent or low expression of HLA class I has been associated with a worse survival in patients with advanced cutaneous melanoma, cervical cancer and rectal cancer[26,40,41]. We did not find a correlation between HLA class I expression and melanoma-related survival in primary CM. However, we did notice that an aberrant

Table 4. HLA class I expression in CM murine xenografts.

	Staining intensity/% Positive tumor cells		
Material	**HLA-A (HCA2)**	**HLA-B/C (HC10)**	**B2M**
CRMM1			
Primary tumor	2/2 (Weak)	2/2 (Weak)	3/3 (Weak)
In vivo-passaged tumor	0/0 (Negative)	2/1 (Weak)	2/2 (Weak)
Lung metastasis	0/0 (Negative)	0/0 (Negative)	0/0 (Negative)
CRMM2			
Primary tumor	2/3 (Weak)	1/2 (Weak)	3/4 (Positive)
CM2005.1			
Primary tumor	3/3 (Weak)	3/2 (Weak)	3/5 (Positive)
In vivo-passaged tumor	3/1 (Weak)	3/2 (Weak)	3/4 (Positive)
Lung metastasis	1/3 (Weak)	2/3 (Weak)	2/3 (Weak)

The staining intensity scoring system is described in the material and methods. B2M: beta-2-microglobulin.

HLA class I expression was significantly correlated with one of the known prognostic factors, i.e. tumor thickness, which is concordant with previous investigations in cervical cancer and cutaneous melanoma[42,43]. The association of HLA class I expression with M2 macrophages and $CD8^+$ T cells suggests a connection of IFN-γ with HLA class I expression in the tumor. The cytokine IFN-γ, mainly secreted by CD4 Th1, CD8 T lymphocytes, macrophages and NK cells[44], is known to be a key modulator of HLA expression. The data on expression and regulation of most of the HLA antigens on three unique CM cell lines, using HLA DNA typing, qPCR and flow cytometry, indeed confirmed this theory: after IFN-γ treatment, mRNA expression levels of CIITA, IRF1, NLRC5, TAP1 and TAP2 were increased, together with HLA class I molecules. Our finding is similar to previous investigations using UM cell lines[36]. Interestingly, the flow cytometry data showed that not all alleles were expressed on the cell surface: although the HLA-A*02:01

and HLA-B*44:02 alleles were detected by HLA DNA typing, they were not expressed on the cell surface of CRMM1 and CRMM2, respectively. This result may be explained by allele-specific mutations, or by post-translational instability due to a missing disulfide bridge[45]. This remains to be investigated.

To further test our theory that the presence of infiltrating immune cells plays a role in HLA expression, we looked at murine xenografts, that were obtained by injection of three CM cell lines into the subconjunctiva of NOD/SCID-mice (with impaired T, B and NK cells). We noticed that primary tumors of the xenograft showed a similarly low HLA class I expression as the cell lines (Figure 3 and Figure 4). In addition, a trend towards gradually decreased HLA class I expression in the xenografts after *in vivo* passaging and on a lung metastasis was seen (Figure 4). A lack of IFN-γ production may be responsible for this finding, as lack of lymphocytic infiltration leads to low IFN-γ production. In a study on uveal melanoma, HLA class I expression was similarly weaker in SCID murine xenografts than in their original freshly-obtained tumors, which had shown high HLA class I expression[35]. However, another study shows an opposite outcome: in a mouse fibrosarcoma model, a HLA class I negative tumor clone led to HLA class I-positive spontaneous lung metastasis in immunodeficient mice which lacked T cells[46].

TCR-based immunotherapies against cutaneous melanoma have also been studied extensively in the last decade, using $CD8^+$ T cells which recognize the tumor-associated antigens of amongst others, tyrosinase, MAGE-A1 (melanoma-associated antigen A1), MART-1 (melanoma antigen recognized by T cells), glycoprotein 100 (gp100)[47]. In this context, a proper HLA class I expression is needed because metastatic cutaneous melanoma with a low HLA class I expression was resistant to T cell-based immunotherapy and progressed[48,49]. A recent study shows that mutations in B2M and IFN genes contribute to the recurrences of four metastatic cutaneous melanoma patients after anti-PD-1 (pembrolizumab) therapy[50]. These findings strongly suggest that both "soft" (reversible) and "hard" (irreversible) types of absence of HLA class I expression can influence the efficacy of T cell-mediated immunotherapy. Our FACS tests showed that some of the HLA antigens were not

expressed, even in the presence of IFN-γ, while other antigens showed a higher expression following exposure to IFN-γ. This indicates that both the soft as well as the hard type of downregulation of HLA expression occurs in CM. PD-L1/PD-1 was not expressed on the same tumors as the HLA antigens, therefore HLA expression cannot be used to predict the effect of PD-L1/PD1 checkpoint inhibitors.

Although our study contains only a small cohort from one medical centre, to the best of our knowledge, this is the first comprehensive view of HLA class I expression of CM *in vivo* and *in vitro*. The downregulation of HLA class I may contribute to the mechanisms of immune escape, and limit effective T-cell immune responses. When designing the immune-therapeutic strategies to treat CM, one should evaluate tumor cell HLA class I expression and potentially enhance it to improve the efficacy of T cell-based immunotherapy.

Acknowledgements

The authors thank T. Huibertus van Essen and Pieter van den Velden for providing the primers for qPCR, Pieter van der Linden and Dave L. Roelen for HLA typing, and Marjolein Sluijter for helping with the flow cytometry. The authors appreciate the effort of Sean P. McGuire and Paraskevi E. Kolovou on the mouse model. And the authors thank Aat A. Mulder for the assistance of IHC and Brendy EWM van den Akker for the assistance with the confocal microscope.

This work was supported partly by grants from the China Scholarship Council (JC, 201206170141), the Bontius Stichting, the Dutch Cancer Society (UL 2013-5757), the LUMC MD/PhD program grant (NJB), Nelly Reef Fund, the Bontius Uveal Melanoma Fund, Ms. I. Brouwer, LOOF and Horizon2020 CURE UM (667787).

References

1. Dunn GP, Bruce AT, Ikeda H, Old LJ, Schreiber RD. Cancer immunoediting: from immunosurveillance to tumor escape. *Nat Immunol*. 2002;3:991-998.

2. Weber JS, D'Angelo SP, Minor D, et al.: Nivolumab versus chemotherapy in patients with advanced melanoma who progressed after anti-CTLA-4 treatment (CheckMate 037): a randomised, controlled, open-label, phase 3 trial. *Lancet Oncol*. 2015;16:375-384.

3. Mahoney KM, Freeman GJ, McDermott DF. The next immune checkpoint inhibitors: PD-1/PD-L1 blockade in melanoma. *Clinical Ther*. 2015;37:764-782.

4. Rizvi NA, Hellmann MD, Snyder A, et al. Cancer immunology. Mutational landscape determines sensitivity to PD-1 blockade in non-small cell lung cancer. *Science*. 2015;348:124-128.

5. Butler M, Hamid O, Ribas A, et al. Efficacy of pembrolizumab in patients with advanced mucosal melanoma enrolled in the KEYNOTE-001, 002, and 006 studies [ECCO abstract]. Eur J Cancer. 2017;72 Suppl 1:S123.

6. Andersen MH, Schrama D, Thor Straten P, Becker JC. Cytotoxic T cells. *J Invest Dermatol*. 2006;126:32-41.

7. Natarajan K, Li H, Mariuzza RA, Margulies DH. MHC class I molecules, structure and function. *Rev Immunogenet*. 1999;1:32-46.

8. Sabbatino F, Schwab JH, Ferrone S, Ferrone CR. Evolution of studies of HLA class I antigen processing machinery (APM) components in malignant cells. *Clin Transpl*. 2013:453-463.

9. Garrido F, Algarra I, García-Lora AM. The escape of cancer from T lymphocytes: immunoselection of MHC class I loss variants harboring structural-irreversible "hard" lesions. *Cancer Immunol Immunother*. 2010;59:1601-160.

10. Isager P, Engholm G, Overgaard J, Storm H. Uveal and conjunctival malignant melanoma in denmark 1943-97: observed and relative survival of patients followed through 2002. *Ophthalmic Epidemiol*. 2006;13:85-96.

11. Tuomaala S, Eskelin S, Tarkkanen A, Kivelä T. Population-based assessment of clinical characteristics predicting outcome of conjunctival melanoma in whites. *Invest Ophthalmol Vis Sci*. 2002;43:3399-3408.

12. Yu GP, Hu DN, McCormick S, Finger PT. Conjunctival melanoma: is it increasing in the United States? *Am J Ophthalmol*. 2003;135:800-806.

13. Triay E, Bergman L, Nilsson B, All-Ericsson C, Seregard S. Time trends in the incidence of conjunctival melanoma in Sweden. *Br J Ophthalmol*. 2009; 93:1524-1528.

14. Wong JR, Nanji AA, Galor A, Karp CL. Management of conjunctival malignant melanoma: a review and update. *Expert Rev Ophthalmol*. 2014;9:185-204.

15. Shields CL, Shields JA, Gündüz K, et al. Conjunctival melanoma: risk factors for recurrence, exenteration, metastasis, and death in 150 consecutive patients. *Arch Ophthalmol*. 2000;118:1497-1507.

16. Werschnik C, Lommatzsch PK. Long-term follow-up of patients with conjunctival melanoma. *Am J Clin Oncol*. 2002;25:248-255.

17. Missotten GS, Keijser S, De Keizer RJ, De Wolff-Rouendaal D. Conjunctival melanoma in the Netherlands: a nationwide study. *Invest Ophthalmol Vis Sci*. 2005;46:75-82.

18. Shields CL, Markowitz JS, Belinsky I, et al. Conjunctival melanoma: outcomes based on tumor origin in 382 consecutive cases. *Ophthalmology*. 2011;118:389-95. e1-2.

19. Tuomaala S, Kivelä T. Metastatic pattern and survival in disseminated conjunctival melanoma: implications for sentinel lymph node biopsy. *Ophthalmology*. 2004;111:816-821.

20. Cao J, Brouwer NJ, Richards KE, et al. PD-L1/PD-1 expression and tumor-infiltrating lymphocytes in conjunctival melanoma. *Oncotarget*. 2017;8:54722-54734.

21. Ford J, Thuro BA, Thakar S, Hwu WJ, Richani K, Esmaeli B. Immune checkpoint inhibitors for treatment of metastatic melanoma of the orbit and ocular adnexa. *Ophthal Plast Reconstr Surg*. [published online Sep 21, 2016]. doi: 10.1097/IOP.0000000000000790.

22. Edge SB, Byrd DR, Compton CC, et al. Malignant melanoma of the conjunctiva. *AJCC Cancer Staging Manual 7th ed*. New York, NY: Springer; 2010:539–546.

23. Gezgin G, Luk SJ, Cao J, et al. PRAME as a Potential target for immunotherapy in metastatic uveal melanoma. *JAMA Ophthalmol*. 2017;135:541-549.

24. de Waard NE, Cao J, McGuire SP, et al. A murine model for metastatic conjunctival melanoma. *Invest Ophthalmol Vis Sci*. 2015;56(4):2325-2333.

25. Ruiter DJ, Ferrier CM, van Muijen GN, et al. Quality control of immunohistochemical evaluation of tumour-associated plasminogen activators and related components. European BIOMED-1 concerted action on clinical relevance of proteases in tumour invasion and metastasis. *Eur J Cancer*. 1998;34:1334-1340.

26. Jordanova ES, Gorter A, Ayachi O, et al. Human leukocyte antigen class I, MHC class I chain-related molecule A, and CD8+/regulatory T-cell ratio: which variable determines survival of cervical cancer patients? *Clin Cancer Res*. 2008;14:2028-2035.

27. Djajadiningrat RS, Horenblas S, Heideman DA, Sanders J, de Jong J, Jordanova ES. Classic and nonclassic HLA class I expression in penile cancer and relation to HPV status and clinical outcome. J Urol. 2015;193:1245-1251.

28. Nareyeck G, Wuestemeyer H, von der Haar D, Anastassiou G. Establishment of two cell lines derived from conjunctival melanomas. *Exp Eye Res*. 2005;81:361–362.

29. Keijser S, Maat W, Missotten GS, de Keizer RJ. A new cell line from a recurrent conjunctival melanoma. *Br J Ophthalmol*. 2007;91:1566–1567.

30. Buyse M, Charrier L, Sitaraman S, Gewirtz A, Merlin D. Interferon-gamma increases hPepT1-mediated uptake of di-tripeptides including the bacterial tripeptide fMLP in polarized intestinal epithelia. *Am J Pathol*. 2003;163:1969-1977.

31. Bronkhorst IH, Jehs TM, Dijkgraaf EM, et al. Effect of hypoxic stress on migration and characteristics of monocytes in uveal melanoma. *JAMA Ophthalmol*. 2014;132:614-621.

32. Koene G, Mulder A, van der Ven K, et al. Human monoclonal antibodies as a tool for the detection of HLA class I allele-specific expression loss in head-and-neck squamous cell carcinoma and corresponding lymph node metastases. *Hum Immunol*. 2006;67:692-699.

33. Mulder A, Kardol MJ, Arn JS, et al. Human monoclonal HLA antibodies reveal interspecies crossreactive swine MHC class I epitopes relevant for xenotransplantation. *Mol Immunol*. 2010;47:809-815.

34. Stam NJ, Vroom TM, Peters PJ, Pastoors EB, Ploegh HL. HLA-A- and HLA-B-specific monoclonal antibodies reactive with free heavy chains in western blots, in formalin-fixed, paraffin-embedded tissue sections and in cryo-immuno-electron microscopy. *Int Immunol*. 1990;2:113-125.

35. Güssow D, Rein R, Ginjaar I, et al. The human beta 2-microglobulin gene. Primary structure and definition of the transcriptional unit. *J Immunol*. 1987;139:3132-3138.

36. van Essen TH, van Pelt SI, Bronkhorst IH, et al. Upregulation of HLA expression in primary uveal melanoma by infiltrating leukocytes. *PLoS One*. 2016;11:e0164292.

37. Campoli M, Ferrone S. HLA antigen changes in malignant cells: epigenetic mechanisms and biologic significance. *Oncogene*. 2008;27:5869-5885.

38. Sabbatino F, Villani V, Yearley JH, et al. PD-L1 and HLA class I antigen expression and clinical course of the disease in intrahepatic cholangiocarcinoma. *Clin Cancer Res*. 2016;22:470-478.

39. Garrido F, Perea F, Bernal M, Sánchez-Palencia A, Aptsiauri N, Ruiz-Cabello F. The escape of cancer from T cell-mediated immune surveillance: HLA class I loss and tumor tissue architecture. *Vaccines*. 2017;5:7. doi:10.3390/vaccines5010007

40. Carretero R, Romero JM, Ruiz-Cabello F, et al. Analysis of HLA class I expression in progressing and regressing metastatic melanoma lesions after immunotherapy. *Immunogenetics*. 2008;60:439-447.

41. Reimers MS, Engels CC, Putter H, et al. Prognostic value of HLA class I, HLA-E, HLA-G and Tregs in rectal cancer: a retrospective cohort study. *BMC Cancer*. 2014;14:486.

42. Ibrahim EC, Aractingi S, Allory Y, et al. Analysis of HLA antigen expression in benign and malignant melanocytic lesions reveals that upregulation of HLA-G expression correlates with malignant transformation, high inflammatory infiltration and HLA-A1 genotype. *Int J Cancer*. 2004;108:243-250.

43. Ferns DM, Heeren AM, Samuels S, et al. Classical and non-classical HLA class I aberrations in primary cervical squamous-and adenocarcinomas and paired lymph node metastases. *J Immunother Cancer*. 2016;4:78.

44. Parker BS, Rautela J, Hertzog PJ. Antitumour actions of interferons: implications for cancer therapy. *Nat Rev Cancer*. 2016;16:131-144.

45. Hinrichs J, Figueiredo C, Hirv K, et al. Discrimination of HLA null and low expression alleles by cytokine-induced secretion of recombinant soluble HLA. *Mol Immunol*. 2009;46:1451-1457.

46. Garcia-Lora A, Algarra I, Gaforio JJ, Ruiz-Cabello F, Garrido F. Immunoselection by T lymphocytes generates repeated MHC class I-deficient metastatic tumor variants. *Int J Cancer*. 2001;91:109-119.

47. Wang RF, Wang HY. Immune targets and neoantigens for cancer immunotherapy and precision medicine. *Cell Res*. 2017;27:11-37.

48. Aptsiauri N, Carretero R, Garcia-Lora A, Real LM, Cabrera T, Garrido F. Regressing and progressing metastatic lesions: resistance to immunotherapy is predetermined by irreversible HLA class I antigen alterations. *Cancer Immunol Immunother*. 2008;57:1727-1733.

49. Carretero R, Wang E, Rodriguez AI, et al. Regression of melanoma metastases after immunotherapy is associated with activation of antigen presentation and interferon-mediated rejection genes. *Int J Cancer*. 2012;131:387-395.

50. Zaretsky JM, Garcia-Diaz A, Shin DS, et al. Mutations associated with acquired resistance to PD-1 blockade in melanoma. *N Engl J Med*. 2016;375:819-829.

Supplementary information

Supplementary Table 1. Secondary antibodies for IF and IHC.

Antibody	Specificity	Isotype	Company	Catalogue	Dilutions
AlexaFluor 488	mouse	IgG1	Life Technologies	A-21121	1：300
AlexaFluor 546	mouse	IgG2a	Life Technologies	A-21133	1：300
AlexaFluor 647	rabbit	IgG	Life Technologies	A-21245	1：300
Biotinylated	mouse	IgG	DAKO	E0433	1：200
Biotinylated	rabbit	IgG	Vector Laboratories	BA-1000	1：300

Supplementary Table 2. An overview of the primers used in qPCR.

Primers	Forward	Reverse
RPL13	GTACGCTGTGAAGGCATCAAC	GGTTGGTGTTCATCCGCTTG
RPS11	AAGCAGCCGACCATCTTTCA	CGGGAGCTTCTCCTTGCC
HLA-A	TGTGTTCGTGTAGGCATA	TTGAGACAGAGATGGAGAC
HLA-B	CTCCATCTCTGTCTCAACTT	CATCAACCTCTCATAGCA
B2M	TGCTGTCTCCATGTTTGATGTATCT	TCTCTGCTCCCCACCTCTAAGT
HLA-DR	CAAAGAAGGAGACGGTCTGG	GGCTCTCTCAGTTCCACAGG
HLA-DQ	TGATGGAGATGAGCAGTTC	GCAGCGGTAGAGTTGTAG
CIITA	GCTGGGATTCCTACACAATGC	TCTCCAGCCAGGTCCATCTG
IRF1	TCACCAAGAACCAGAGAA	TCCATCAGAGAAGGTATCAG
NLRC5	CTGGAGGAGTTGATGCTT	GATGGCTGAATGGTAGGT
TAP1	CGAAGCCCAGAAGTTTAG	CCACCAATGTAGAGGATTC
TAP2	CTATTCTGGTCGTGTGATTG	CTGTCTTAGTCTCCTGGAA

Supplementary Table 3. An overview of the HLA allele-specific antibodies used in the FACS analysis.

Cell line	Antibody clone	HLA-specificity defined by CDC	Isotype
CRMM1			
	SN607D8	A2/A28	IgG
	SN230G6	A2/B17	IgG
	DMS1B10	B62/B21/B37/B56/B72/B52/B45/A23/B44	IgM
	TRA2G9	Cw1/Cw3/Cw4/Cw*1402	IgM
CRMM2			
	MUL4C8	A3/A11	IgG
	WIM8E5	A1/A10/A11/A9/A29/A30/A31/A33/A28	IgG
	ROU9A6	B12/B13/B40/B21/B41	IgG
	DMS1B10	B62/B21/B37/B56/B72/B52/B45/A23/B44	IgM
	WK4C11	Cw1/Cw3/Cw*0801/Cw*1202/Cw*1402	IgM
CM2005.1			
	BRO11F6	A11	IgG
	MUS4H4	Bw4/A24/A32/A25	IgG
	KG30A7	B27/B12/B14/B49	IgM
	HDG8D9	B51/B35	IgG
	TRA2G9	Cw1/Cw3/Cw4/Cw*1402	IgM

CDC= Complement dependent cytotoxicity.

Supplementary Table 4. Information and data of the studied cohort.

Study number	Sex	Age at diagnosis (yr)	Follow-Up (months)	Local Recurrence	Time to recurrence (months)	Metastases	Time to metastasis (months)	Location of Metastases	Status	Location on Conjunctiva	Thickness (mm)	Largest Basal Diameter (mm)	cTNM (7th ed)
1	Female	59	43.6	No		No			Alive	Non-epibulbar	1.2	8	2
2	Female	47	246.8	Yes	48.9	No			Alive	Epibulbar	0.6	12	1
3	Male	64	78.6	Yes	24.6	No			Alive	Epibulbar	0.3	7	1
4	Female	84	42.3	No		Yes	27	Distant skin	Death due to metastases	Non-epibulbar	6	20	2
5	Male	61	51.9	No		No			Alive	Non-epibulbar	1.4	17	2
6	Male	46	6.7	No		No			Alive	Non-epibulbar	2.5	30	2
7	Male	33	107.6	Yes	37.8	No			Alive	Epibulbar	0.2	6	1
8	Female	69	35	No		No			Alive	Non-epibulbar	16	16	2
9	Male	58	64.9	No		No			Alive	Epibulbar	4	13	1
10	Female	49	37.3	No		No			Alive	Non-epibulbar	4.2	10	2
11	Female	84	3.3	No		No			Death due to unknown cause	Epibulbar	4	15	1
12	Female	73	37.2	No		No			Alive	Epibulbar	0.8	7	1
13	Male	60	98.3	Yes	70.3	Yes	91.9	Brain. visceral	Death due to metastases	Epibulbar	Unknown	5	1
14	Female	67	45.7	No		No			Alive	Epibulbar	1.2	12	1
15	Female	56	23.8	No		No			Alive	Epibulbar	0.2	5	1
16	Male	56	34.2	Yes	32.7	No			Alive	Epibulbar	0.2	12	1
17	Female	56	27.1	Yes	8.5	No			Alive	Epibulbar	2.5	Unknown	1
18	Female	75	41.9	Yes	8.4	No			Death due to unknown cause	Epibulbar	5	Unknown	1
19	Female	40	58.1	Yes	34.8	No			Alive	Epibulbar	1	9	1
20	Female	86	12.8	No		No			Alive	Epibulbar	0.1	6	1
21	Male	68	46.4	Yes	17.8	No			Alive	Epibulbar	0.2	2	1
22	Male	68	29.5	No		No			Alive	Epibulbar	0.2	12	1
23	Male	80	52.4	Yes	42.1	Yes	51.4	Unknown	Death due to metastases	Non-epibulbar	Unknown	Unknown	2

Supplementary Table 4. Information and data of the studied cohort (Continued).

Study number	CD4 T helper (cells/mm2)	CD4 (cells/mm2)	Tregs (cells/mm2)	CD68+ (cells/mm2)	CD68+CD163+ (cells/mm2)	CD3 (cells/mm2)	CD8 (cells/mm2)	HLA-A score	HLA-A category	HLA-BC score	HLA-BC category	B2M score	B2M category
1	32.1	70	37.9	57.3	45.6	124.5	54.5	0	total loss	3	partial loss	3	partial loss
2	52.7	94.4	41.7	63.4	58.1	264.1	169.7	6	partial loss	6	partial loss	6	partial loss
3	39.1	70.9	31.8	75	51.2	173.1	102.2	7	normal expression	7	normal expression	7	normal expression
4	12.6	29.5	16.9	46.6	22.1	109.6	80.1	6	partial loss	6	partial loss	6	partial loss
5	35.5	62.9	27.4	63.1	58.8	120	57.1	5	partial loss	6	partial loss	6	partial loss
6	51.4	76.2	24.9	19.1	11.9	144.1	67.8	0	total loss	0	total loss	0	total loss
7	45.2	64.5	19.3	24.8	10.9	129.5	65	5	partial loss	6	partial loss	6	partial loss
8	42.2	63.4	21.2	47.8	18.1	113	49.6	1	total loss	1	total loss	1	total loss
9	30.2	64	33.8	20.9	7.7	91.9	27.9	3	partial loss	3	partial loss	3	partial loss
10	38.7	64	25.3	27.2	11.3	121.5	57.5	3	partial loss	5	partial loss	5	partial loss
11	29.7	39.6	9.9	59.9	46.7	85.4	45.8	4	partial loss	4	partial loss	4	partial loss
12	46	67.8	21.8	85.3	50.7	158.8	91	2	total loss	2	total loss	2	total loss
13	91.8	132.7	41	27.3	19	206.6	73.9	7	normal expression	7	normal expression	7	normal expression
14	115.9	225.2	109.4	95.9	74.8	278.6	53.3	6	partial loss	6	partial loss	7	normal expression
15	99.6	157.3	57.7	51.8	40.6	290.9	133.6	3	partial loss	4	partial loss	4	partial loss
16	15	25.9	10.9	73.2	58.8	84.6	58.8	7	normal expression	6	partial loss	7	normal expression
17	57.7	83.3	25.7	66.8	38.4	171.2	87.9	8	normal expression	8	normal expression	8	normal expression
18	67.3	89.7	22.4	62.8	31.7	157.8	68.1	3	partial loss	3	partial loss	3	partial loss
19	38.8	55.1	16.3	22	14.9	97.8	42.7	3	partial loss	3	partial loss	4	partial loss
20	189.4	313.8	124.4	188.7	161.1	616.5	302.7	8	normal expression	7	normal expression	8	normal expression
21	201.5	301.8	100.3	248.3	219.9	636.6	334.8	7	normal expression	7	normal expression	7	normal expression
22	32.7	45	12.3	18.6	29.6	70.8	25.8	7	normal expression	7	normal expression	7	normal expression
23	12.9	60.8	47.8	40.3	38.8	123.2	62.5	6	partial loss	7	normal expression		Not-Scorable

Chapter 7

Summary, Discussion, and Perspective

Summary and general discussion

Although conjunctival melanoma (CM) is not a common disease, many aspects need to be considered in terms of medical care: treating the primary malignancy and preventing local recurrences, regional and distant metastases. The subject of this thesis is to better understand the biology of CM and look for potential targets of personalized treatment, as conventional chemotherapy has little effect on metastatic CM. Instead of the conventional medical concepts of "one disease, one target" and "one-size-fits-all", personalized medicine monitors the individual's comprehensive profile, and facilitates the development of multiple therapeutic strategies which may provide the best option. Therefore, I first set out to do experiments to identify the potential targets within CM, and subsequently studied the efficacy and safety of some pharmacological compounds, which have already shown therapeutic effects in other malignancies, on CM in laboratory circumstances.

Understanding the molecular mechanisms and pathways of CM may unmask oncogenic targets and explain how tumor cells escape from immune surveillance, thereby providing new therapeutic strategies to prolong survival of patients with CM. It would be great if our pre-clinical laboratory studies will lead to new treatment options with clinical applications, although many challenges remain to be addressed.

Cancer is a genetic abnormality. On the one hand, mutations occur in proto-oncogenes and can activate the oncogenic signaling pathway, letting tumor cells grow out of control. On the other hand, mutations existing in tumor suppressor genes may reverse the downregulation of cell division, thereby promoting tumor cell growth. Recognizing and targeting the right mutations is of great importance for targeted therapy, and for minimizing undesirable side effects. In **Chapter 2**, by performing immunohistochemistry (IHC) with specific antibodies, we discover frequent *BRAF* V600E mutations in conjunctival nevi (19%) and CM (26%). On the contrary, primary acquired melanosis (PAM) with or without atypia in the conjunctiva did not show any *BRAF* V600E mutation. Since CM mainly derives from PAM with atypia rather than a nevus, one may assume that only the presence of a

BRAF V600E mutation is not enough for tumor formation, and that other mutations in oncogenes and/or tumor-suppressor genes are needed to form CM. In addition, phosphorylated-ERK and phosphorylated-AKT are expressed in conjunctival melanocytic lesions, indicating that the MAPK and PI3K/AKT pathways are constitutively activated and can serve as targets for CM. *In vitro* experiments show that the BRAF inhibitors Vemurafenib and Dabrafenib inhibit the growth of *BRAF* V600E-mutated cell lines, while the MEK inhibitor MEK162 and AKT inhibitor MK2206 inhibit the proliferation of all CM cell lines, regardless of their mutation status. Moreover, combining MEK162 and MK2206 shows a synergistic effect on cell viability and the cell cycle profile, and induces more cell death than the single compounds. Our findings suggest that clinical investigations should be carried out to test the efficacy and safety of those small molecule inhibitors in CM.

Besides genetics, epigenetics is of great importance in regulating cell cycle and survival. Epigenetics changes the genome without altering nucleotide sequences. Epigenetic modifications play an important role in cellular transformation to malignancy: tumor-suppressor genes are frequently silenced by epigenetic alterations in cancer. Targeting epigenetic alterations has been shown to affect cancer prevention, detection, and treatment [1,2]. Enhancer of zeste homolog 2 (EZH2) is a core subunit of the polycomb repressive complex 2 (PRC2) family. Overexpression of EZH2 has been shown in many cancers, and has been associated with poor survival [3]. Some drugs that target epigenetic changes have been developed and have shown a high potency *in vitro* and *in vivo* against some cancers [4]. In **Chapter 3**, similar to cutaneous melanoma and prostate cancer, we also observe frequent overexpression of EZH2 in primary CM, and show that EZH2 expression is associated with tumor thickness. In contrast, EZH2 is not expressed in normal conjunctival melanocytes. Subsequently, we carried out *in vitro* experiments using genetic knockdown or pharmaceutical inhibition, and reveal that both types of inactivation of EZH2 lead to a significant decrease of cell viability, colony formation, EZH2-mediated protein expression and induce cell cycle arrest. EZH2 inhibitor GSK503 shows similar apoptosis induction as EZH2 depletion does, however,

another EZH2 inhibitor UNC1999 does not induce apoptosis in all CM cell lines, suggesting additional effects of the first drug. Furthermore, GSK503 inhibits growth of CM cells in zebrafish at a well-tolerated concentration. Our findings suggest that EZH2 may provide a new therapeutic option for CM patients.

Animal models have many advantages for studying cancer. Researchers can control and/or exclude potential confounding factors which may affect the results. Especially regarding such a rare malignancy as CM, the lack of human tissues limits the material available for further investigations. Animal models, therefore, may provide more opportunities to study tumor behavior and therapeutic strategies for CM. Currently, there are only a few proper animal models for CM research. While the treatment of primary CM has gained success in past years, we aim to explore potential therapies for distant metastasis. In **Chapter 4**, we first subconjunctivally injected three primary CM cell lines into nonobese diabetic (NOD)/severe combined immunodeficiency (SCID) IL-2 rγ^{null} mice. Primary tumor growth was successfully detected in all cases subsequently, whereas no metastasis developed. Therefore, we next applied an *in vivo* passaging technique: cells derived from subconjunctival xenografts were implanted into the subconjunctival space of the same strain of immunodeficient mice, and this method eventually resulted in frequent lung metastases. This murine model mimics the natural route of human metastasis as CM often spreads to the lung. Another benefit of this model is that corresponding xenografts maintain their mutation status present in the cell lines. This is especially important for testing new drugs targeting these mutations. Our research can provide novel options to prevent metastatic dissemination, and furthermore, to treat lung metastases. However, we should be aware that the lack of a functional immune system in immunodeficient mice limits the possibility to study the immunology of CM.

The discovery of immune checkpoints inhibitors has opened a new era of personalized treatment for advanced cutaneous melanoma, non-small cell lung cancer, bladder and renal cancer [5]. Considerable efforts have taken place to translate these exciting investigations towards clinical treatment. As targeted

therapies may induce resistance, current efforts of drug development pay a lot of attention to boost T-cell function, thereby killing tumor cells. The inhibitory immune checkpoint molecules cytotoxic T lymphocyte antigen 4 (CTLA-4) and programmed death 1 (PD-1) play an essential role in inhibiting T cell signaling. Antibodies blocking these two molecules have achieved great success in treating advanced malignancies and have led to good clinical responses [6]. The successful achievement of blocking PD-1/PD-L1 axis may be dependent on PD-L1 expression on the tumor cell membrane [7,8]. Recently, the predictive value of PD-L1 expression by tumor-infiltrating lymphocytes (CTL), which constitute the tumor microenvironment, for the clinical effect of the inhibitors has also been addressed [9]. In **Chapter 5**, we wonder whether treatment of immune checkpoint blockade can be applied to CM, and we study the expression of PD-L1 in CM, and the relation to the tumor microenvironment. Our results show that PD-L1 is expressed on tumor cells of 19% primary CMs and stromal cells (mainly $CD68^{+}CD163^{+}$ M2 macrophages) of 59% tumors. The tumoral PD-L1 expression is correlated with distant metastases and worse prognosis. Interestingly, the density of TILs is negatively associated with tumor size: large tumors contain less TILs than small tumors, suggesting tumor cells grow out when there are not enough infiltrating immune cells. These results suggest that advanced CM patients could be recruited for PD-1/PD-L1 axis blockade therapies.

Cancer utilizes multiple methods to escape immune recognition and attack. Currently, seven parameters have been characterized in relation to cancer-immune interactions, including general immune status, tumor foreignness, tumor sensitivity to immune effectors (human leukocyte antigen (HLA) expression and IFN-γ sensitivity), absence of inhibitory tumor metabolism, absence of soluble inhibitors, and absence of checkpoints [11]. The activation of cytotoxic T lymphocyte (CTL) responses by antigen-presenting cells demands the presence of HLA class I-associated peptides. HLA expression is often impaired on tumor cells, thus avoiding "visualization" by the immune system. No studies have as yet shown the correlation between HLA expression and clinical outcomes of anti-PD-1 or anti-CTLA-4

immunotherapies. However, studying tumor sensitivity will be helpful to understand the mechanisms of resistance of immunotherapy and to find out which patients are less likely to respond to T-cell mediated therapies. Furthermore, downregulation of HLA class I expression is considered a biomarker of poor prognosis in many cancer types [12]. In **Chapter 6**, we therefore examine HLA class I expression, and analyzed its correlation with some clinical parameters in CM. The immunofluorescence staining shows frequent downregulation of HLA class I expression, and that its expression is associated with the presence of some TILs but not with PD-L1/PD-1 status. We also observe that thick tumors often present weak or no HLA class I expression. T cell effector cytokines, especially IFN-γ, are a crucial promotors of HLA expression. The association of HLA class I expression and TILs may suggest that in thick tumors, less TILs produce IFN-γ, thereby impairing HLA expression, decreasing immune sensitivity and allowing tumors to grow unrestrained. We tested the influence of IFN-γ *in vitro* by incubating CM cell lines with IFN-γ to mimic the tumor environment and study the molecular changes. The mRNA and membranous protein expression of HLA class I and components of the antigen presentation machinery indeed were increased upon IFN-γ treatment. *In vivo* results show that HLA class I expression was maintained in a murine xenograft. In summary, our findings suggest that downregulation of HLA class I may contribute to the mechanisms of immune escape in CM. And it is necessary to enhance tumor HLA class I expression and improve the efficacy of T cell-based immunotherapy.

Conclusions and future perspectives

CM is a disease with its own characteristics: it is often mismanaged by family doctors at its early stages because of its rarity; ophthalmologists treat the primary malignancy and cooperate with pathologists to determine the accurate diagnosis and to schedule the necessary therapeutic strategies. Frequent local recurrences reduce the quality of life and the development of metastases may result in death. Therefore,

more collaborations should be made by ophthalmologists, pathologists, oncologists, geneticists and biochemists to provide better medical options to prevent and treat metastases in CM patients. Understanding tumor biology and immunology is a tedious but essential task. Nowadays, still, conventional chemotherapies may not show an effect in some malignancies and cause severe side effects; more attention therefore needs to be paid to personalized treatments and many studies indeed are showing promising clinical outcomes. One is encouraged to evaluate the patients' condition and make precise decision, intervention and treatment strategies for patients with cancer.

In this thesis, we have explored biological and immunological mechanisms in CM. We reveal that HLA class I expression is frequently downregulated in CM, which may contribute to tumor immune evasion. Our studies demonstrate that *BRAF* and *NRAS* mutations, EZH2 overexpression and PD-L1 expression can be targets for personalized therapies. We show that the establishment of a murine metastatic CM model mimics the human malignancy and can facilitate further pre-clinical analysis for CM. Our findings will support knowledge-based treatments of this disease. It is no doubt that more and more potential molecular targets will be uncovered by basic science and oncology research. Future studies will most likely investigate the combination treatment targeting multiple pathways and activating the function of immune cells. We hope our attempts may provide novel therapeutic options and prolong survival of CM patients.

References

1. Novak, K . Epigenetics Changes in Cancer Cells. MedGenMed. 2004;6:17.
2. Banno K, Kisu I, Yanokura M, Tsuji K, Masuda K, Ueki A, Kobayashi Y, Yamagami W, Nomura H, Tominaga E, Susumu N, Aoki D. Epimutation and cancer: a new carcinogenic mechanism of Lynch syndrome. Int J Oncol. 2012;41:793-797.
3. Bachmann IM, Halvorsen OJ, Collett K, Stefansson IM, Straume O, Haukaas SA, Salvesen HB, Otte AP, Akslen LA. EZH2 expression is associated with high proliferation rate and aggressive tumor subgroups in cutaneous melanoma and cancers of the endometrium, prostate, and breast. J Clin Oncol. 2006;24:268-273.
4. Kim KH, Roberts CW. Targeting EZH2 in cancer. Nat Med. 2016;22:128-134.
5. Bersanelli M, Buti S. From targeting the tumor to targeting the immune system: Transversal challenges in oncology with the inhibition of the PD-1/PD-L1 axis. World J Clin Oncol. 2017;8:37-53.
6. Sharma P, Allison JP. The future of immune checkpoint therapy. Science. 2015;348:56–61.
7. Taube JM, Anders RA, Young GD, Xu H, Sharma R, McMiller TL, Chen S, Klein AP, Pardoll DM, Topalian SL, Chen L. Colocalization of inflammatory response with B7-h1 expression in human melanocytic lesions supports an adaptive resistance mechanism of immune escape. Sci Transl Med. 2012;4:127ra37.
8. Mahoney KM, Freeman GJ, McDermott DF. The next immune checkpoint inhibitors: PD-1/PD-L1 blockade in melanoma. Clinical Ther. 2015;37:765–782.
9. Santarpia M, Karachaliou N. Tumor immune microenvironment characterization and response to anti-PD-1 therapy. Cancer Biol Med. 2015;12:74-78.
10. Teng MW, Ngiow SF, Ribas A, Smyth MJ. Classifying cancers based on T-cell infiltration and PD-L1. Cancer Res. 2015;75:2139-2345.
11. Blank CU, Haanen JB, Ribas A, Schumacher TN. Cancer immunology. The "cancer immunogram". Science. 2016;352:658-660.
12. Speetjens FM, de Bruin EC, Morreau H, Zeestraten EC, Putter H, van Krieken JH, van Buren MM, van Velzen M, Dekker-Ensink NG, van de Velde CJ, Kuppen PJ. Clinical impact of HLA class I expression in rectal cancer. Cancer Immunol Immunother. 2008;57:601-609.

SAMENVATTING

Hoewel conjunctiva melanoom (CM) een zeldzame aandoening is, is de medische zorg voor de aandoening veelomvattend: zowel het behandelen van de primaire tumor, het voorkomen van lokale recidieven, als het voorkomen van regionale metastasen en metastasen op afstand is van belang. Het doel van dit proefschrift is tweeledig. Enerzijds gaat het om het verkrijgen van een beter inzicht in de biologie van CM, anderzijds gaat het om het ontwikkelen van doelgerichte gepersonaliseerde therapie, aangezien gangbare chemotherapie niet goed werkt bij gemetastaseerd CM. In tegenstelling tot de gebruikelijke principes van "één ziekte, één doel" en "one-size-fits-all" voor behandelingen, betrekt gepersonaliseerde therapie een uitgebreid persoonlijk profiel, en maakt het meerdere behandelstrategieën mogelijk waaruit een beste optie kan worden gekozen. Om dit doel te bereiken, heb ik experimenten uitgevoerd om aangrijpingspunten te identificeren voor de behandeling van gemetastaseerd CM en vervolgens heb ik de effectiviteit en veiligheid van farmacologische middelen, die al gebruikt worden bij andere maligniteiten, onder laboratoriumomstandigheden bij CM onderzocht.

Begrip van de moleculaire mechanismen van CM kan leiden tot de ontdekking van aangrijpingspunten voor behandeling ("therapeutische targets") en verklaren hoe tumorcellen ontkomen aan opruiming door het immuunsysteem ("immune surveillance"). Hiermee hopen we de levensverwachting van patiënten met CM te verbeteren. Hoewel er nog vele uitdagingen moeten worden overwonnen, zou het mooi zijn als ons pre-klinische onderzoek resulteert in klinisch toepasbare behandelopties.

Kanker is een genetische aandoening. Enerzijds kunnen mutaties in proto-oncogenen groei-stimulerende 'pathways' aanzetten en anderzijds kunnen mutaties in 'tumor-suppressor genen' de natuurlijke rem op celdeling ongedaan maken waardoor tumorcellen ongecontroleerd kunnen delen. Het herkennen van, en het aangrijpen op

de juiste mutaties is een wezenlijk onderdeel van 'targeted' therapie; tevens om het risico op bijwerkingen te minimaliseren. In **Hoofdstuk 2** hebben we via immunohistochemie (IHC) met specifieke antilichamen aangetoond dat *BRAF* V600E mutaties vaak voorkomen in conjunctivale nevi (19%) en CM (26%). Die specifieke mutatie vonden we echter niet in primair verworven melanose (primary acquired melanosis, PAM) van de conjunctiva, met of zonder atypie. Aangezien CM veelal vanuit PAM met atypie ontstaat, en zelden vanuit een nevus, is het aannemelijk dat alleen een *BRAF* V600E mutatie onvoldoende is voor tumorvorming en dat andere mutaties in oncogenen en/of tumor suppressor genen nodig zijn voor de ontwikkeling van CM. Bovendien zagen wij expressie van gefosforyleerd ERK en gefosforyleerd AKT in conjunctivale melanocytaire laesies, wat wijst op een activatie van de PI3K/AKT pathway, hetgeen een target voor doelgerichte therapie kan zijn. Onze *in vitro* experimenten toonden aan dat de BRAF inhibitoren Vemurafenib en Dabrafenib de groei van cellijnen met de *BRAF* V600E mutatie remmen, terwijl de MEK inhibitor MEK162 en AKT inhibitor MK2206 de proliferatie van CM cellijnen remmen, ongeacht de mutatiestatus. Bovendien laat de combinatie van MEK162 en MK2206 een synergistisch effect zien op cel-overleving en celcyclus, en resulteert de combinatie in meer celdood dan wanneer deze middelen apart worden toegepast. Onze bevindingen tonen aan dat klinisch onderzoek naar de effectiviteit en veiligheid van deze 'small molecule inhibitors' in CM nodig is.

Naast genetische veranderingen zijn ook epigenetische veranderingen van belang voor de regulering van de celcyclus en overleving van tumorcellen. Epigenetica omvat veranderingen aan het genoom die geen wijziging van de volgorde van nucleotiden betreft. Epigenetische veranderingen spelen een belangrijke rol in de transformatie van normale cellen tot tumorcellen: tumor suppressor genen zijn vaak geremd door epigenetische veranderingen bij kanker. Van verschillende behandelingen die gericht zijn op epigenetische veranderingen is bewezen dat zij effectief zijn bij de preventie, detectie en behandeling van kanker [1,2]. Enhancer of

zeste homolog 2 (EZH2) is een onderdeel van de 'polycomb repressive complex 2' (PRC2) familie. Overexpressie van EZH2 is in meerdere kankersoorten aangetoond en is geassocieerd met een slechte overleving [3]. Van bepaalde middelen die gericht zijn op epigenetische veranderingen is in sommige kankersoorten zowel *in vitro* als *in vivo* de effectiviteit aangetoond [4]. In **Hoofdstuk 3** laten we zien dat overexpressie van EZH2, net zoals in huidmelanoom en prostaatkanker, regelmatig voorkomt in primair CM en we tonen aan dat EZH2 expressie is geassocieerd met tumordikte. EZH2 komt daarentegen niet tot expressie in normale conjunctivale melanocyten. Vervolgens hebben we *in vitro* experimenten uitgevoerd waarbij we middels genetische 'knock-down' en farmacologische inhibitie EZH2 hebben geïnactiveerd. We tonen aan dat beide manieren resulteren in een significante vermindering van de levensvatbaarheid van tumorcellen, een vermindering van kolonievorming van tumorcellen in celweek, een vermindering van expressie van EZH2-gemedieerde eiwitten en leiden tot blokkade van de celdeling. Hoewel de EZH2-inhibitor GSK503 leidt tot een vergelijkbare mate van apoptose als EZH2 depletie, resulteert EZH2 inhibitie met de inhibitor UNC1999 niet in apoptose in alle CM cellijnen, wat suggereert dat GSK503 bijkomende effecten heeft. Meer nog, GSK503 remt de groei van CM cellen in een zebravismodel bij een goed te verdragen concentratie. Onze bevindingen suggereren dat aangrijpen op EZH2 een nieuwe therapeutische optie voor patiënten met CM kan zijn.

Het gebruik van diermodellen voor onderzoek naar kanker heeft verschillende voordelen. Het biedt onderzoekers de mogelijkheid om factoren die de resultaten van het onderzoek kunnen beïnvloeden, te controleren en/of te excluderen. In zeldzame maligniteiten als CM is er een gebrek aan voldoende humaan weefsel wat de mogelijkheden voor onderzoek beperkt. Diermodellen kunnen extra mogelijkheden bieden om het gedrag van tumoren en therapeutische strategieën te onderzoeken. Momenteel zijn er slechts enkele diermodellen die geschikt zijn voor onderzoek naar CM. De afgelopen jaren is er vooruitgang geboekt in de behandeling van primair CM. Wij hebben als doel om potentiële behandelingen voor metastasen op afstand

te ontwikkelen. In **Hoofdstuk 4** hebben we 3 primaire CM cellijnen subconjunctivaal geïnjecteerd in 'nonobese diabetic (NOD)/severe combined immunodeficiency (SCID) IL-2 rγ^{null}' muizen. We detecteerden in alle muizen primaire tumorgroei zonder ontwikkeling van metastasen. Daarom hebben we vervolgens een *in vivo* passage techniek toegepast: tumorcellen verkregen uit de subconjunctivale xenotransplantaten werden geïmplanteerd in de subconjunctivale ruimte van hetzelfde type immunodeficiënte muizen. Dit resulteerde uiteindelijk in een aanzienlijk aantal longmetastasen. Omdat CM vaak naar de longen metastaseert, komt dit muismodel overeen met het natuurlijke gedrag van CM. Een ander voordeel van dit muismodel is dat in de xenotransplantaten dezelfde mutaties werden gevonden als in de bijbehorende cellijnen. Dat is vooral van belang voor het testen van nieuwe middelen die gericht zijn tegen deze mutaties. Ons onderzoek kan leiden tot nieuwe mogelijkheden om uitzaaiingen te voorkomen, en verder om longmetastasen te behandelen. We moeten echter beseffen dat de afwezigheid van een functionerend immuunsysteem in immunodeficiënte muizen de mogelijkheden beperkt om de immunologie van CM te bestuderen.

De ontdekking van immunologische 'checkpoint remmers' heeft geleid tot een nieuw tijdperk in de gepersonaliseerde behandeling van gemetastaseerd huidmelanoom, niet-kleincellig longcarcinoom, blaaskanker en nierkanker [5]. Er is veel inspanning geleverd om deze bevindingen te vertalen naar klinisch toepasbare behandelingen. Omdat targeted therapie resistentie kan opwekken, is veel van het huidige onderzoek gericht op het stimuleren van de functie van T cellen, om zo tumorcellen te doden. De immunologische checkpoint moleculen 'cytotoxic T lymphocyte antigen 4' (CTLA4) en 'programmed death 1' (PD-1) spelen een essentiële rol in de remming van de T cel signaaloverdracht. Antilichamen die deze twee moleculen blokkeren zijn effectief gebleken in de behandeling van gevorderde maligniteiten en hebben geleid tot een goede klinische respons [6]. De succesvolle blokkade van de PD-1/PD-L1 as is mogelijk afhankelijk van PD-L1 expressie op de tumorcelmembraan [7,8]. Onlangs is onderzocht of PD-L1 expressie op tumor-

infiltrerende lymfocyten (TIL) een voorspellende waarde heeft voor het klinische effect van checkpointremmers [9]. In **Hoofdstuk 5** hebben we ons afgevraagd of immunologische checkpoint blokkade toegepast kan worden in CM, hebben we de expressie van PD-L1 in CM bestudeerd en hebben we de relatie met de tumor-omgeving bestudeerd. We laten zien dat PD-L1 tot expressie komt op tumorcellen bij 19% van de primaire CM, en op stromale cellen (vooral $CD68^{+}CD163^{+}$ M2 macrofagen) bij 59% van de primaire CM. Verder laten we zien dat PD-L1 expressie op tumorcellen gecorreleerd is met de ontwikkeling van metastasen op afstand en een slechte prognose. Opmerkelijk is dat de dichtheid van TILs een negatieve associatie met tumorgrootte laat zien: grotere tumoren hebben minder TILs dan kleinere tumoren. Dit suggereert dat tumoren beter groeien als er minder infiltrerende immuuncellen zijn. Deze resultaten geven aan dat blokkade van de PD-1/PD-L1 as mogelijk effectief kan zijn bij patiënten met gevorderde CM.

Kankercellen gebruiken verschillende manieren om te ontkomen aan herkenning en vernietiging door het immuunsysteem. Momenteel zijn er 7 parameters bekend die betrokken zijn bij kanker-immuunsysteem interacties: de algemene toestand van het immuunsysteem, 'tumor foreignness' (de mate waarin een tumor als lichaamsvreemd wordt gezien door het immuunsysteem), de gevoeligheid van tumoren voor het immuunsysteem (human leukocyte antigen (HLA) expressie en IFN-γ gevoeligheid), de afwezigheid van remmend tumormetabolisme, de afwezigheid van remmende stoffen en de afwezigheid van checkpoints [11]. De activatie van cytotoxische T lymfocyten (CTL) door antigeen-presenterende cellen vereist de aanwezigheid van HLA klasse I-geassocieerde peptiden. Tumorcellen hebben vaak een lage HLA expressie om zo minder 'zichtbaar' te zijn voor het immuunsysteem. Een correlatie tussen HLA expressie en klinische effectiviteit van anti-PD-1 of anti-CTLA-4 immunotherapieën is alleen nog niet aangetoond. Het bestuderen van de gevoeligheid van tumoren voor immunotherapie zal bijdragen aan inzicht in de manier waarop resistentie voor immunotherapie ontstaat en zal helpen bij het identificeren van patiënten het beste reageren op T cel gemedieerde

behandelingen. Bovendien wordt een verminderde expressie van HLA klasse I in vele maligniteiten als een biomarker van slechte prognose gezien [12]. In **Hoofdstuk 6** hebben we daarom de expressie van HLA klasse I bestudeerd en de correlatie met bepaalde klinische parameters van CM geanalyseerd. Immunofluorescentie laat in veel gevallen een verminderde expressie van HLA klasse I zien en toont een associatie tussen expressie van HLA klasse I met de aanwezigheid van sommige TILs, maar niet met de PD-L1/PD-1 status. Ook laten we zien dat tumoren met een grotere dikte vaak weinig tot geen HLA klasse I expressie vertonen. T cel effector cytokines, zoals IFN-γ, zijn cruciale promotoren van HLA expressie. De associatie tussen expressie van HLA klasse I en TILs suggereert dat in dikkere tumoren minder TILs IFN-γ produceren, waardoor de HLA expressie lager is. Hierdoor is de tumor minder gevoelig voor het immuunsysteem en kan deze ongestoord groeien. We hebben de invloed van IFN-γ *in vitro* getest door CM cellijnen te incuberen met IFN-γ. Dit bootst demicro-omgeving van de tumor na en stelt ons in staat de moleculaire veranderingen te bestuderen. We zagen inderdaad dat incubatie met IFN-γ resulteerde in een verhoging van de mRNA en membraaneiwit expressie van HLA klasse I en HLA-geassocieerde moleculen. *In vivo* resultaten lieten zien dat expressie van HLA klasse I behouden bleef in het muis-xenotransplantaat. Samengevat suggereren onze bevindingen dat een verminderde expressie van HLA klasse I kan bijdragen aan de manier waarop CM herkenning door het immuunsysteem ontloopt. Het is noodzakelijk de expressie van HLA klasse I op te hogen om de werkzaamheid van T-cel gebaseerde immuuntherapie te verhogen.

Conclusies en toekomstperspectieven

CM is een aandoening die in de vroege fase vaak wordt gemist door huisartsen vanwege de geringe tumorgrootte. Oogartsen behandelen de primaire maligniteit en bepalen in samenwerking met patholoog-anatomen de daadwerkelijke diagnose en verdere therapie. Frequente lokale recidieven verminderen de kwaliteit van leven, terwijl metastasen kunnen resulteren in de dood. Meer samenwerking tussen oogartsen, patholoog-anatomen, oncologen, genetici en biochemici is zodoende

nodig om betere opties te ontwikkelen voor de preventie en behandeling van metastasen van CM. Begrip van de tumorbiologie en tumor-immunologie is hierbij een lastige maar essentiële voorwaarde. Gangbare chemotherapie is niet effectief bij sommige maligniteiten en kan ernstige bijwerkingen hebben; er moet daarom meer aandacht besteed worden aan gepersonaliseerde behandelingen. Gelukkig laten meerdere studies naar gepersonaliseerde behandelingen veelbelovende klinische resultaten zien. Het verdient de voorkeur om bij patiënten met kanker de conditie van de patiënt te evalueren en een zorgvuldige beslissingover interventie en therapie te maken.

In dit proefschrift hebben we de biologische en immunologische mechanismen van CM bestudeerd. We hebben aangetoond dat er in CM veelal verminderde expressie van HLA klasse I optreedt, wat mogelijk bijdraagt aan het ontkomen van tumorcellen aan het immuunsysteem. Onze studies tonen aan dat *BRAF* en *NRAS* mutaties, EZH2 overexpressie en PD-L1 expressie aangrijpingspunten voor gepersonaliseerde therapie kunnen zijn. We laten zien dat het muismodel van CM metastasen de humane maligniteit goed nabootst en verdere pre-klinische analyses naar CM kan bevorderen. Onze bevindingen ondersteunen de ‘knowlegde-based’ behandelingen voor deze aandoening. Ongetwijfeld zullen steeds meer potentiële targets ontdekt worden door fundamenteel (oncologisch) onderzoek. Toekomstige studies zullen zich naar waarschijnlijkheid richten op de combinatie van doelgerichte therapie van meerdere moleculaire pathways en immuuntherapie door activatie van immuuncellen. Wij hopen dat ons onderzoek nieuwe therapeutische opties biedt voor de behandeling van CM en de levensverwachting van patiënten met CM verbetert.

LIST OF PUBLICATIONS

1. **Cao J**, Jager MJ.
   Animal eye models for uveal melanoma.
   Ocul Oncol Pathol. 2015; 1 (3):141–150.

2. Yang H, **Cao J**, Grossniklaus HE.
   Uveal melanoma metastasis models.
   Ocul Oncol Pathol. 2015; 1 (3):151–160.

3. De Waard NE, Kolovou PE, McGuire SP, **Cao J**, Frank NY, Frank MH, Jager MJ, Ksander BR.
   Expression of multidrug resistance transporter ABCB5 in a murine model of human conjunctival melanoma.
   Ocul Oncol Pathol. 2015; 1 (3):182–189.

4. De Waard NE*, **Cao J***, McGuire SP, Kolovou PE, Jordanova ES, Ksander BR, Jager MJ.
   A murine model of metastatic conjunctival melanoma.
   Invest Ophthalmol Vis Sci. 2015; 56 (4):2325–2333.

5. Versluis M, de Lange MJ, van Pelt SI, Ruivenkamp CA, Kroes WG, **Cao J**, Jager MJ, Luyten GP, van der Velden PA.
   Digital PCR validates 8q dosage as prognostic tool in uveal melanoma.
   PLoS One. 2015; 10 (3): e0116371.

6. **Cao J**, Heijkants RC, Jochemsen AG, Dogrusöz M, de Lange MJ, van der Velden PA, van der Burg SH, Jager MJ, Verdijk RM.
   Targeting of the MAPK and AKT pathways in conjunctival melanoma shows potential synergy.
   Oncotarget. 2016; 8 (35):58021-58036.

7. **Cao J***, Brouwer NJ*, Richards KE, Marinkovic M, van Duinen S, Hurkmans D, Verdegaal EME, Jordanova ES, Jager MJ.
   PD-L1/PD-1 expression and tumor-infiltrating lymphocytes in conjunctival melanoma.
   Oncotarget. 2017; 8 (33):54722-54734.

8. Gezgin G, Luk SJ, **Cao J**, Dogrusöz M, van der Steen DM, Hagedoorn RS, Krijgsman D, van der Velden PA, Field MG, Luyten GPM, et al.
   PRAME as a potential target for immunotherapy in metastatic uveal melanoma.
   JAMA Ophthalmol. 2017; 135 (6):541-549.

9. Pontes KC, Groenewoud A, **Cao J,** Ataide LM, Snaar-Jagalska E, Jager MJ. Evaluation of (fli:GFP) Casper zebrafish embryos as a model for human conjunctival melanoma. (*In press, Invest Ophthalmol Vis Sci*. 2017).

10. **Cao J**, Pontes KC, Heijkants RC, Brouwer NJ, Groenewoud A, Jordanova ES, Marinkovic M, van Duinen SG, Teunisse AFAS, Robert M Verdijk, Snaar-Jagalska E, Jochemsen AG, Jager MJ.
    Overexpression of EZH2 in conjunctival melanoma offers a new therapeutic target. (*Submitted for publication*).

11. **Cao J**, Brouwer NJ, Jordanova ES, Marinkovic M, van Duinen SG, de Waard NE, Ksander BR, Mulder A, Claas FHJ, Heemskerk MHM, Jager MJ.
    HLA class I antigen expression in conjunctival melanoma is not associated with PD-L1/PD-1 status. (*Submitted for publication*).

12. Dogrusöz M, Trasel AR, **Cao J**, Olak S, van Pelt SI, Pfeffer U, van Duinen SG, Luyten GPM, van der Velden PA, Jochemsen AG, Jager MJ.
    Differential expression of DNA repair genes in prognostically-favorable versus prognostically-unfavorable uveal melanoma. (*Submitted for publication*).

* These authors contributed equally to the work.

CURRICULUM VITAE

The author of this thesis was born on February 17th, 1982 in Changchun, Jilin Province, P.R. China. In 2001, after finishing his high school education at Jilin Provincial Experimental School in Changchun, he decided to study clinical medicine at the Norman Bethune Health Science Center of Jilin University. The author obtained his M.D. degree in 2006, and he was admitted as a master student of Ophthalmology by Jilin University Second Hospital in 2007. After completion of his master education in 2010, the author continued his clinical doctor career at the Ophthalmology Department of Jilin University Second Hospital for two years.

In 2012, he was supported by the China Scholarship Council Scholarship Program and came to the Netherlands to start his PhD career under supervision of Professor Martine J. Jager, at the Ophthalmology Department of Leiden University Medical Center. During his PhD training, the author had the chance to present his work in Europe, Asia and the United States and established international collaborations with other institutes. The author will go back to China where he will continue his clinical and scientific research.

ACKNOWLEDGEMENTS

When I wrote this thesis, all the memories of past five years emerged in my mind. I still remember on the day that I first arrived at Leiden Central station, my dear landlady Christine drove me home and I started to realize that my adventure in Netherlands had begun.

Expressing my gratitude with only words is not enough. Many kind and lovely people have helped me overcome the hard times, and make my life better. I am so lucky to have met you all.

My dear promotor, Prof. Dr. Martine J. Jager, thank you for providing me the great opportunity to perform my PhD program under your supervision in the LUMC. Your scientific views, attitudes and enthusiasm have encouraged me all the time. You always inspired and supported me, and gave me enough freedom to think, to practice, and to finish. I really appreciate your supervision style. Special thanks to my co-promotor Dr. Aart G. Jochemsen. You are so patient, and have taught me many useful techniques and created a lot of excellent ideas. I am also lucky to have Dr. Rob Verdijk as my co-promotor: we had a nice collaboration and you showed me how to become a rigorous researcher. Dear Prof. Dr. Ludwig Heindl, Dr. Mei Wang and Dr. Renbing Jia, I am very grateful for your kind help and suggestions regarding my thesis.

I would like to express my appreciation to my colleagues in Ophthalmology: Gre, Pieter, Mehmet, Mieke, Herbert, Niels, Annemijn, Gulcin, Kelly, Rogier, Marina, Mark, Judith, Annelies and Nadine. It was very nice to share so much good time with you.

I would also thank my friends and collaborators from other departments: Sjoerd, Els, Thorbald and Marjolein (Clinical Oncology, LUMC); Renier, Amina and Aat (MCB, LUMC); Katja and Sjoerd (Pathology, LUMC); Mirjam and Dirk (HEM, LUMC); Arend and Pieter (IHB, LUMC); Marco (Pediatrics, LUMC); Arwin and Ewa (IBL,

Leiden). Without you, the studies could not be finished. It was great to work with you.

I am very grateful to my ex-landlords Jan and Willem, and ex-landlady Christina, for sharing your wonderful experiences of Netherlands and for your kind help.

My dear friends Mengmeng, Min, Zhenyu, Yaojin, Hao, Feng, Peng, Zhuang and Jiaxin, thank you very much for taking care of me during my long-term injury. I appreciate the kind help from Junling, Wenbo and Jianxin for my scientific research. Dear Frank, Yuchuan, Jian, Feng, Lin, Jinxian, Dejian, Jianxin, Ruslan, Rind, Florence, Zoraida, Joep, Teresa, Tom, Anran, Alexander, Maartje, Claire, Pjotr, Junzeng and Jieya, I am very happy to get to know you brilliant people. The kind help and wonderful time that we spent together are always in my mind.

I am very grateful to my teachers and friends in China. Despite the long distance, your encouragements inspire me all the time.

Last but not least, I would like to thank my family members. My dear parents Guihe and Chunshun, thank you for showing me how to be a kind, brave, confident and independent person. Although I went so far away, my heart is always with you. My dear wife Yan, thank you for your company during my injury. And thank you for your understanding, supporting and letting me pursue my dream thousands of kilometers away. The end is just another beginning. Now it is time to go home and start a new journey!

Sincerely,
Jinfeng